MAX-PLANCK-INSTITUT
FÜR POLYMERFORSCHUNG

Noncoherent Upconversion in Multimolecular Organic Systems

Dissertation

zur Erlangung des Grades
„Doktor der Naturwissenschaften“

im Promotionsfach Physikalische Chemie
am Fachbereich Chemie, Pharmazie und Geowissenschaften

JOHANNES GUTENBERG
UNIVERSITÄT MAINZ

Dzmitry Busko
geboren in Mozyr, Weißrussland

Mainz, Juli 2013

Die vorliegende Arbeit wurde am
Max-Plank-Institut für Polymerforschung in Mainz
unter Anleitung von

in der Zeit von Mai 2009 bis Juli 2013 angefertigt.

Dekan:

Erster Gutachter:

Zweiter Gutachter:

Tag der mündlichen Prüfung: 21. Oktober 2013

Abstract.

The dissertation is devoted to the investigation of the process of triplet-triplet annihilation assisted upconversion (TTA – UC). The semiclassical theory of the process, a theoretically possible maximum of the quantum yield, requirements to the characteristics of a sensitizer and an emitter, as well as methods of a quantum efficiency determination are described.

The current state of the art of the used nowadays emitters and sensitizers, as well as the main directions in a creation of the new ones, is overviewed.

Due to the cooperation with chemists from our group the new emitters, synthesized mainly on the base of perylene, are created and analyzed for the applicability for the TTA – UC process in the combination with the sensitizers from tetrabenzo- and tetranaphtoporphyrine families. The modification allowed to create the library of the dyes, emitting in the blue up to yellow regions of the spectrum, and simultaneously to increase the quantum efficiency of the TTA – UC process. The maximal obtained quantum efficiency of the TTA – UC reached 13.4%.

The optimization of the conditions for the efficient TTA – UC observation was done. A strong influence of the excitation beam parameters on the resulting UC efficiency is shown and discussed. The dependence of the quantum yield of TTA – UC on excitation radiation intensity and a relative ratio between the sensitizer and emitter concentrations is reported.

The new strategy of an effective UC emitter's creation by comprising the functions of two chromophors in a dyad, where the function of the triplet-triplet transfer (TTT) and the triplet-triplet annihilation (TTA) are attributed to different parts of the molecule, is represented. It is shown that the quantum efficiency of the TTA – UC with the synthesized bichromophore emitter can be significantly higher than for each dye separately or being mixed.

The successful transfer of an UC medium into the water environment by the encapsulation of hydrophobic UC dyes into the micelles, formed by the PTS surfactant was done. Resulting quantum efficiency, in compare to the previously reported values, is comparable with that in an organic solvent.

Additionally, an extremely strong dependence of the efficiency of the TTA – UC process on temperature in such micellar structures was obtained. As a consequence, the use of PTS micelles for the local temperature sensing in bio objects is theoretically possible. It is shown, that by a variation of the surfactant one can extend the usable temperature range up to 70ºC and increase the temperature sensitivity of the system

Zusammenfassung

In der vorliegenden Dissertation wird der Prozess der Triplett-Triplett-Annihilation-Aufkonversion (TTA-UC) untersucht. Dabei wird zunächst die semi-klassische Theorie des Prozesses und die theoretisch maximale Quantenausbeute beschrieben. Des Weiteren werden die Anforderungen an die charakteristischen Eigenschaften von Sensitizer und Emitter diskutiert und unterschiedliche Methoden zur Bestimmung der Quanteneffizienz vorgestellt.

Zudem wird ein Überblick über den bisherigen Stand der aktuell verwendeten Farbstoffe (Sensitizer und Emitter) sowie ein Ausblick auf deren zukünftige und mögliche Weiterentwicklungen gegeben.

Die von Chemikern aus unserer Gruppe synthetisierten Emitter, überwiegend auf der Basis von Perylen, und Sensitizer aus der Familie der Tetrabenzo- oder Tetranaphtaporphyrine wurden auf eine mögliche Anwendbarkeit im TTA-UC-Prozess untersucht. Die zahlreichen Modifikationen ermöglichten die Zusammenstellung einer Farbstoffauswahl mit variabler Emission vom blauen bis hin zum gelben Bereich des Farbspektrums. Gleichzeitig konnte eine Erhöhung der Quanteneffizienz des TTA-UC-Prozesses bis zu einem Maximum von 13,4% erreicht werden.

Um eine effiziente Beobachtung der TTA-UC zu ermöglichen, wurde eine Optimierung der Bedingungen durchgeführt. Dabei wurde ein starker Einfluss der Parameter des Anregungsstrahls auf die resultierende UC-Effizienz nachgewiesen und diskutiert. Außerdem wurde die Abhängigkeit der Quantenausbeute des TTA-UC-Prozesses von der Strahlungsintensität und vom relativen Verhältnis zwischen Sensitizer- und Emitterkonzentration gezeigt.

Durch die Kombination der Eigenschaften von eigentlich zwei Farbstoffen in einer Dyade, wird eine neue Strategie für die Darstellung effektiver UC-Emitter beschrieben. Dabei wird ein Teil des Farbstoffmoleküls für die Funktion des Triplett-Triplett-Transfers (TTT) verwendet, während der andere Teil des Moleküls für die Funktion der Triplett-Triplett-Annihilation zuständig ist. Es wurde gezeigt, dass die Quanteneffizienz bei der Verwendung der Dyade im Vergleich zum Einsatz von einzelnen Farbstoffen oder nur zwei miteinander vermischten Farbstoffen signifikant größer ist.

Der erfolgreiche Transfer des UC-Mediums in eine wässrige Umgebung wurde mittels Verkapselung der hydrophoben UC-Farbstoffe in Mizellen, aufgebaut aus PTS-Tensid, dargestellt. Die dabei erhaltene Quanteneffizienz ist mit der Effizienz in einem organischen Lösungsmittel vergleichbar.

Des Weiteren wurde in diesen micellaren Strukturen ein extrem starker Temperatureinfluss auf die Effizienz des TTA-UC-Prozesses beobachtet. Theoretisch könnten solche PTS-Mizellen als Temperatursensoren in biologischen Proben verwendet werden. Es wurde gezeigt, dass durch die Variation des Tensides der nutzbare Temperaturbereich auf bis zu 70 °C ausgedehnt werden kann und die Temperatursensitivität des Systems erhöht werden kann.

List of content

1 Introduction

Spreading of light photons in any medium can lead to the conversion of their energy. Thus, absorption of light photons can lead to the substance heating, phase transmission, photochemical reactions, electric current generation and others. The process of reemission of the absorbed light photon is known as photoluminescence. Usually, this process is accompanied by loss of part of energy by the substance and, therefore, the emitted photon has energy lower than the energy of the absorbed one. This is called down-shifting. The spectrum of the resulting emission is shifted into the region of lower light frequencies (or longer wavelengths). The corresponding difference between the maxima of the absorption and emission spectrum is called the Stokes shift.

In contrast, the process, leading to an increase of the energy of emitted photon, is called upconversion (UC). The spectrum of the converted radiation will be correspondingly shifted into the region of higher light frequencies (shorter wavelengths). This so-called Anti-Stokes emission was first observed in processes involving the thermal energy of the substance. However, the frequency shift, which can be obtained in such processes, is very small. For the higher shift values generally the combination of energy parts obtained from at least two light photons is required.

There are many physical processes, leading to such UC. They can be virtually divided into two types. The first type deals with so-called virtual levels, introduced in order to simplify the description of correlated processes. The following physical effects can be assigned to this type [1]: multi-photon absorption [2], harmonic generation [3, 4], frequency mixing [5]. For such type of processes the simultaneous presence of at least two photons in one point of space is required. For the observation of UC emission in such processes an excitation radiation should possess extremely high intensity (on the order of $MW \cdot cm^{-2}$ or even $GW \cdot cm^{-2}$). Such light intensities could be provided only by coherent light sources – lasers.

The second type of UC processes is related with so-called sequential processes. For their operation the presence of a metastable state, which is placed intermediate in energy between the ground and the excited states and acts like a short-lived reservoir of energy, is necessary. One can attribute to this type the sequential two-photon absorption upconversion, the cooperative energy transfer and the photon avalanche upconversion [6]. Due to the presence of the metastable, but real state, the requirement to the intensity of pump radiation is significantly lowered for this type of processes, however, it still has an order of 10^3 - 10^6 $W \cdot cm^{-2}$.

Introduction

In the first decade of 21st century it was proposed [7] a new method for effective photon UC, which nowadays attracts a lot of interest from many scientific groups and industrial companies. Actually being first observed in 1960s by Parker [8] and partially being investigated [9-12], this effect (p-type delayed fluorescence) was somehow forgotten with time. However, with a newly rising interest in technologies based on organic materials it starts to be investigated with double efforts. The method is based on “annihilation" of triplet states of organic chromophors (called emitters) which are populated by energy transfer from molecules of another type (sensitizers). In comparison to previously mentioned UC methods the fundamental advantage of triplet-triplet annihilation photon upconversion (TTA – UC) is its *inherent* independence [13] on the coherence parameters of the excitation radiation. As a consequence, the requirements on the intensity of the excitation light are considerably reduced. Efficient TTA – UC can be obtained at an extremely low intensity of the irradiation light – in order of $mW \cdot cm^{-2}$. Due to the usage of organic molecules, having a broad spectra of absorption, the spectral power density of an excitation source can be also extremely low – in order of tens of $\mu W \cdot nm^{-1}$. Such requirements match to the parameters of low concentrated sunlight. Thus, in 2006 effective TTA – UC excited by the focused green part of sunlight was shown [13]. In 2008 the conversion of the broadband green-far-red part of the sun radiation into the blue region of spectra was reported [14]. It opened the way for potential applications of TTA – UC for the improvement of the performance of photovoltaic organic devices, such as organic solar cells [15, 16] and creation of photocatalytic hydrogen generators [17].

From the other side, already functioning prototypes of devices based on TTA – UC like flexible transparent displays [18, 19] and highly sensitive oxygen sensors [20] were recently shown.

The following objectives were pursued during this dissertation:

- Creation of an experimental setup for multiparametric characterization of the TTA – UC process
- Investigation of the main relations of TTA – UC process
- Creation and characterization of new efficient sensitizer-emitter UC pairs
- Investigation of new effects based on TTA – UC

2 Semi-classical description and basic principles of TTA – UC

2.1 Upconversion system and participating processes

The conventional TTA – UC system consists of two kinds of organic molecules dissolved in an organic solvent. The first type, called a sensitizer, absorbs the optical energy and stores it for further transformations. The second type, called emitter, is commonly represented by aromatic hydrocarbons, having very high fluorescence quantum yield (Q.Y.).

The energetic scheme of the TTA – UC process is shown in Figure 2.1. It has to be considered as an essentially connected chain of successive processes [21]: intersystem crossing (ISC), triplet-triplet transfer (TTT), triplet-triplet annihilation (TTA) and subsequent emitter fluorescence. After absorption of photon in the Q-band of the sensitizer ($S^1_{sensitizer}$) through the process of intersystem crossing (ISC) a metastable sensitizer triplet state ($T^1_{sensitizer}$) is formed:

$$S^0_{sensitizer} + h\nu_{exc} \longrightarrow S^1_{sensitizer} \xrightarrow{ISC} T^1_{sensitizer} \qquad (2.1)$$

where h is Planck's constant and ν_{exc} – frequency of excitation light.

It is known, that intramolecular transitions between states with different multiplicity is forbidden. However, the probability of the ISC process can be strongly enhanced by spin-orbit coupling with a heavy metal atom. Thus, in the presence of such atoms like palladium or platinum ISC efficiency can be close to unity [22]. Four channels for the sensitizer triplet state relaxation are possible: (i) emission of a phosphorescent photon; (ii) the quenching of the excited triplet state by molecular oxygen (if present); (iii) the triplet state relaxation in a non-radiative manner, dissipating the optical energy as heat and (iv) the transfer of the sensitizer triplet state energy to an emitter triplet state ($T^1_{emitter}$) by the process of triplet-triplet transfer (TTT):

$$T^1_{sensitizer} + S^0_{emitter} \xrightarrow{TTT} S^0_{sensitizer} + T^1_{emitter} \qquad (2.2)$$

Due to the negligible small ISC-coefficient, the populated through the scenario (iv) excited triplet state of the emitter molecule even at room temperature can store the energy for a long time without energy dissipation or phosphorescence photon emission. If the process (2.2) is

performed by another pair of sensitizer-emitter molecules, one more emitter molecule will be transferred into the excited triplet state.

There are three channels for further energy dissipation: the TTA process between two triplet excited emitter molecules, the relaxation in non-radiative manner or quenching of the emitter triplet state by a molecule of oxygen. In a non-precise description, during the TTA process one of the two triplet excited emitter molecules returns to the ground state, but the another molecule accumulate the total energy and populate the excited emitter singlet state.

$$T^1_{emitter} + T^1_{emitter} \xrightarrow{TTA} S^0_{emitter} + S^1_{emitter} \qquad (2.3)$$

Finally, because of high fluorescence ability, the emitter molecule radiates a fluorescent photon.

$$S^1_{emitter} \longrightarrow S^0_{emitter} + h\nu_{UC} \qquad (2.4)$$

where ν_{UC} – is the frequency of emitted UC fluorescence.

To sum up, a photon with an energy higher than the energy of excitation radiation ($h\nu_{UC} > h\nu_{exc}$) is finally emitted and the UC process occurred.

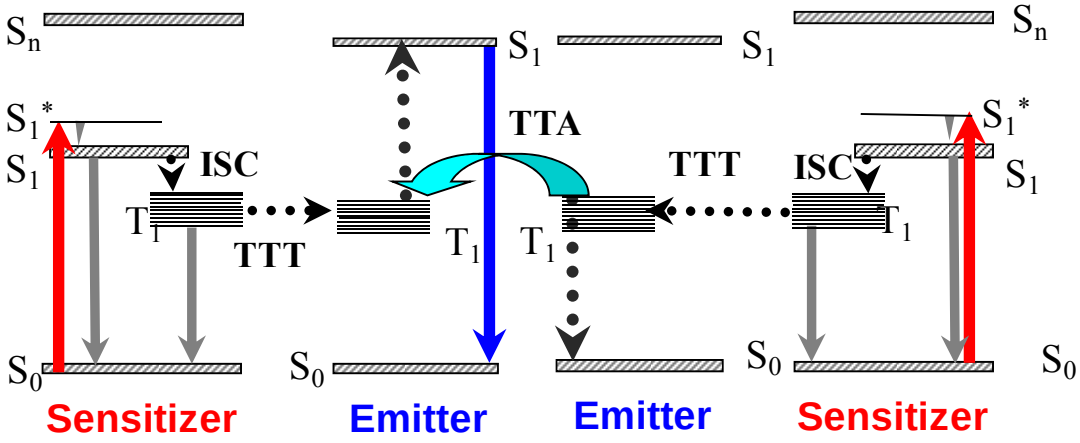

Figure 2.1 Energetic scheme of TTA – UC process. Red arrows mean excitation, blue arrow – emission of UC photon, gray solid arrows – other processes leading to energy dissipation, like phosphorescence, non-radiative decay or quenching by molecular oxygen.

2.2 Conditions for efficient TTA – UC observation

As mentioned earlier, the TTA – UC process is represented by an essentially connected chain of successive processes: ISC, TTT, TTA and subsequent emitter fluorescence. For that reason, for the observation of efficient UC fluorescence, the efficiency of each step in the chain should be maximized [14].

As it was mentioned above, the high triplet state population of the sensitizer via single photon absorption is required. Therefore, the sensitizer molecule must have a high ISC-coefficient. At the same time the radiative decay (phosphorescence) from the triplet state of the emitter molecule should be strongly prohibited, i.e. the ISC-coefficient for the emitter molecule must be small. These two requirements can be summarized in the following:

$$c^{ISC}_{sensitizer} >> c^{ISC}_{emitter} \tag{2.5}$$

The probability for triplet-triplet energy transfer from the sensitizer to the emitter is proportional to the overlap of their triplet states [23, 24]. Accordingly the energy of the levels should be similar:

$$E(T^1_{sensitizer}) \cong E(T^1_{emitter}) \tag{2.6}$$

It is obvious, that the TTA process is efficient only if the combined energy of two emitter triplet states is larger or of comparable size with the energy of the excited emitter singlet state:

$$2 \times E(T^1_{emitter}) \geq E(S^1_{emitter}) \tag{2.7}$$

The last relation creates additional requirements for the absorption spectra of the participating sensitizer and emitter molecules. Simultaneously in the UC – medium are existing sensitizer and emitter molecules, which could be both in triplet state and in ground states. All those states can absorb the generated UC photons, radiated by the emitter, either through the process of absorption by excited triplet states to higher lying triplet states, or by absorption by the sensitizer molecule from the ground state.

In order to reduce this so-called reabsorption, the emission of UC photons should take place in a region of the spectrum free from the sensitizer and emitter ground state absorption. For an emitter molecule with enough large Stokes shift, or at relatively low concentration of emitter this requirement is fulfilled automatically. However, for the sensitizer molecule (or other additional substances being used) the special attention should be given to match this requirement. Namely reabsorption is mainly responsible for the low efficiency of TTA − UC based systems, where sensitizers with consolidated and continuous absorption spectrum, such as $Ir(ppy)_3$, are used [25]. In these systems, the singlet absorption band of the sensitizer

overlaps completely with the fluorescence spectrum of the emitter, causing the strong reabsorption of the generated UC light.

At the same time, sensitizers which belong to the family of metallated macrocycles, such as porphyrins and phthalocyanines, are reported to have high efficiency in TTA – UC. They have a band-like absorption spectrum, consisting of two strong bands – the Soret (corresponds to absorption $S^0 \rightarrow S^2$) and the Q-band ($S^0 \rightarrow S^1$). For the wavelengths lower than the Q-band and significantly higher than the Soret-band no optical absorption is observed. Those wavelengths represent the so-called transparency window of the metallated macrocycles (shown in Figure 2.2). In an optimized TTA – UC system, the UC emission should take place into the transparency window.

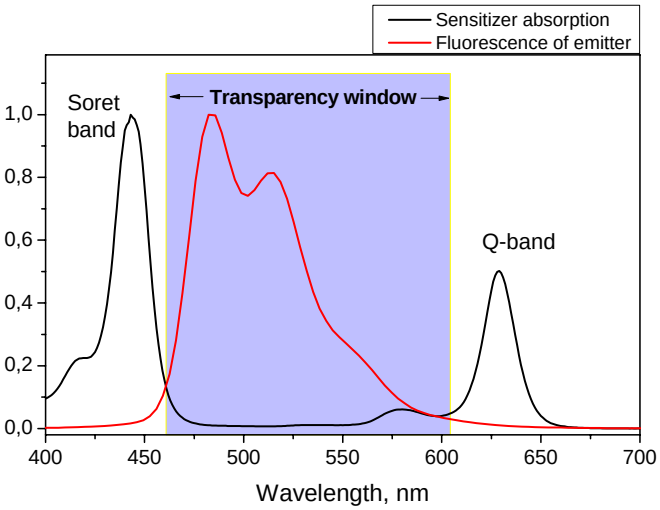

Figure 2.2 Illustration to requirement of correspondence of sensitizer absorption and emitter fluorescence for the case of usage of metallated macrocycles as sensitizers.

In energetic terms, the meaning of the transparency window can be presented as:

$$E(S^0_{sensitizer} \rightarrow S^2_{sensitizer}) > E(S^1_{emitter} \rightarrow S^0_{emitter}) >> E(S^0_{sensitizer} \rightarrow S^1_{sensitizer}) \quad (2.8)$$

If all other requirements for TTA – UC, except the last one, are fulfilled, the TTA – UC process will have a low external efficiency.

The main outcome of these experimentally established requirements to the multi – component organic UC system is: if the equations (2.5), (2.6), (2.7) and (2.8) are fulfilled, very efficient TTA – UC will be observed. Having these selection criteria, the search for new and effective sensitizer-emitter pairs, working in different regions of visible (VIS) and infra-red (NIR) spectrum, can be considerably accelerated.

2.3 Theoretical maximum of TTA – UC efficiency

The theoretical maximum of efficiency of the UC process is consisted from a particular efficiency of each involved process. Thus, the Q.Y. of the process of ISC is approaching unity [22] for metallated macrocycles with heavy atoms such as Pt, Pd. The efficiency of the TTT process is dependent many factors like mutual arrangement of the triplet states of sensitizer and emitter, the lifetime of the triplet state of sensitizer and the viscosity of the solvent [23, 26], but its highest value is not limited by any physical reason and can be close to unity as well.

The quantum yield of an emitter fluorescence also can be close to 100% for many of the aromatic hydrocarbons [27-29].

After all, one of the processes limiting the production of UC photons is the TTA. Two molecules (*M*) excited in the triplet state can form a virtual complex having singlet, triplet or quintet spin state with a statistical ratio 1:3:5, respectively [30]:

$$M_3^* + M_3^* \rightarrow \left\{ \begin{array}{l} 1/9 : [MM]_1^* \\ 3/9 : [MM]_3^* \\ 5/9 : [MM]_5^* \end{array} \right\} \qquad (2.9)$$

where *M* is the molecule,

[*MM*] is the molecular complex,

the presence of an asterisk (*) in superscript means excited state, the absence of it – ground state, subscript represents a corresponding multiplicity of the spin state.

Being formed, the singlet complex dissociate into two separate molecules, one of which will be in the highly excited singlet state having all the energy from the both original triplet states and the other in the singlet ground state. The excited molecule will undergo a fast internal relaxation giving up an excess of energy and finally will appear to be in the S_1 stage.

$$[MM]_1^* \xrightarrow{\text{complex dissociation}} M_1^{**} + M_1 \xrightarrow{\text{internal relaxation}} M_1^* + M_1 \qquad (2.10)$$

From this level with a high probability the energy will be emitted as a photon. Following the classical representation, only 1/9 of the complete triplet ensemble is “useful” and can create an excited single state of emitter, resulting in photon emission. All other formed complexes are estimated to be quenched to the ground state without creating of singlet excited state. As a result, it gives only 5.5% for the maximal possible external Q.Y. This value was for long time kept as the highest one. Often the published efficiencies of the TTA –

UC in different compounds overcome this value, so it was obvious that this assumption should be revised.

In 2009 the following full scheme of complex formation and dissociation was proposed [31]:

$$M_3^* + M_3^* \rightarrow \begin{cases} 1/9: [MM]_1^* \xrightarrow{\text{complex dissociation}} M_1^{**} + M_1 \xrightarrow{\text{internal relaxation}} M_1^* + M_1 \\ 3/9: [MM]_3^* \xrightarrow{\text{complex dissociation}} M_3^{**} + M_1 \xrightarrow{\text{internal relaxation}} M_3^* + M_1 \\ 5/9: [MM]_5^* \xrightarrow{\text{complex dissociation}} M_3^* + M_3^* \xrightarrow{\text{internal relaxation}} M_3^* + M_3^* \end{cases} \quad (2.11)$$

Actually, the scheme was presented already in 2000 by Bachilo and Weisman [30], but was not applied to TTA – UC process up to aforementioned paper.

In this scheme the formed triplet complexes are not fully quenched but dissociate in two molecules back to one being excited in a higher triplet state (for example T_2 or higher) and another into the ground state. The higher triplet state undergoes a fast spin-allowed radiationless transition to a lower triplet state, thereby returning one excited molecule in the triplet state back into the process.

The quintet complexes in their turn will just dissociate, returning two triplet excited molecules back into a “reaction bath”, because the energy of a possible quintet state is too high and usually is not accessible [32]. The discussion devoted to dissociation of quintets to original species rather than the previously supposed full quenching to the ground state is presented in the “Implications” part of [31]. In this way, the quintet complexes are not taken into account, because their formation does not lead to a change in the population of triplet states.

Under the revised scenario for each 4 formed double-complexes (one singlet and three triplet complexes) five emitter molecules in the triplet state are quenched to form one UC photon. It gives 40% of valuable use of the emitter triplet states. Given in other words, the maximum obtainable external Q.Y. of UC is equal to 20%.

Last investigations in this field are dedicated to theoretical overcoming of even this limit by suggestion of impact of strength of spin-orbital coupling [33] and reverse intersystem crossing [31].

2.4 Photon energy conversion

Up to now the discussion was dedicated to the efficiency of the TTA – UC process. But what is with a photon energy transformation? How much energy in comparison with the energy of excitation photon can carry the converted photon?

It is important to note, that all energy levels of molecules, involved in the process of TTA – UC, are real molecular levels; and no virtual energetic levels are involved in UC photon creation. Therefore, the processes of internal energy relaxation (i.e. thermalization of the electronic states of the molecules involved) and, consequently, their influence on the energetic schema of the process of TTA – UC cannot be neglected. The main losses of energy are caused by the following processes:

- the vibrational relaxation of the excited singlet state
- an energy difference between the sensitizer singlet and triplet states and the following vibrational relaxation of the excited triplet state (losses during ISC-process):

$$E(S^1_{sensitizer}) - E(T^1_{sensitizer}) > 0$$

- an energy mismatch between the triplet states of sensitizer and emitter and corresponding losses during the TTT process:

$$E(T^1_{sensitizer}) - E(T^1_{emitter}) \neq 0$$

- an excess of doubled emitter triplet energy regarding to the single state in the emitter molecule during the TTA process:

$$2 \times E(T^1_{emitter}) - E(S^1_{emitter}) \geq 0$$

As a result, the processes of internal energy conversion lead to a noticeable loss of excitation photon energy, and the UC emission *a priori* has a frequency lower than the doubled frequency of the excitation light [21]

All these losses can be minimized by optimization of the energy structures of used sensitizer and emitter molecules. Unfortunately, the conventional amount of the total losses during efficient TTA – UC are close to 1 eV. Up to now the highest energy gap between absorbed and emitted photons was demonstrated to be 0.8 eV [34] (conversion from 615 nm to 450 nm) with the energy losses of around 1.15 eV, and further in the far-red region of spectra with a similar gap of 0.77 eV [35] (conversion from 706 nm to 490 nm), but with a much less amount of the lost energy (0.92 eV).

2.5 Oxygen and its influence on TTA – UC process

To understand the critical role of oxygen in the processes of UC one should take a look at the electronic configuration of oxygen [36]. Atomic oxygen has eight electrons. Using electronic orbitals and filling them, one can find three possible configurations of the external shell of an atom (shown in Figure 2.3). According to the Hund's rule the lowest possible energy and the corresponding higher stability will have a configuration having a maximal multiplicity of a resulting electronic state. For the atomic oxygen the resulting stable state ^3P will have two unpaired electrons with the total multiplicity of 3 and meaning that the ground state is triplet.

The same reasoning, being applied to molecular oxygen (electronic configuration is shown in Figure 2.4), will give a result that again two unpaired electrons are in the $2\pi^*$ orbital. These electrons, like for atomic oxygen, can be found in 3 different arrangements $^3\Sigma^+_g$, $^1\Delta_g$ and $^1\Sigma^-_g$. The ground state has the highest multiplicity and corresponds to $^3\Sigma^+_g$ configuration. In other words, the ground state of molecular oxygen is a triplet as well.

Like it was noted above, almost all the processes participating in TTA – UC are closely associated with triplet states of the molecules. These processes take place during tens or even hundreds of microseconds, that is extremely long period of time from the point of view of molecular movements. This time is more than enough for the molecule of sensitizer or emitter being in excited triplet state to meet the molecule of oxygen. Interaction with it will result in the corresponding loss of the carried energy and excitation of molecular oxygen into the singlet state $^1\Delta_g$.

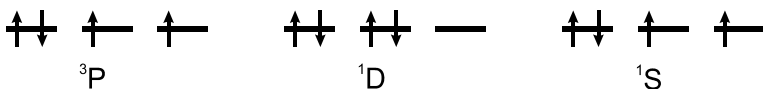

Figure 2.3 Electronic configuration of partially filled 2p orbitals of atomic oxygen.

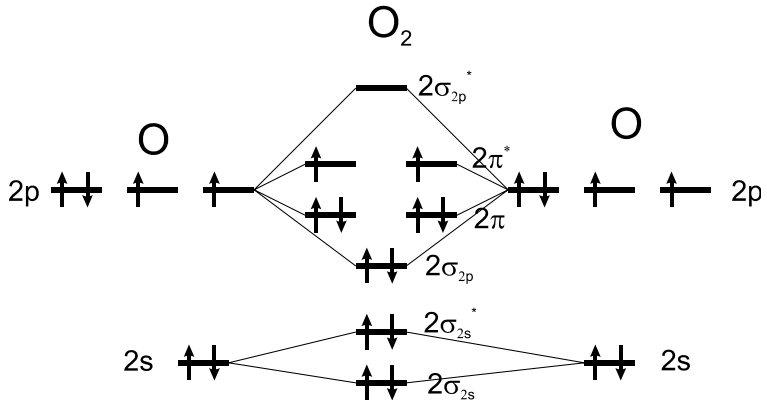

Figure 2.4 Molecular oxygen (O_2) orbital diagram.

The process of triplet energy transfer from a sensitizer is widely used for oxygen sensing [20, 37-39] and generation of singlet oxygen [40, 41], but in TTA – UC process it leads to critical loses in efficiency of UC generation. The molecular oxygen with a concentration even in the range of ppm crucially influences the efficiency and aging properties of UC samples.

For deoxygenation of investigated samples several techniques can be used:

- The first possibility is to use a glovebox with an inert atmosphere like nitrogen or argon. Argon is preferable because of its higher mass density and therefore faster substitution of oxygen dissolved in solutions.
- The second possibility is to purge the investigated solution by a neutral gas for some time. Because of higher partial pressure of the incoming neutral gas, oxygen will be removed. However, as a drawback of this method one can note the simultaneous evaporation of the solvent with consequent undefined change of the total concentrations of dissolved dyes.
- The third frequently used method is the so called freeze-pump-thaw process. The solution is frozen using liquid nitrogen, and thereafter, is warmed up to melt, allowing trapped bubbles of gas to escape under a controlled low pressure. This method is also concerned with solvent evaporation and requires liquid nitrogen. It should be noted that the application of such a procedure to some substances can result in unwanted phase separation.
- The fourth method is based on using so called oxygen scavengers, which chemically react with oxygen and trap it. Evident drawbacks are possible unwanted reactions between the scavenger and the investigated materials and an influence of additional compound on the investigated system over all. Another drawback is the necessity of having several scavengers for different solvents to be used in investigations.

From the practical point of view, all devices using the TTA – UC principle should have a long-term stability. Therefore, their development is closely connected with an evolution of oxygen scavengers, oxygen protectors and the search for oxygen stable UC dyes.

3 Experimental setup and methods

3.1 Evolution of experimental setup

The experimental investigation of a recently discovered process is often associated with measurements of different parameters. Therefore, the design of an experimental setup should be always done considering further possible modifications, improvements or upgrades. It will provide a way for measurements of characteristics of the investigated process, previously not taken into account.

As a base for the new setup for the UC measurements the scheme from our partners in Sony Deutschland GmbH (see Figure 3.1) was taken. For the excitation it was proposed to use two diode lasers with the wavelength 635 nm for UC excitation of sensitizers (mainly TBP sensitizers) and 405 nm for the direct excitation of the fluorescence of emitters. The radiation of the diode laser should be collimated by short-focus aspheric lenses mounted on the translation stages to improve the accuracy of collimation. The use of removable reflecting mirrors should give the opportunity to choose the radiation needed for the experiment. The stability of mirror positioning is provided by magnetic kinematic bases, having a high precision with a repeatability of positioning claimed by manufacturer of 1 μrad. An additional defocusing lens with a focal distance of around 1 meter should be used to increase the diameter of excitation spot on the sample. A round continuously variable metallic neutral density filter (NDC-50C-2M-A, OD = 0÷2, Thorlabs Inc.) and the additional set of neutral filters were used for measurements of emitted spectra in dependence on the excitation intensity. In order to minimize the influence of distortions rising from the setup geometry and sample cuvette position, the co-alignment of the optical axes of the excitation beam and the collection angle of the luminescence emission of the sample was done. For this purposes the excitation beam was reflected by an edge of a small rectangular mirror to a notch filter, which possesses the high reflectance on the small band of wavelengths close to the excitation and is transparent for all other wavelengths. By using of a system of dielectric mirrors (E02, 50 mm diameter, Thorlabs Inc) the excitation beam was directed to the sample and focused by an achromatic lens (diameter 50mm, focal distance 100 mm, numerical aperture NA=0.24).

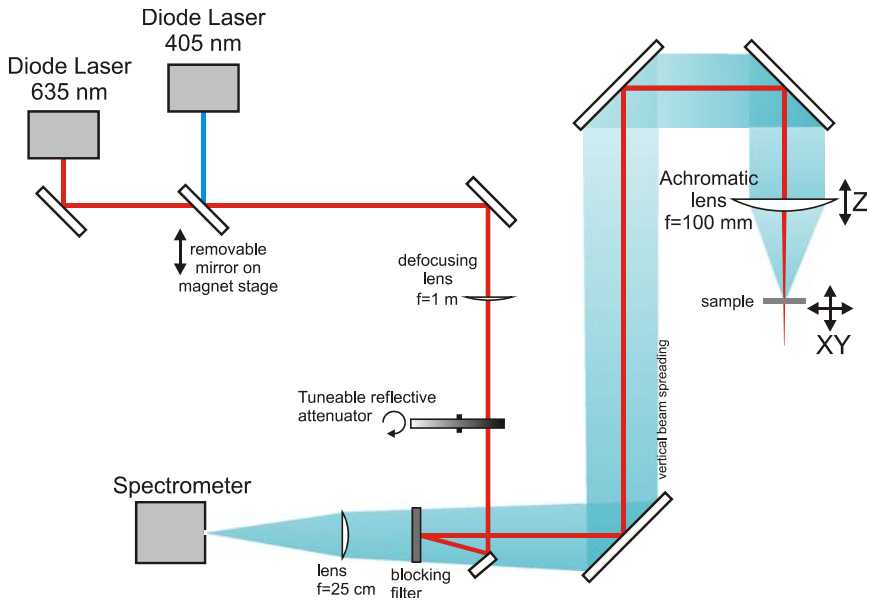

Figure 3.1 Initial design of the experimental setup.

The same lens collects the emission, irradiated by the sample, and directs it backwards to a spectrometer. Notch filters (Semrock Inc), designed for the specific laser wavelength, separate the useful signal from the scattered or reflected excitation laser light. These filters have a very high transmission (~97 %) in the transparency window almost without spectral distortion, high suppression characteristics (OD ~ 6) in the blocked region and very sharp transition fronts (down to 1 nm). The obtained luminescence signal is focused onto an entrance slit of the spectrometer to be detected and analyzed.

This scheme was used by our partners for a long time, but it has a couple of evident drawbacks. There are a limited number of excitation sources (restricted from the wavelengths of commercially available diode lasers). Their use is additionally limited by the existence of suitable commercially available notch filters with a high surface planarity, while up to now filters are developed mainly for commonly used laser sources.

In order to resolve the excitation wavelength limitation, the initial design of the setup was changed. The new experimental scheme is shown in Figure 3.2. A supercontinuum (SC) laser (SC450-2-PP, Fianium Ltd.) was introduced as an excitation source. The laser is operating in quasi – continuous wave mode, with a repetition rate of 20 MHz and a pulse duration of 5 ps. The SC radiation has a spectrum in a region of wavelengths 415 - 2000 nm with mean spectral power density of 1 $mW \cdot nm^{-1}$. In order to reject in the experiments not useful IR- part of the laser emission an ultrabroadband mirror (Semrock Inc.) with a reflection coefficient >98% in the range 300 - 1100 nm and transparent in IR region of spectrum was used.

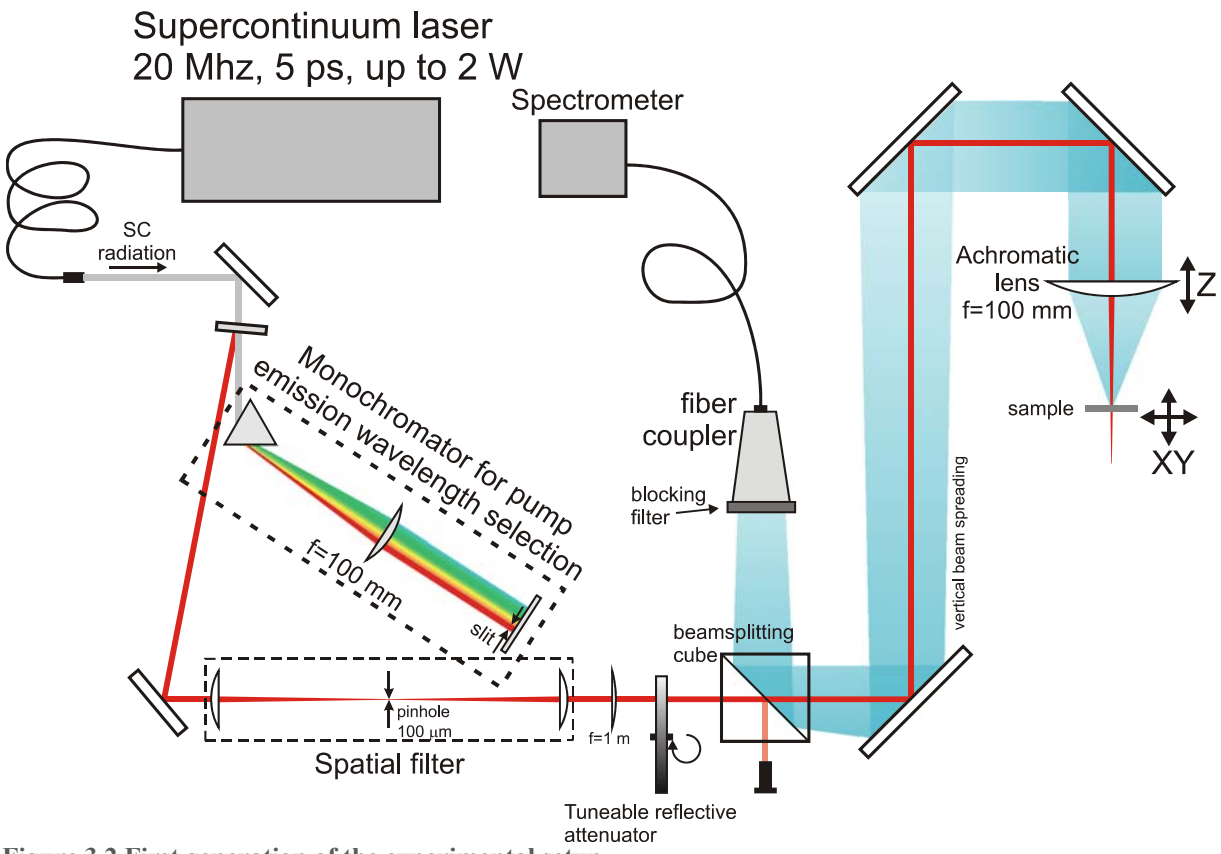

Figure 3.2 First generation of the experimental setup.

A selection of the needed spectral band had to be performed with a negligible shift of the beam position, i.e. without a perceivable change of the optical axis of the set-up. For this purposes a 4-f monochromator (see Figure 3.3) based on a highly dispersive Brewster prism (SF59, Schott AG, Mainz, Germany) was built. In this scheme a beam having a broad spectrum was first dispersed on a glass prism (horizontal plane). The entrance point of the beam on the prism is placed in the focal plane of a lens, so that after passing the lens the beam is collimated in the horizontal plane, but focused in the vertical one. To avoid focusing one can use a cylindrical lens instead. The beam, being spread in a space according to the wavelength, falls on a vertically situated slit, which is placed on a translation stage driven by micrometric actuator. The mechanical slit should be placed as close as possible to the broadband high-refractive mirror placed in the focal plane of the used lens.

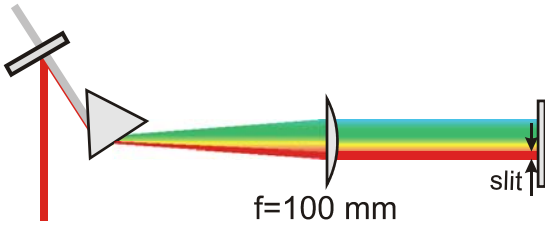

Figure 3.3 Scheme of the 4-f monochromator.

The radiation passed through the slit is reflected back and focused by the lens onto the prism, where it collapses back because all the parts of the beam move back on the same way (retro-reflecting scheme). To extract the resulting beam from the plane of the initial one, its position is changed in the vertical plane by the upper mentioned reflecting mirror. At all, having a perfect monochromator alignment and the widely opened slit one should obtain the beam with the same diameter and spectrum as the one incident to the monochromator. Therefore, by the translation of the slit and tuning of its width via the micro-actuator, one can determine a desired spectral band with a desired central wavelength and a desired spectral bandwidth with the resolution of 1/10 nanometer, without any displacement of the resulting beams.

After this scheme was correctly realized, an unexpected disadvantage was observed. A bright extremely broadband halo spreading in the same direction as the beam appears. This is a consequence of the scattering of the powerful SC (white) light pulse on the prism. For suppressing this halo a spatial filter consisting of two identical focusing lenses with a focal distance of 10 cm and one pinhole (diameter of 100 μm) placed in the beam waist was built.

It is obvious that the use of a blocking filter as a mirror was not possible in the modified scheme. Instead, it was decided to use a non-polarizing cube beamsplitter with a splitting ratio 50:50 and an aperture of 50x50 mm. A huge disadvantage of the cube beam splitter is the loss of a half of the excitation power and the detected signal, but from other point of view, the benefit of independence in the choice of an excitation spectrum overcomes it.

The radiation emitted by the sample is detected by a high-sensitive CCD spectrometer (C10083CA, Hamamatsu Inc.), which has a fiber input. A double-lens collimator was used for the collection of light and focusing into the multimode fiber. For the careful tuning of light coupling the collector was placed in 4D-translation mount, having the possibility to move in the horizontal and vertical planes and to be tilted in both planes as well.

A blocking filter (usually notch-filter) should be also applied in this version of the setup, but with much higher flexibility. Being placed on a rotational mount, by tilting of the filter up to to 45º one can tune a blocking range up to $0.9 \cdot \lambda_{designed}$. Although filters can be attached and detached without any additional tuning of the setup (the fiber coupler tuning will be necessary at the tilted filter usage because of the displacement of the beam).

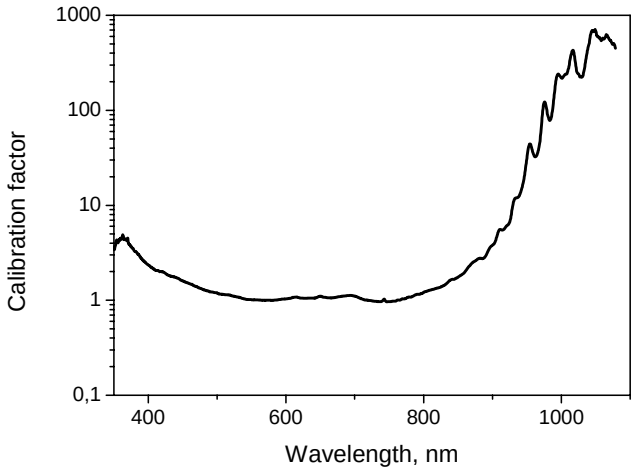

Figure 3.4 Calculated correction function F_{corr} for the first generation of the experimental setup.

After assembling and tuning, the experimental setup was calibrated according to a procedure described in part 3.2. The corresponding calibration curve is shown in Figure 3.4. It is seen, that in the blue region of the spectrum (up to 500 nm) the signal should by corrected by several times whereas in the infra-red region of spectrum by tens or even hundreds of times, that results in big scaling-mistakes. Based on this calibration figure a next step in the improvement of the setup was chosen.

In a second generation of the experimental setup the reflective mirrors which directed the excitation to the sample and the irradiation collected from a sample to the spectrometer were changed by ultrabroadband mirrors (2 inch size, MM2-311-25, Semrock Inc.). For the adjustment of the excitation beam spot on the sample, the de-collimation lens was removed, but the collimation lens of the spatial filter was placed on the two combined linear translation stages. This makes it possible to vary the beam spot diameter in the range from 35 μm up to 420 μm (see Figure 3.5). The setup was calibrated again, thus the corresponding correction function is shown in Figure 3.6. One can note the highly improved transmission of a detected signal in the regions of the spectrum that should by strongly corrected before. Thus, in the range 400 – 800 nm almost no correction is needed. The detection in the region of the spectrum near to $\lambda \sim 1$ μm was also enhanced that made it possible to measure the phosphorescence spectra of naphthoporphyrins (see part 0).

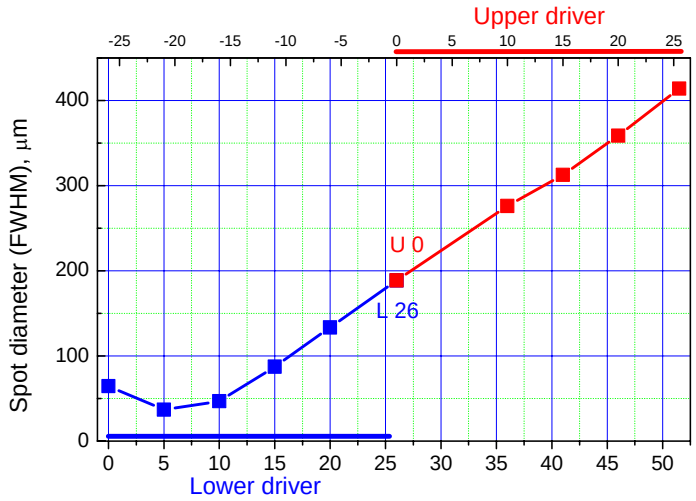

Figure 3.5 Beam spot diameter on a sample in dependence on the rear spatial filter lens position.

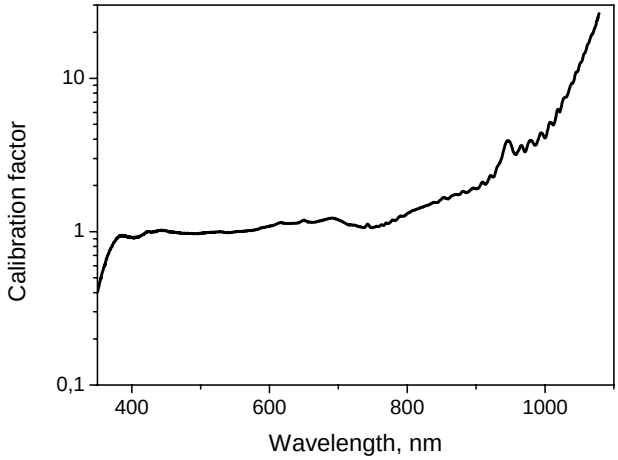

Figure 3.6 Correction function F_{corr} for the second generation of the experimental setup.

Up to this point, only the steady state characteristic spectra in dependence on the excitation power could be measured. However, for an investigation of the dynamical properties of the TTA – UC process for different sensitizer-emitter pairs and an influence of the media's viscosity on the efficiency of the TTT and TTA processes one should measure temporal characteristics as well. For these purposes the setup was one more time modernized.

The carried out changes are shown on a principal scheme (see Figure 3.7). With a help of reflective mirror, which was placed on the magnet kinematical stage, the emission of the continuous-wave diode laser (QL63H5S-A, 635 nm, 20 mW, mounted in a laser diode mount TCLDM9 from Thorlabs Inc.) was tuned to spread on the same path as the main beam from the super-continuum laser. The emission was modulated by the application of an external voltage from a pulse generator (TTi TGA1244, 40MHz Arbitrary waveform generator) to a laser current driver (LDC8001, Thorlabs Inc.). An additional removable mirror was placed

before the spectrometer to direct the collected sample emission to a time-resolving registration part. The scattered and reflected excitation radiation was blocked by the same notch filter (NF03-633E-25, Semrock Inc.) used for the measurements of the spectra. The radiation, which passed through the filter, was separated by short-pass filter (FF01-694/SP-25, Semrock Inc.), tilted at the angle of 45º, on two parts. The turned part of the radiation, with the wavelength higher than 625 nm (694 nm multiplied by coefficient·0.9 from tilting of the filter to 4º), passed through the additional long-pass filter (FF01-692/LP-25, Semrock Inc.). The transmitted part of the radiation with the wavelength shorter than 625 nm was additionally cleaned by a short-pass filter (SP01-633RU-25, Semrock Inc.) and a band-pass filter (BP530/200), which were tilted at ~15 degrees in order to shift their cutting-edge wavelengths. The emission in both cases was detected by photo-multiplier-tubes (type R374, Hamamatsu Inc.) connected to a digital oscilloscope (Agilent 54622A Oscilloscope 100MHz). All obtained oscillograms were averaged over 32 - 128 pulses.

To obtain the characteristics of the TTA – UC process in dependence on sample temperature the regular sample holder was changed by a thermo stabilized stage from LINKAM Inc, originally designed to be used in a microscope. The stage can be controlled by a driver within the range from -190°C up to 120°C with the accuracy of 0.1°C. For the exact temperature control a cooling system providing cold water or a vapor of a liquid nitrogen should be assembled.

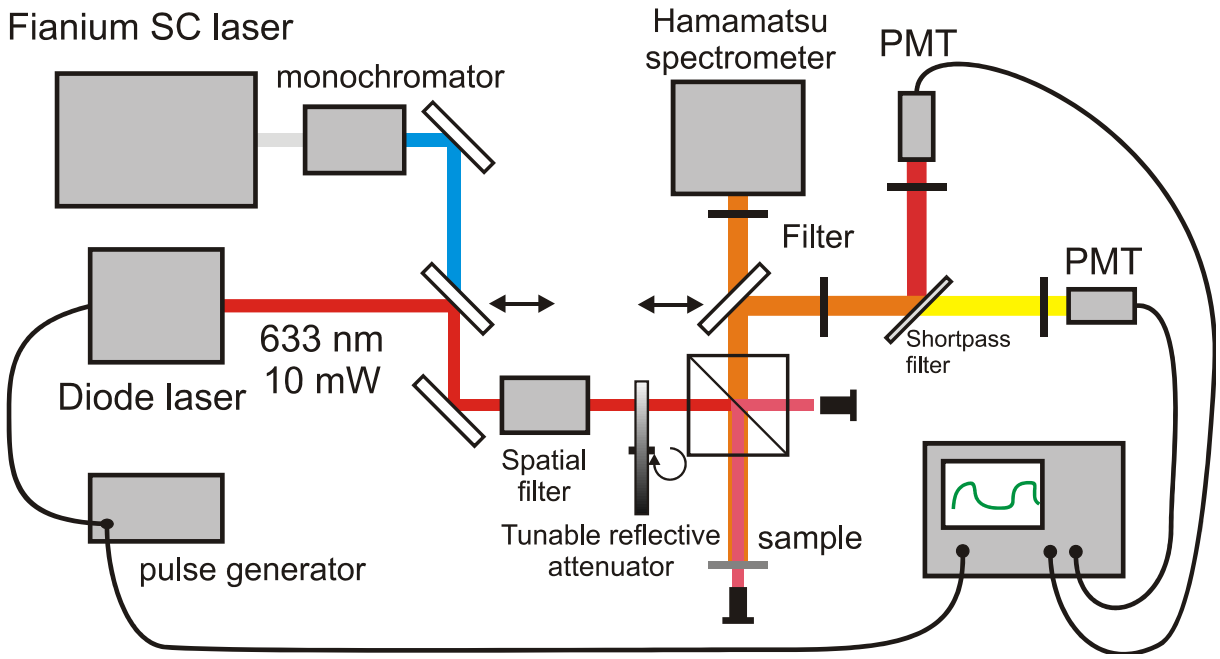

Figure 3.7 Principal scheme of the third generation of the experimental setup.

3.2 Calibration of the experimental setup

For the correct Q.Y. determination one should use spectra which are not distorted by a device response. Therefore the experimentally measured data should be spectrally corrected by a response-transmission function of the device. For the calibration of our experimental setup a tungsten halogen calibrated light source (AvaLight-HAL-CAL, Avantes Inc.) was used. The exit pupil of the light source was placed on the position of the sample in the experimental setup and the spectrum was measured by the CCD spectrometer. This method gives one correction function, which takes into account both the transmission of the setup itself and the spectral sensitivity of the spectrometer sensor. The correction function value in dependence on a wavelength was obtained according to a following formula:

$$F^*_{corr}(\lambda) = \frac{S_{cal}(\lambda)}{S_{measured}(\lambda)} \qquad (3.1)$$

where λ - wavelength corresponding to a given pixel on the CCD matrix,

F^*_{corr} - correction function value for the given wavelength,

S_{cal} - calibration source intensity on the given wavelength,

$S_{measured}$ - measured value for the given wavelength.

For a further usage the correction function F^*_{corr} was normalized to be unity in a region of a minimal distortion (λ ~ 500-550 nm) with the resulting function F_{corr}. By this method no absolute magnitude of the sample's luminosity can be observed. Actually, the measurement of absolute values is quite complicate and is not limited by the determination of correction function. Fortunately, one can use the comparative method (described in part 3.4) for the determination of an absolute Q.Y, where only the correction of the spectral shape of the detected spectra by the function F_{corr} is needed.

3.3 Absorption measurements

The absorbance in ultraviolet and visible spectra was measured by the help of a calibrated Perkin Elmer Lambda 25 UV/VIS Spectrometer. The absorption spectra of prepared solutions were measured in commercially available quartz cuvettes (Hellma Analytics Inc.) having a thickness of 1 or 10 mm. The same cuvettes with the pure solvents were used as blank samples for a baseline correction. For the accurate Q.Y. determination the absorptions were measured directly in the samples sealed in vitrotubes (see part 3.7). Such procedure allows

avoiding mistakes in recalculation of an optical density with respect to the real thickness of the vitrotube. To limit the light beam being used in the spectrometer and correlate it with a size of the vitrotubes a black mask with a slit of 2 mm width was placed before the sample. Due to a non-ideal planarity of the vitrotube surface their use for the solvent transparency correction was not helpful. Since in the experiments relatively high concentrations of dyes were used, the variation in the transparency of the solvents was assumed to be negligible and obtained spectra were manually corrected for a background by subtraction of a linear function.

3.4 Quantum yield determination

The emissive processes, such as fluorescence and phosphorescence, characterize the energy levels and the processes taking place in different substances. One of the main characteristics, having often the crucial role in a characterization of dyes, is the quantum yield (Q.Y.) of the emission.

There are two different ways to obtain the Q.Y. value: relative to a standard with the known Q.Y. value or as an absolute measurement (needs complicated setup). The most recent review on the methods of Q.Y. measurements was published in 2008 by Rurack [27]. The classical work of Demas and Crosby [42] describes the main methods, problems and contributions for the accurate Q.Y. measurements.

Starting from a classical determination – the Q.Y. is the fraction of molecules, which can be found in the state under the interest from a total number of the initially excited molecules. For example, the Q.Y. of the ISC is the ratio of the created triplet states to the overall number of the initially excited molecules. From the other side, mainly under the quantum efficiency one mean the Q.Y. of luminescence – the fraction of the total number of the emitted photons to the total number of the absorbed photons:

$$Q = \frac{N_{emm}}{N_{abs}} \qquad (3.2)$$

where Q is the quantum yield of luminescence,

N_{emm} – the number of the emitted photons,

N_{abs} – the number of the absorbed photons.

The number of the absorbed photons is usually calculated through a macroscopic absorbance of a material at the wavelength of the excitation and the energy of the excitation radiation:

$$N_{abs} = \frac{\left(1-10^{-A\cdot L}\right)}{h\nu} E \qquad (3.3)$$

where A is the absorbance of the sample at the excitation wavelength,

L – the thickness of the sample,

E – an energy of the excitation radiation,

ν – a frequency of the excitation radiation,

h – the Planck's constant.

To count the number of the emitted photons one should have a corresponding collecting scheme with a detector. All the factors like the sensitivity of a detector, a figure of merit of a photon's collector, an overall ability of the setup to transmit the radiation from the sample to the detector and many other parameters can be combined in a total scaling coefficient for the number of detected photons:

$$N_{emm} = N_{\det} \cdot k \qquad (3.4)$$

where N_{det} is the number of the detected photons,

k – a response coefficient of the experimental setup.

The most commonly used method to determine the absolute Q.Y. of a dye is the comparison of its emission with the emission of a compound, the Q.Y. of which is already known. The main idea is to measure the standard and the investigated sample in the same conditions. It reduces the difference in the detection parameters and the unknown factors k for both samples becomes equal and could be neglected during the comparison. The optimized equation for the Q.Y. for this method can be written as follow:

$$Q_x = Q_{st} \frac{N_x}{N_{st}} \frac{\left(1-10^{-A_{st}\cdot L_{st}}\right)}{\left(1-10^{-A_x\cdot L_x}\right)} \frac{\nu_x}{\nu_{st}} \frac{E_{st}}{E_x} \qquad (3.5)$$

where Q_{st}, Q_x is the absolute Q.Y. of the standard and the investigated sample, respectively,

N_{st}, N_x – the total number of the detected emitted photons for the standard and the investigated sample, respectively,

A_{st}, A_x – the absorbancies of the standard and the investigated samples at the wavelengths of the excitation, respectively,

L_{st}, L_x – the length of the standard and the investigated sample, respectively,

ν_{st}, ν_x – the frequency of the excitation radiation for the measurements with the standard and the investigated sample, respectively,

E_{st}, E_x – the energy of the excitation for the measurements with the standard and the investigated sample, respectively.

The number of photons can be calculated in two ways: using a broadband sensitive photon counter, or by integration of area under spectra of luminescence, which is corrected according to the conditions of measurement (accumulation time, transmission of used filters et al.). It is necessary to note that for the correct calculations the spectra should be presented in terms of photon flux (not in terms of energy flux) depending on the radiation frequency (not wavelength dependent). Mathematically it can be described as following:

$$N_{x,st} = \int S_{x,st}(\nu) d\nu \qquad (3.6)$$

where $S_{x,st}(\nu)$ is the corrected spectrum of luminescence for the investigated sample (x) or the standard (st) in dependence on a frequency of radiation.

To make the formula for the Q.Y. determination suitable for the different cases, one can describe the fraction of incident light being absorbed (B) in three ways [42]:

1. In general case, for solutions, excited by a monochromatic light, especially when the absorbancies of the standard and the sample strongly differ (optically dense solutions):

$$B = 1 - 10^{-AL} \qquad (3.7)$$

2. For optically diluted solutions excited by the monochromatic light the exponential of equation (3.7) can be expanded in a power series of (AL) with a further truncation of the result:

$$B = 2.303\, AL \qquad (3.8)$$

3. For the case of non-monochromatic radiation the form of absorption spectrum $A(\nu)$ and the spectral distribution of the excitation light $I(\nu)$ would also be taken into account:

$$B = \frac{\int I(\nu)(1 - 10^{-A(\nu)L}) d\nu}{\int I(\nu) d\nu} \qquad (3.9)$$

For the conventional schemes without an integration sphere, when the light is collected from one side of the sample in a limited solid angle, the number of collected photons will depend on the refractive index of the solvent being used. In the case of usage of different

solvents for the sample and the standard an additional correction should be done in the response to the change of the refraction index of the solvents [42].

$$\frac{I_x}{I_{st}} \sim \frac{n_x^2}{n_{st}^2} \tag{3.10}$$

where n_x, n_{st} – the refraction indices of the solvents used for the sample and the standard on the wavelengths of sample emission.

Summing up all above, the resulting formula for the Q.Y. determination will look as following:

$$Q_x = Q_{st} \frac{N_x}{N_{st}} \frac{B_{st}}{B_x} \frac{\nu_x}{\nu_{st}} \frac{E_{st}}{E_x} \frac{n_x^2}{n_{st}^2} \tag{3.11}$$

There are some main contributions and recommendations complying of which will increase the accuracy of the measurements. The standard should have the spectrum of emission in nearly the same region where the investigated matter emits. It will reduce the mistakes rising from the spectral sensitivity of the detector. Both samples should be optically diluted in order to avoid the aggregation, the concentration quenching and reabsorption. An excitation light has to be monochromatic and the samples should be measured in the same conditions (most accurately – in the same optical cuvettes).

For more than fifty years of the luminescence investigation it appears many dyes claimed to be standards for comparative method [43-46]. Unfortunately, only a few of them are fully characterized and are reliable to be standards. The situation becomes even more difficult because often values of Q.Y. are taken from a literature without taking into account the conditions of their measurement. Sometimes even the values for two different cases from the same article are mixed (for example values for the air-saturated and the deoxygenized solutions). As well there are many cases when the contributions for the proper Q.Y. measurements are just ignored and the results are not corrected for the cases of using substances at the different temperatures, while pumping by a broadband radiation, using optically dense solutions or not deoxygenized solutions.

From our point of view, only some dyes from the Rhodamine family [29, 47] can serve now as a standard. For example, the Rhodamine 6G is multilaterally characterized. Its emitting ability is almost not changed in a huge concentration range [28, 48], in different solvents [49] and in a presence of the oxygen. As well Rhodamine-123 have a high Q.Y.

value of 0.9 [29, 50] and was characterized being dissolved in solvents with a different polarity [51].

3.5 Determination of quantum yield of TTA – UC

The value of an external Q.Y. has a decisive role for practical applications. Therefore the method of its determination should be free from any possible uncertainties and the obtained in accordance to it results should allow to recalculate an experimentally observed photon flux. On the other hand the definition of Q.Y. must allow a clear comparison of the Q.Y. values of other similar processes (other methods of the UC, for example). The classical definition [52] is applicable only to a single molecule system. As mentioned earlier, the studied TTA – UC process incorporates a chain of closely connected processes (ISC, TTT, TTA and consequent emitter fluorescence), all of which can be characterized by the particular efficiency (Q_{ISC}, Q_{TTT}, Q_{TTA} and η_{F}, respectively). The resulting external Q.Y. can be represented as a multiplication of the efficiencies of all participating processes (see part 2.1):

$$Q_{ext} = Q_{ISC} \cdot Q_{TTT} \cdot Q_{TTA} \cdot \eta_F \qquad (3.12)$$

where Q_{ext} is the external Q.Y.,

Q_{ISC} – the efficiency of the ISC process for a sensitizer,

Q_{TTT} – the efficiency of the TTT process,

Q_{TTA} – the efficiency of the TTA process,

η_{F} – the Q.Y. of the emitter's fluorescence.

The measurement of the absolute Q.Y. value of the emitter fluorescence can be done by the ordinary procedure. The efficiency of the ISC process of sensitizer molecule usually is estimated by the simplest form of the Ermolaev's rule ($Q_{ISC} = 1 - \eta_{\mathrm{F},sens}$). Oppositely, the efficiencies of the TTT and TTA processes cannot be defined enough precisely. The theory of those processes is still not developed enough to predict the accurate values of the processes efficiencies. Therefore, the extensive way to predict the Q.Y. of the TTA – UC process seems not be productive.

In our investigations we apply the classical methodology of the Q.Y. determination even for the UC process. It means that the TTA – UC is considered as a two-step process – the absorption of an incident photon in the absorption band of the sensitizer and the emission of an upconverted photon by the emitter. As a result, all details of the processes which are taking part in the so-called "upconversion black-box" [21] are not examined individually.

After the performed simplification, actually every method for the Q.Y. determination of the UC could be applied.

It should be also noted, that the described above method deals with the experimentally observable Q.Y. value – it means the fraction of obtained upconverted photons to the absorbed photons. Starting from the publication of review [53] many other research groups began to use a hypothetical efficiency of the UC of absorbed photons, which maximum has to reach 100%. For this purposes the factor 2 was introduced in the equation of the Q.Y. determination, "since the absorption of 2 photons is required for the observation of 1 upconverted photon" [53]. More important is that the classical term «quantum yield» is started to be used for designation of some internal efficiency of the studied process. This leads to a huge mishmash during comparison of experimental results obtained by different authors and in different time (for example, up to appearance of above noted review even the group, which have published it, used the classical determination of the Q.Y. [54, 55]).

In this dissertation for all Q.Y. values the classical method of calculation according to the equation (3.11) was used.

3.6 Materials employed

The perylene (sublimed grade, 99.5%), rubrene (98%), PTS (15 wt% in water), THF (99%) were obtained from the Sigma-Aldrich. Extra dry toluene (99.8%, Acroseal) was obtained from Acros Organics.

All other employed in experiments dyes were synthesized by colleagues of our group. Substituted perylene dyes, tetrabenzo- and tetranaphtoporphyrins, were synthesized by xxxxxxxxxxx. Bodipy dye was synthesized by xxxxxxxxxxx. The Bodipy-based dyads were created by xxxxxxxxxxx and xxxxxxxxxxx together.

3.7 Sample preparation

The synthetic dyes were weighed under ambient conditions by the use of analytical weights having a precision of 0.01 mg. Most of the analytical grade solvents were available in the sealed under argon packages. Solvents which were not available commercially in deoxygenated form were previously placed in the glovebox (Uni Lab, mBraun) filled by nitrogen. The oxygen level in glovebox was kept below 5 ppm. Sample solutions, prepared in the ambient conditions, were purged by nitrogen for 5 min and kept in glovebox for around 24 hours with a partially opened cap. Afterwards the bottles with deoxygenated solutions were

closed and stored in the glovebox. It was experimentally proven that after 24 hours the oxygen is removed also from highly viscous solutions even without stirring.

In order to avoid additional contamination by the oxygen, dry weighted chemicals were evacuated and filled with the nitrogen 6 times in a chamber box and dissolved directly in the glovebox. To improve the accuracy in the concentrations, the amount of the needed solvent was weighed on the analytical balances instead of measuring by the volume. The required weight of the solvent was preliminary calculated in respect to its mass density.

The mixing of the dye's solutions was performed by the same method. Solutions were weighed on the analytical balances instead of the conventional mixing by the volume. The accuracy of such method was proven many times by the absorption measurements. For example, seven prepared in a row samples with the same assumed concentration of sensitizer show that the real concentration differs in the range of maximum 7% (see Figure 3.8).

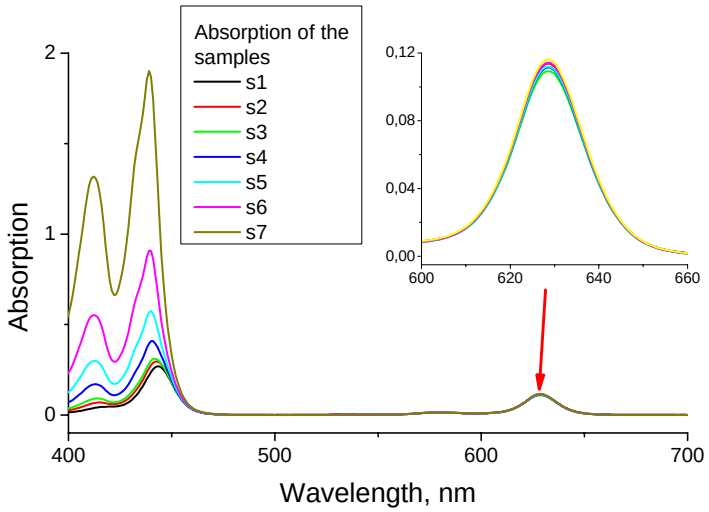

Figure 3.8 Absorption of seven prepared in row samples like a demonstration of advantage of the mixing method.

The samples solutions were investigated by the use of glass tubes (VITROTUBES™, Hollow Rectangle Capillaries - N2540-50): thickness of 400±10 μm (shown in Figure 3.9). The glass tubes were pre-sealed from one side and kept permanently in the glove box in order to minimize the amount of oxygen physically adsorbed on the capillary walls. The ready for investigation solutions were filled by a syringe with an insulin needle having outer diameter of 300 μm. Use of the syringe for the tubes filling instead of capillary effect prevents adsorption of a sample solution on the walls close to the opened end of the tube and improves subsequent glue adhesion. After filling, the open end of the tube was sealed in order to prevent the oxygen penetration in the sample solution. The sealing was done with a UV-light

curing glue or a commercially available transparent two-component fast hardening epoxy (UHU Plus 5 min epoxy). After hardening, the epoxy resin is stable against organic solvents (except ethanol), that is important for long-term storage of the samples. After being measured, the samples were placed back in the glove box in order to create a sample-library with the long term availability.

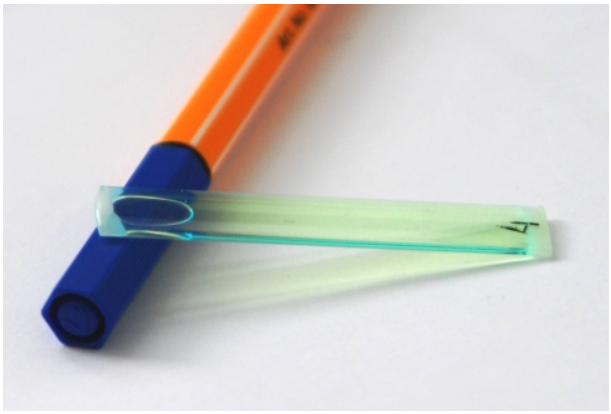

Figure 3.9 UC sample solution filled in the glassy vitrotube having thickness of 400 μm and width of 8 mm glued by the UV-light cured glue.

4 Sensitizer-emitter pairs. Present state of the art

In the pioneering work of Parker and Hatchard [8] the participation of the triplet state in formation of the p-type delayed fluorescence was assumed. Those studies were restricted to only two pairs of interacting molecules. The first pair consists of phenathrene (sensitizer) and naphthalene (emitter). The second tested pair was proflavine hydrochloride (sensitizer) and anthracene (emitter). The dyes were dissolved in the ethanol and frozen (–72 ºC). A reported Q.Y. of the p-type delayed fluorescence process was estimated to be around 1% and 0.1% for phenanthrene / naphtalene and proflavine hydrochloride / anthracene, respectively.

Being reborn in the new century, the process of TTA – UC was demonstrated in technologically important conditions, namely at room temperature. Following the experimentally postulated requirements (2.5 - 2.8), a large amount of optimized UC pairs (sensitizer /emitter) were already demonstrated.

In this part the current state of art in the region of the used sensitizers and the emitters will be overviewed and the investigations on the creation of a new set of perylene-based emitters with a subsequent utilization for the TTA – UC will be reported.

4.1 Sensitizers

Taking into account, that the starting energy level for the process of the TTA – UC is the highly populated sensitizer triplet state, it is obvious, that dyes, demonstrating high Q.Y. of the phosphorescence or the efficient singlet oxygen generation have to be tested as possible TTA – UC sensitizers. To mention some of these dyes [41]: methylene blue, xanthene dyes usually with halogen substituents, porphyrins, phthalocyanines and related tetrapyrroles, transition metal complexes of ruthenium, platinum and palladium.

4.1.1 Ruthenium (II) complexes

In 2005 Castellano and coworkers used $[Ru(dmb)_3][PF_6]_2$ (Ru-1 in Figure 4.1) as the sensitizer in a mixture with 9,10-diphenylanthracene (DPA in Figure 4.1) as the emitter to obtain the TTA – UC [56]. The studied ruthenium complex demonstrates an absorption maximum located at 460 nm and the phosphorescence maximum at 620 nm (the corresponding triplet level energy is around 2 eV). In UC regime the complex was excited by use of green line of an Ar^+ laser (laser line 514.4 nm).

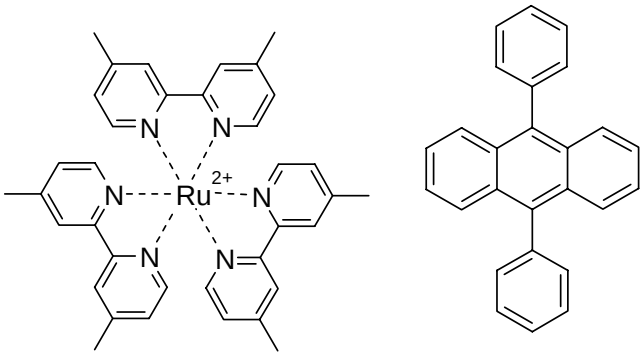

Figure 4.1 Chemical structure of $[Ru(dmb)_3][PF_6]_2$ dmb = 4,4-dimethyl-2,2´-bipyridine and 9,10-diphenylanthracene (DPA) used in [56]

The UC fluorescence of DPA was observed with a maximum of the emission at around 430 nm. No Q.Y. values of the TTA – UC were reported.

Investigations with the ruthenium complexes, used as the sensitizers, were continued by a group of Jianzhang Zhao [57]. In order to enhance the TTT process efficiency they tried to increase a lifetime and a position of the triplet state by modification of the coordination geometry of the Ru(II) center by choice of an appropriate ligand and by the functionalization of molecule with different groups, such as pyrene or phenyl. The molecules shown in Figure 4.2 were synthesized. The phosphorescence of the modified complexes is located in the region 600 – 680 nm that corresponds to the triplet level energy in 1.8-2 eV. Most promising complexes were tested for the TTA – UC using again DPA as the emitter. The highest UC external Q.Y. values were obtained for Ru-7 (Q.Y. = 4.9%), Ru-8 (Q.Y. = 4.8%) and Ru-6 (Q.Y. =2.25%) complexes.

As a first drawback of such type of complexes one can note the relatively low decay time of the triplet state (nearly some microseconds, the exceptions are Ru-7 and Ru-8 complexes with phosphorescence decay times of round 100 μs) and a low extinction coefficient of the complexes in the region of used excitation (532 nm or 514 nm). Even more, such systems demonstrate a crucial drawback: a strong overlap between the emission spectrum of the used emitter (DPA) and the absorption spectrum of the sensitizers. Thus, a significant reabsorption of the UC photons by the sensitizer will take place and the overall efficiency of the process will be lowered accordingly to the optical density of the sensitizer solution. If the concentration of sensitizer will be increased in order to enhance the photon flux of UC radiation, with high probability almost all UC photons will be absorbed by the sensitizer and the external Q.Y. will be very low.

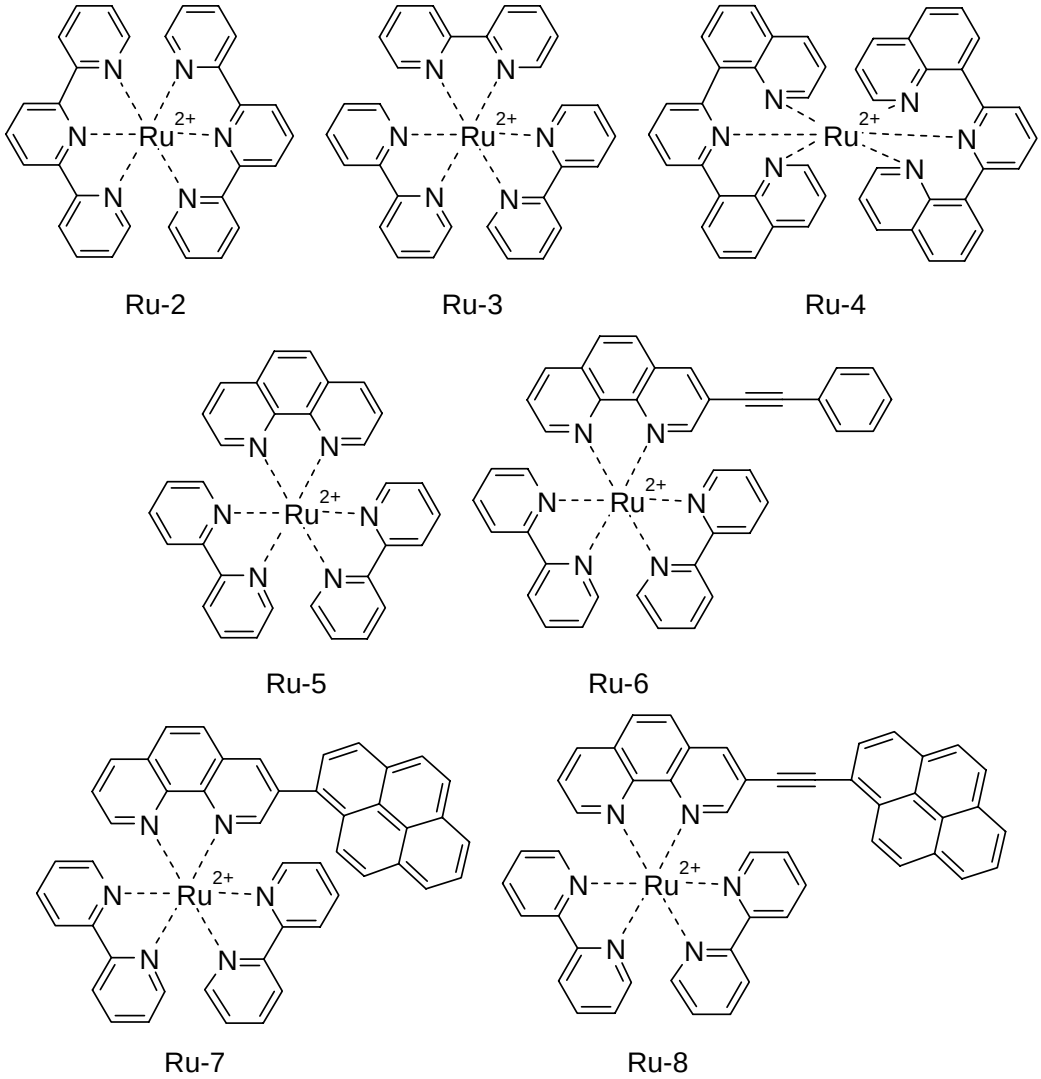

Figure 4.2 Molecular structures of the ruthenium complexes [58-61].

4.1.2 Platinum complexes

Platinum acetylide complexes were also used in the TTA – UC process as the sensitizers. They usually show high phosphorescence even at room temperature. Thus, in 2010 the observation of the UC radiation with a platinum(II) terpyridyl acetylide complex [62] (see Figure 4.3) as the sensitizer was reported. In a deoxygenated solution the complex has the strong phosphorescent radiation located at 610 nm (corresponding energy 2.03 eV). The DPA molecule was chosen again as emitter, although as well as in the case of ruthenium complexes its emission spectrum coincides with the main absorption band of the complex. Being excited at 514 nm the mixture shown UC emission with the Q.Y. around 1%, which strongly decreases as the emitter concentration increases.

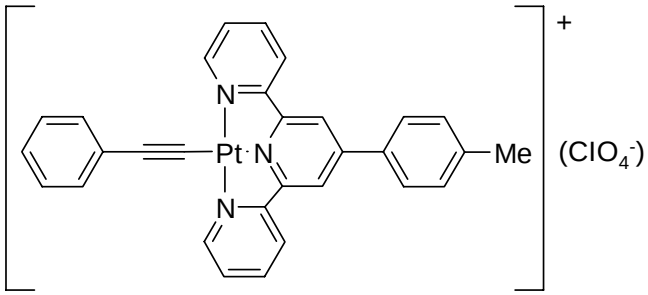

Figure 4.3 Platinum(II) terpyridyl acetylide complex served as the sensitizer in [62].

The work on the platinum complexes was extended by the group of Jianzhang Zhao [39]. Using different substituents the set of molecules was synthesized (structures are shown in Figure 4.4). Due to the variation of the ligand the longest wavelength of a complex absorption was shifted to the region near 550 nm and the lifetime was increased in 7 times (comparing the parent Pt-1 molecule with the modified Pt-6 complex). The strong UC signal of the delayed fluorescence from DPA molecule, used as the emitter, was detected in combination with the complexes Pt-5 and Pt-6. Phosphorescence of these complexes takes place at ~ 610 nm (2.03 eV) for Pt-5 and ~ 670 nm (1.85 eV) for Pt-6. As claimed by the authors external Q.Y. values reached 4.9% for the Pt-5 complex and 17.7% for the Pt-6 complex.

It is important to mention the optical standard chosen in this article. The fluorescence signal of DPA, which is located in the region 400-470 nm, was compared with the phosphorescence of $[Ru(dmb)_3][PF_6]_2$ (shown previously in Figure 4.1), which maximum is placed at 630 nm. The small Q.Y. value for the ruthenium complex (0.073 reported in [63]), its strong dependence on a presence of the molecular oxygen as well as above noted the strong spectrum mismatch, make doubtful the specified values of the UC efficiency.

The drawbacks of these complexes are the same as the noted above for the ruthenium complexes. The presence of the strongly absorbing band without gaps, which absorb the radiation in the range 300 – 550 nm, will highly restrict the applicability of the complexes for the TTA – UC.

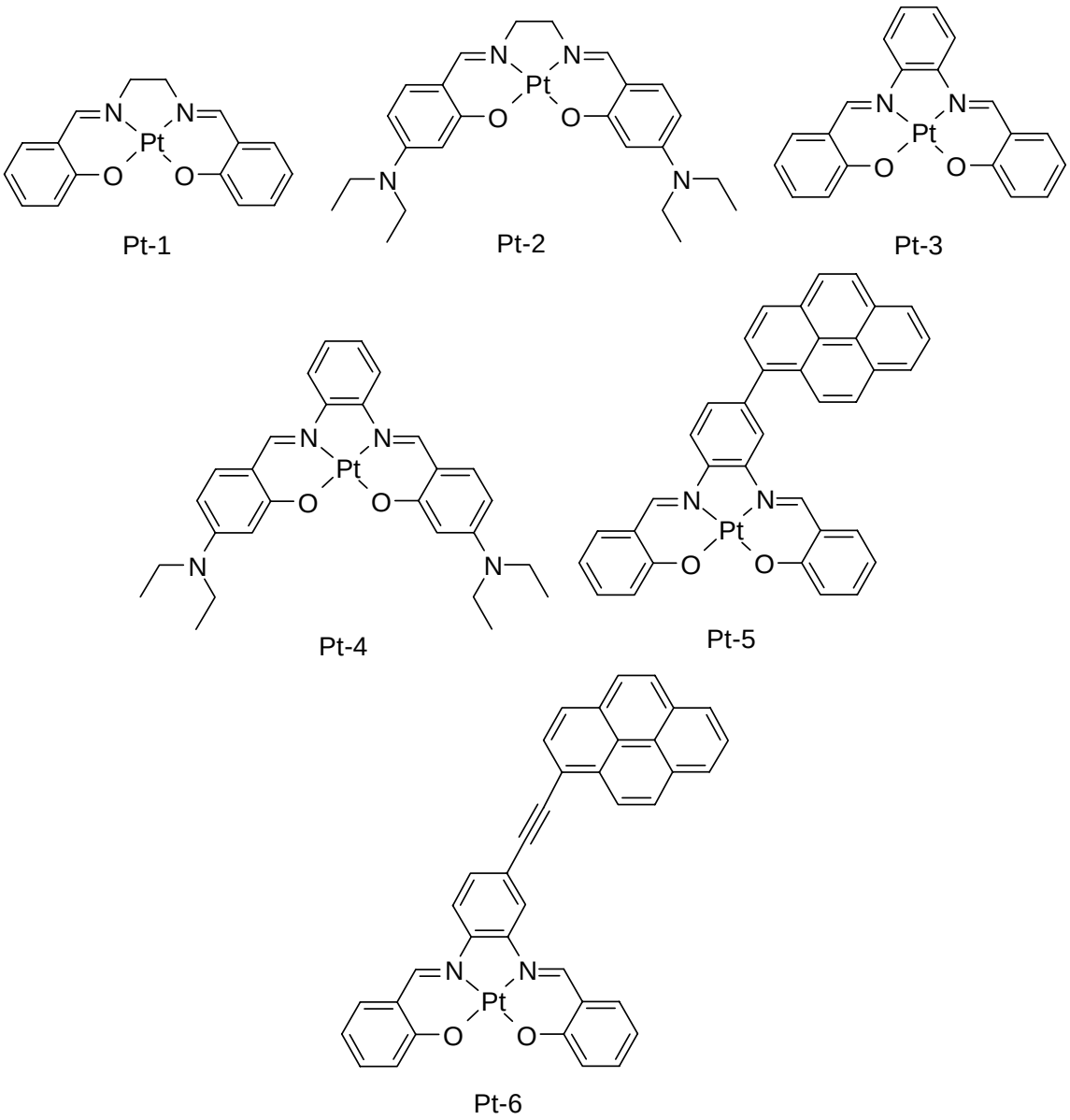

Figure 4.4 Molecular structures of platinum complexes [39].

4.1.3 Iridium complexes

It was also reported the use of coumarin containing Ir(III) complexes (see Figure 4.5) as a sensitizer [64] for the TTA – UC. UC efficiencies were claimed to reach 11% that was achieved with the use of the DPA as the emitter. The reported anti-Stokes shift was extremely low, actually less than 0.21 eV. Unfortunately, the previously mentioned comments such as the Q.Y. measurements procedure, as well as the strong overlapping of the sensitizer absorption and the region of emitter radiation, are valid also for this publication.

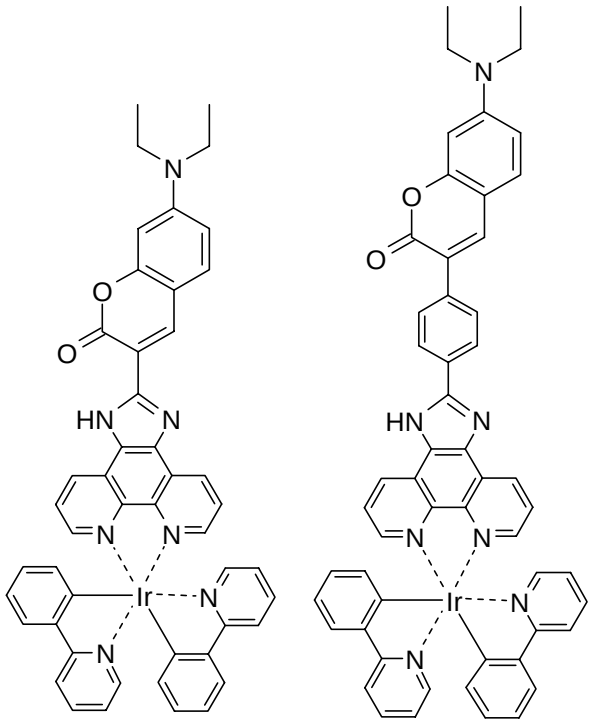

Figure 4.5 Molecular structures of iridium complexes [64].

4.1.4 Organic Bodipy dyes

There is interesting paper devoted to the synthesis of organic sensitizers based on Bodipy molecule [65]. Bodipy dyes usually possess a high fluorescent Q.Y. and were also used as efficient emitters for TTA – UC [55, 66, 67]. It was shown that in the presence of a heavy atom (for example Iodine), the ISC-probability for such Bodipy molecule can be substantially increased, which leads to efficient population of the triplet state of this molecule. The newly synthesized Bodipy-derivatives (see Figure 4.6) possess a long lifetime of the triplet state (50 μs), which leads to a potential increase of the efficiency of the TTT process. The energy positions of the triplet state were calculated to be around 1.51 eV (phosphorescence maximum should be located at 820 nm). Nevertheless, being optically excited, the complexes show only fluorescence emission. Although the phosphorescence of these compounds were not detected, the ISC-coefficients were estimated (calculated according to the simplest form of Ermolaev's rule) to be as high as 95%. In the presence of the perylene (shown in Figure 4.7), which serves as the emitter, the TTA – UC was detected. The estimated external Q.Y. reached 3%.

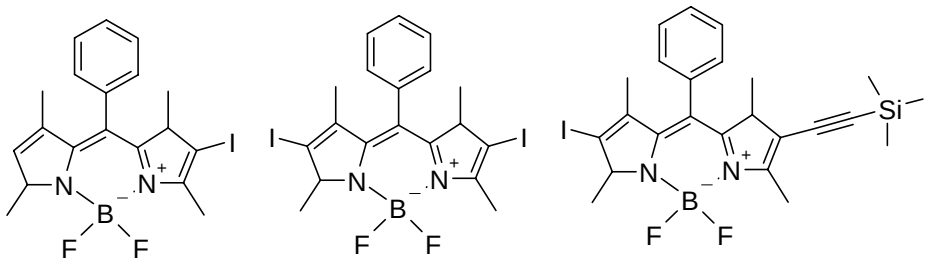

B-1 B-2 B-4

Figure 4.6 Molecular structures of the organic sensitizers from the Bodipy family [65].

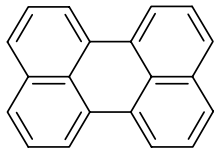

Perylene

Figure 4.7 Chemical structure of the perylene used in [65] as the emitter.

4.1.5 Metallated porphyrins

Porphyrins are related to the large family of molecules called tetrapyroles. Due to the similarity with natural pigments – chlorophyll and haem, which are contained in living systems, a synthesis and an investigation of their photophysical properties was very popular in 1930-1970s. The diversity of developed porphyrin dyes and a big variety of their properties results in their wide usage in the drug development, the electron-transfer, the photodynamic therapy and the oxygen sensing.

All porphyrins have the similar band-like structure of the absorption spectra. Conventionally it consists of two main absorption bands: the Soret-band and the Q-band (see Figure 4.8). The very intensive Soret-band is located in the ultraviolet region of spectrum and is a result of the electronic excitation from the ground level to the second excited singlet level ($S^0 \rightarrow S^2$). The Q-band usually consists of two bands, which are placed in a more red part of the spectrum with a gap 150-250 nm from the Soret-band and correspond to the electronic excitation into the first singlet state ($S^0 \rightarrow S^1$) (the stronger one) and into the first vibronic level of S^1 state (weaker band). The extinction coefficients of metallated porphyrins usually are very high and reach $(1 \div 5) \cdot 10^5$ ($L \cdot mol^{-1} \cdot cm^{-1}$).

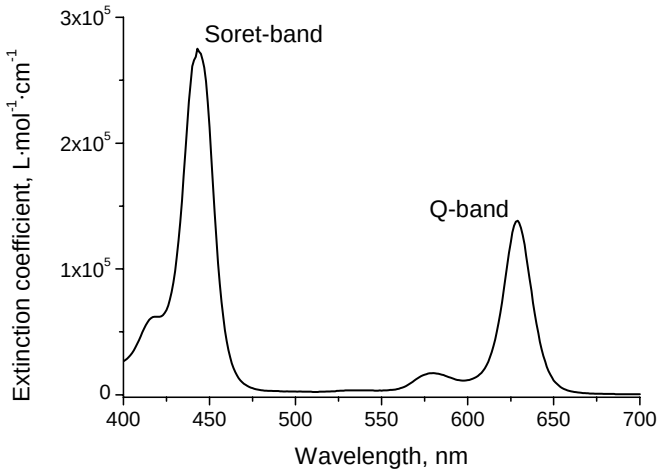

Figure 4.8 Typical absorption spectrum of metallated porphyrin (namely PdTBP).

It is known that the efficiency of intersystem crossing depends on the metal atom introduced in the porphyrine structure and can reach 100% [68]. Also the metal can influence on the absorption spectrum of the porphyrin, resulting in hypsochromic or bathochromic shifts. The atomic mass and size of the metal ion is also critical for a lifetime of the triplet state and the Q.Y. of the phosphorescence. Thus, palladium porphyrin usually provide the extremely long living triplet states (lifetime is near 300 μs), whereas platinum complexes show an order less lifetime [69]. For applications the chemical stability of synthesized compounds is also crucial characteristic. The platinum and palladium porphyrins require a planar coordination geometry provided by a porphyrin macrocycle. Usually the both ions are placed very tight in the structure that makes them almost impossible to escape from the macrocycle, allowing using them in different solvents and over a large region of temperature.

Due to all above-mentioned characteristics the porphyrin's family attracts a big interest of scientists working with the TTA – UC. Nowadays, the most part of published papers in this field of science are dealing with porphyrins as the sensitizers.

Thus, in 2005 by Baluschev et al. the UC in polymer matrices of poly(9,9-bis(2-ethylhexyl)fluorene) (PF2/6) and poly(ladder-type pentaphenylenes) (L-5Ph) doped with (2,7,8,12,13,17,18-octaethyl-porphyrinato)Pt(II) (PtOEP) (see Figure 4.9) was reported. Under reported excitation by continuous-wave laser with reported wavelength of 532 nm the films show the UC photoluminescence in the region of 400-500 nm.

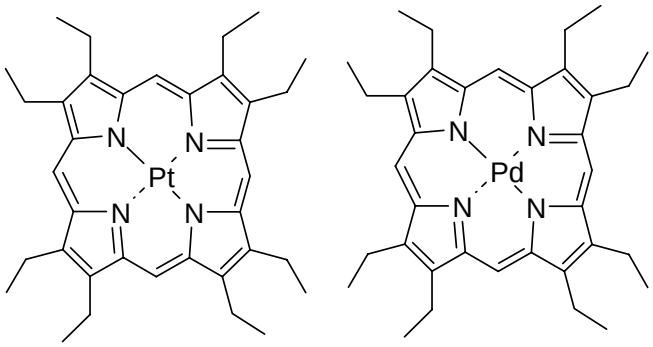

PtOEP PdOEP

Figure 4.9 Chemical structure of (2,7,8,12,13,17,18-octaethyl-porphyrinato) metallated by Pt(II) and Pd(II) (shortly named PtOEP and PdOEP).

Further in 2006 by this group the UC of a noncoherent sunlight with low intensity (as low as 10 $W \cdot cm^{-2}$) was shown [13]. Excited at 545 nm, the porphyrin complex (2,7,8,12,13,17,18-octaethyl-porphyrinato)Pd(II) (PdOEP) (see Figure 4.9) served as the sensitizer and DPA molecule as the emitter. The external Q.Y. of UC was estimated to be more than 1%.

Octaethylporphyrins (OEP) are highly phosphorescent with a phosphorescence maximum located around 670 nm (correspond to the energy of the triplet level of 1.85 eV). These porphyrins are commercially available and therefore are commonly used in investigations of the TTA – UC both in a solution and in a polymer matrix. They were utilized in many publications of different scientific groups [14, 17, 70-79].

The use of tetraphenyltetranaphtoporphyrins (TNP) (shown in Figure 4.10) as sensitizers allows pushing a red border of the excitation further into the NIR region of the spectrum. Thus, in 2007 the UC under the excitation by the NIR part of the sunlight spectrum was shown [35]. Upon excitation of PdTNP (maximum of absorption is placed near to 700 nm) by a noncoherent sunlight having bandwidth 20 nm and mean excitation intensity around 1 $W \cdot cm^{-2}$, the intense fluorescence of bis(tetracene) in the region 500-600 nm was observed. The external Q.Y. of UC was calculated to reach 4%. PdTNP complex has the phosphorescence maximum at 920 nm that corresponds to the triplet state position in 1.35 eV.

A simultaneous utilization of two sensitizers could broad the spectrum of a sun-light photons harvesting. In 2007 Pd(tetraphenyltetrabenzoporphyrin) (PdTPTBP or PdTBP) (structure is shown in Figure 4.10) was used in a couple with above noted PdTNP to upconvert the separated from a sun-light broadband radiation in the range 610-720 nm [80]. The maximum of the phosphorescence of PdTBP is located at 800 nm (energy is around 1.55 eV). Rubrene (chemical structure is shown in Figure 4.11), which emission is located in the range 550-630 nm, was chosen to serve as the emitter.

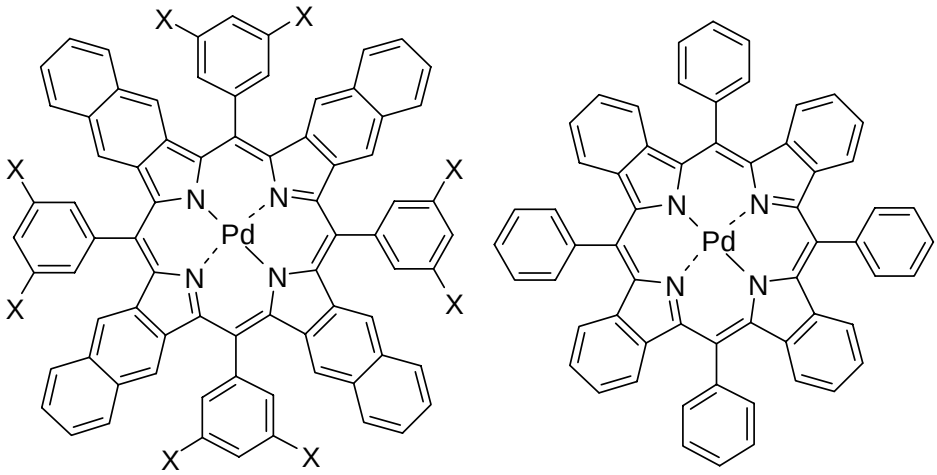

PdTNP PdTBP

Figure 4.10 Chemical structures of palladium derivative of tetrakis-*meso*-(3,5-dimethoxyphenyl) tetranaphthaloporphyrin (short name PdTNP) used in [35], where X = OCH_3 ; and Pd (tetraphenyltetrabenzoporphyrin) (short names are PdTPTBP and PdTBP) used in [80].

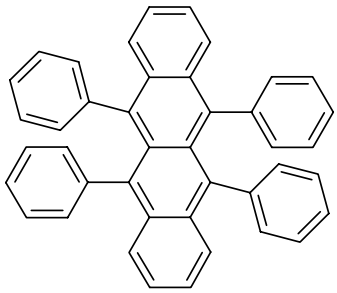

Rubrene

Figure 4.11 The structure of rubrene molecule used as the emitter in [80].

Its usage provides efficient UC signal generation in a combination both with PdTBP and PdTNP sensitizer, as well as at the simultaneous presence of both sensitizers in the mixture.

For some reasons the metallated TBP nowadays are not more available commercially. Therefore, they are not so widely used compared to OEP, but still their palladium and platinum complexes attract a big interest of researchers [20, 34, 66, 67, 81-85].

In 2008 a new porphyrin working as an IR-absorbing sensitizer was presented [86]. It is a palladium derivative of a tetraanthraporphyrin (TAP) (see Figure 4.12). The maximum of its absorption is placed near 800 nm that makes it the most far placed sensitizer used in the TTA – UC. The phosphorescence of the porphyrin was obtained at 1100 nm (1.13 eV). Despite of so low position of the PdTAP triplet state the strong UC signal was measured in a combination with rubrene as the emitter. The external Q.Y. was calculated to be as high as 1.2%. The UC signal was detectable even at ultra-low pump radiation intensities (100 $mW \cdot cm^{-2}$).

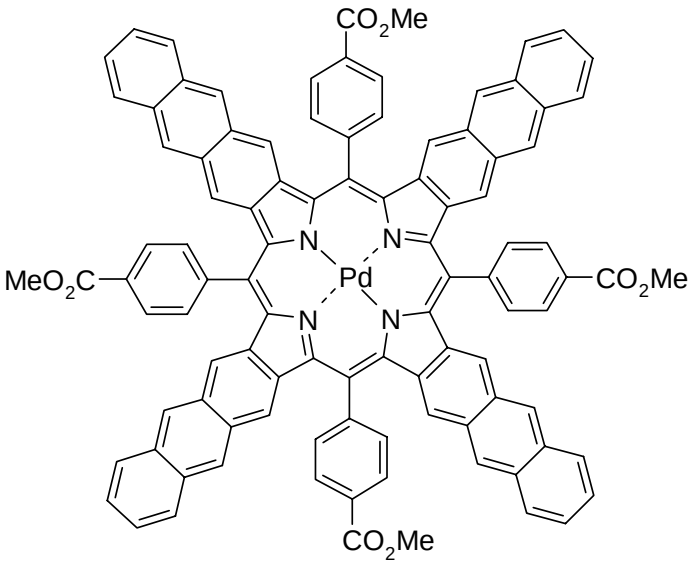

PdTAP

Figure 4.12 Chemical structure of tetrakis-5,10,15,20-(p-methoxycarbonylphenyl) tetraanthra [2,3-b,g,l,q] porphyrin (shortly PdTAP) used as the sensitizer in [86].

In 2010 Schmidt et al. published an article [31] devoted to the maximal possible conversion efficiency of UC. In the experimental part a porphyrin molecule tetrakisquinoxalinoporphyrin palladium(II) (shortly PQ_4Pd) (shown in Figure 4.13) was used as the sensitizer. The porphyrin was excited by the radiation of a femtosecond TOPAS OPA laser system at 670 nm. Excitation intensity was equal to 13 $GW \cdot cm^{-2}$ (mean power was $2W \cdot cm^{-2}$, repetition rate 1 kHz). With the use of rubrene as the emitter the external Q.Y. was estimated to be 12.5%, while the comparison with a directly excited prompt fluorescence of the emitter in ready UC solution gives the efficiency of TTA process to be as high as 33% (it means that from 100 of triplet states 33 was used for creation of UC radiation). This and a slightly modified porphyrin PQ_4PdNA was used in further experiments of this group [15, 33, 87, 88].

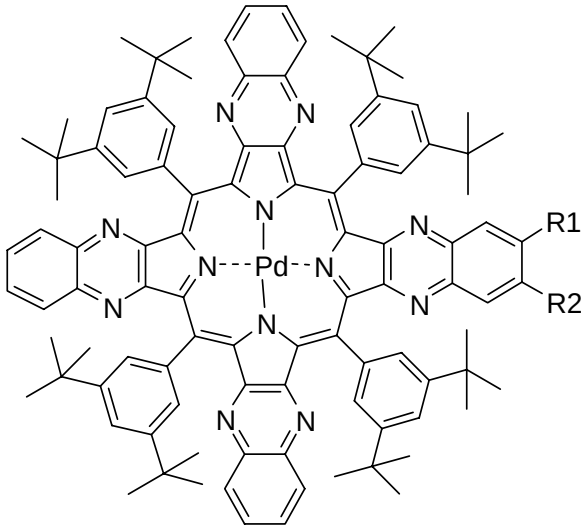

PQ_4Pd: R1,R2 = H
PQ_4PdNA: R1 = NO_2, R2 = NH_2

Figure 4.13 Chemical structure of tetrakisquinoxalinoporphyrin palladium(II) (shortly PQ_4PD) and its modification nitroaminopalladiumtetrakis porphyrin (shortly PQ_4PDNA) used as the sensitizers in [15, 31, 33, 87, 88].

Phthalacyanines belong to the same family of the tetrapyrolic dyes and have the chemical structure similar to the porphyrins. As a result, they have comparable photophysical properties. In 2008 the group of Castellano has reported the use of octabutoxyphthalacyanine ($PdPc(OBu)_8$) as the sensitizer [89]. It has maximum of the absorption at 725 nm while the phosphorescence is placed at 1 μm (corresponds to the energy of 1.24 eV). Rubrene dye was used as the emitter also for this experiment. Under the pulsed excitation by Nd:YAG laser/OPO system at 725 nm the UC signal was measured both in toluene and in ethyleneoxide/ epichlorohydrin copolymer films.

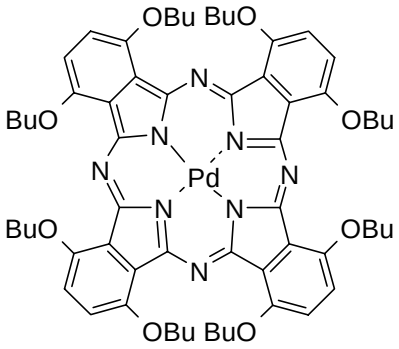

$PdPC(OBu)_8$

Figure 4.14 Chemical structure of Pd(II) 1,4,8,11,15,18,22,25-octabutoxypthalacyanine (shortly $PdPc(OBu)_8$) used in [89].

4.2 Emitters

The contributions to the correct choice of an appropriate emitter for a used sensitizer were discussed in the theoretical part of this work (please see parts 2.2 and 2.4). The emitting dye should have a high fluorescence Q.Y., the energy of its triplet state should correspond to the energy of the triplet state of the sensitizer, and a spectrum of the emitted fluorescence should not overlap with any absorption bands of chemicals used in the sample. As it was noted above, surprisingly often the last contribution is infringed. It is also incomprehensible that despite the huge number of existing and commercially available fluorescent dyes only few were used for the TTA – UC.

Up to now the following dyes were most commonly used in the experiments:

- **DPA** (9,10-diphenylanthracene) (shown in Figure 4.1). In the normal conditions its Q.Y. in deaerated solution in cyclohexane is around 0.97 [45]. It emits in the region 390-470 nm. The energies of its singlet and triplet states are equal to 2.82 eV and 1.77 eV, correspondingly. It is probably the most used emitter nowadays. Commonly, DPA is used in the experiments with the excitation of the sensitizer in a green region of spectrum (510-550 nm).
- **Perylene** (shown in Figure 4.7). It emits in the region 430-510 nm. Its Q.Y. strongly depends on concentration and oxygen presence. Thus, in the air-saturated solution of toluene the Q.Y. is equal to 0.75, while in deaerated one is closing to unity [43]. The energies of levels are 2.83 eV and 1.53 eV [90] for the singlet state and the triplet state, correspondingly. Because of the lower than for DPA position of the triplet state the perylene was used at the excitation in green and red regions of spectrum in dependence on the used sensitizer. Perylene shows a high photostability and is established as the efficient emitter for the process of the TTA – UC [34, 65]. That is one of the reasons why in our group the perylene was chosen as the promising compound for a chemical tuning of the photo-physical properties.
- **Rubrene** (shown in Figure 4.11). The spectrum of emission is located in the region 530-650 nm. Q.Y. of rubrene in deaerated solution is close to unity [91]. However, it should be noted that rubrene is a good photosensitizer for the singlet oxygen generation [92] and in the presence of oxygen it fast oxidizes forming nonfluorescent complexes [93]. The energies of its singlet and triplet state are 2.21 eV and 1.14 eV [94], respectively. The low position of the triplet state opens a possibility to use this emitter in combination with

sensitizers which are excited in the near IR region of the spectrum and have the phosphorescence emission at the wavelength longer than 1 μm.

- **Bodipy** (Boron Dipyrromethene) which base structure is presented in Figure 4.15. The original structure is usually modified by addition of different substituents into position 1-7 of the parent Bodipy structure that leads to a change of the absorption and the emission spectra [95]. Some of the Bodipy dyes show the Q.Y. of fluorescence closing to 100% [96] and the low photobleaching even under highly intense irradiation [97]. Up to now the dyes used as the emitters in the TTA – UC investigations [66, 67] (please see Figure 4.16) look very likely and had the fluorescence spectrum in the region 500-600 nm (energies of singlet state in the region 2.15-2.3 eV). Their triplet state energies were estimated to be around 1.65 eV (corresponds to the phosphorescence emission at 750 nm). Because of the close position of the singlet and the triplet states for these molecules the number of sensitizers is strongly restricted and up to now they were used only with platinum and palladium complexes of TBP. Bodipy dyes with other substituents probably can be used in a combination with other sensitizers.

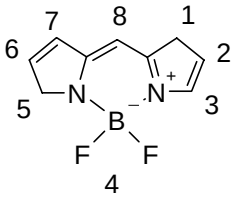

Figure 4.15 Molecular structure of Boron Dipyrromethene, the root base for the Bodipy-dyes.

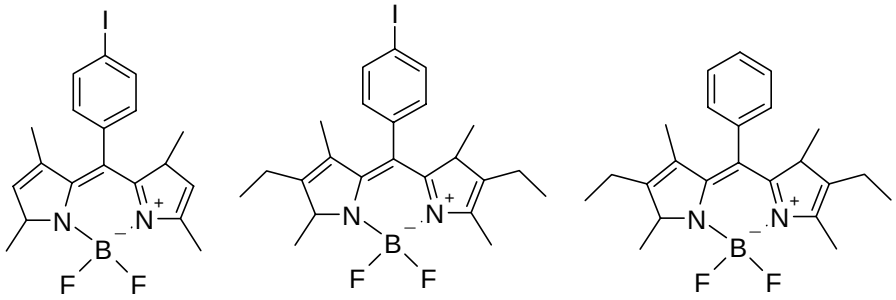

B-5 B-6 B-7

Figure 4.16 Chemical structures of Bodipy-dyes used as emitters in [66, 67].

5 New perylene-based emitters

Whereas other groups modify sensitizer molecules in order to tune the characteristics of their triplet state, our approach is based on a modification of both types of active molecules – sensitizers, and as well emitters. The optimization of the emitter structure in order to meet the requirements stated in parts 2.2 and 2.4 will be presented in this chapter.

A chemical modification of an emitter molecule can be carried out by addition of π-extending groups. The decorated emitter molecule will undergo simultaneous shifts of energy position of the singlet and the triplet states. By a variation of parameters of substituents one can bring the energy of the triplet state into conformity with the known energy position of the sensitizer triplet state. Thus, a substantial increase in the efficiency of the TTT process should be observed. On the other hand, tuning of the singlet state position at the slight influence on the position of the triplet state can result in increase of the TTA process efficiency, if the energies of the sensitizer and emitter triplet states are already brought into the conformity. During all these modifications is also important to not suppress a fluorescent ability of the emitter, or in other words to keep the Q.Y. of fluorescence on the high level.

The reasonable idea is to tune structures of molecules, already tested to be effective for TTA – UC. Thus, efficient UC generation with DPA as the emitter in combination with a few sensitizers was already shown. Also it is known, that the extension of the π-conjugated system in the linear acene dyes by the substituents like annelated aromatic rings leads to a significant red shift in the absorption spectrum and the fluorescence spectrum. Consequently, the corresponding position of the triplet state should be red-shifted as well, but to a lower extent. Unfortunately, acene dyes are not chemically stable in the presence of oxygen even during sample preparation, which lowers the stability of UC systems, based on them.

Perylene seems to be an efficient emitter for UC, possesses a high chemical- and photo- stability, however, it has several drawbacks. One of them is the limited solubility in organic solvents because of so-called π-stacking. In order to improve the solubility and tune the absorption properties of perylene, one can consider the introduction of electron-donating or electron-withdrawing groups, like alkoxy, nitro or amino groups. The extension of perylene π-system usually leads to a tailored bathochromic shift of the absorption on the value up to 65 nm. These groups change the energy levels in the molecule, the HOMO - LUMO gap and allow a fine tuning of the singlet and triplet excited state energies. At the same time such groups often lower the fluorescence Q.Y. drastically. The extension of the π-system with

conjugated double and triple bonds works in the same way but usually does not have an influence on the emission ability of a molecule and improve solubility due to the presence of groups that prevent the π-stacking of dye molecules in the solution. For that reason the substitution of the perylene core with one or two phenyl, ethynyl or phenylethynyl groups was chosen as a route for a fine tuning of the singlet and triplet states of the perylene. All these groups were decorated with the alkyl chains, mostly tert-butyl groups.

The number of perylene-based molecules was synthesized in our group. By the reason of a negligible ISC coefficient of all investigated emitter molecules the direct observation of the phosphorescence and the corresponding determination of the triplet state energy was not possible. Because of this, all the molecules are to be experimentally tested to serve as emitters in combination with PdTBP and PtTBP (the chemical structure for PdTBP is shown in Figure 4.10, PtTBP have the same structure with the changed central metal atom to Pt(II)). To have a starting point of the estimation of the efficiency change of TTA – UC with new created perylene-based emitters the characteristics of the sensitizers and their efficiency in a combination with the perylene itself was analyzed.

5.1 Pd and Pt tetraphenyltetrabenzoporphyrins (PdTBP and PtTBP)

For the first measurements the concentration of sensitizers was chosen to be equal $1 \cdot 10^{-6}$ M. The spectra of phosphorescence were measured at different excitation powers starting from as low as 35 μW and ending at 3.7 mW. The excitation beam diameter on a sample was measured to be equal 100 μm. The spectra of excitation radiation had smooth peak shape close to Gaussian distribution (red lines in Figure 5.1). The central wavelength of the excitation was tuned to match the maximum of absorption of the Q-band of the used sensitizer and was nearly 630 nm (with full-width half maximum (FWHM) of 14 nm) for the investigation of the samples with PdTBP (the absorption spectrum is shown left in Figure 5.1) and nearly 615 nm (with FWHM of 9 nm) during the investigations with PtTBP sensitizer (the absorption spectrum is shown right in Figure 5.1). For an effective (more than in 10^6 times) suppression of the reflected and scattered parts of the excitation radiation the notch filter (NF03-633E-25, Semrock Inc.) was used. As a result of the usage of the excitation radiation having the relatively broad spectrum an unsuppressed part of the excitation radiation is usually presented on the measured spectra as two narrow sharp peaks, which are situated near the wavelength of excitation.

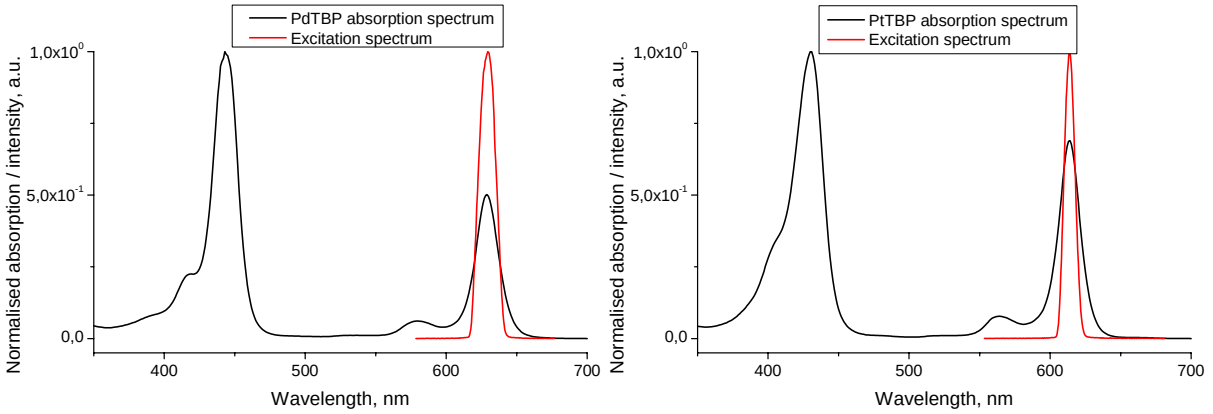

Figure 5.1 Absorption spectra of PdTBP (left) and PtTBP (right) sensitizers and spectra of corresponding excitation radiations.

For the case of PtTBP sensitizer the notch filter was additionally tilted to the angle of approximately 15º to match blocking band of the filter to the wavelength of the excitation radiation. To compensate the resulting walk-off of the detected beam the light collecting system was tuned to the observation of maximum possible detectable signal.

It should be noted that the measured spectra of the phosphorescence of PdTBP (shown in Figure 5.2) and especially their long-wavelength part are distorted and therefore look not fully similar to the real one. The reason for it is described in the part 3.1 and is concerned with the reflective mirrors used in the experimental setup. Afterwards the problem was partially solved by the calibration on the transmission function of the experimental setup and at last fully solved by the replacement of the mirrors on new broadband mirrors. For further discussions only the intensity of the phosphorescence spectrum has the main importance. Taking into account this admission, the shape of the phosphorescence spectrum and its modification during UC and luminescence processes (that was up to now never observed) will be not considered as those having sense.

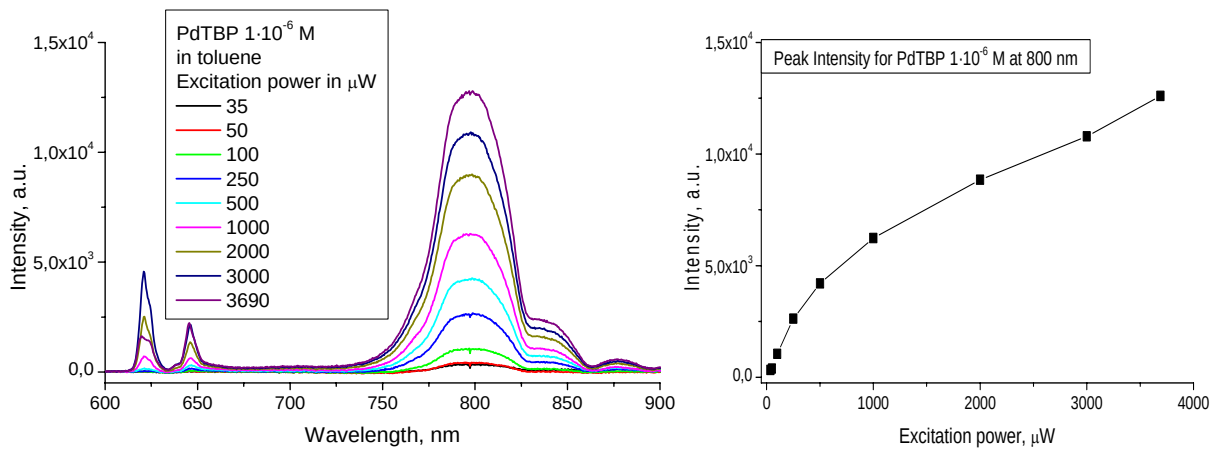

Figure 5.2 The measured spectra of phosphorescence (left) and their peak intensity (right) in dependence on excitation power for PdTBP sensitizer.

Analyzing the spectra shown in Figure 5.2 one can see the evident increase of the phosphorescence signal with the increase of the excitation power. From the other side, the dependence of peak intensity of phosphorescence on the excitation radiation power, plotted at the right side of Figure 5.2, shows saturation, which started to take place even at the moderate level of irradiation (excitation power is 500 μW) and strongly increased at higher excitation levels.

From the opposite side, the phosphorescence of platinum porphyrin has much less pronounced saturation (see Figure 5.3). The reason for that lies in the characteristics of the excited levels of the molecules. In toluene the lifetime of the triplet state of platinum porphyrin is equal to 47 μs and the Q.Y. of the phosphorescence is around 0.2, whereas for the palladium porphyrin the lifetime of the triplet state is almost an order longer (286 μs) whereas the Q.Y. is lower and is equal to 8% [37]. Taking these parameters into account, one can say that PtTBP molecule faster and more efficient utilizes incoming photons than PdTBP. In the same time the efficiency of the TTT process in TTA – UC directly depends on the lifetime of the triplet state. Therefore, for the TTA – UC process the longer lifetime has the crucial significance, but not the Q.Y. of phosphorescence.

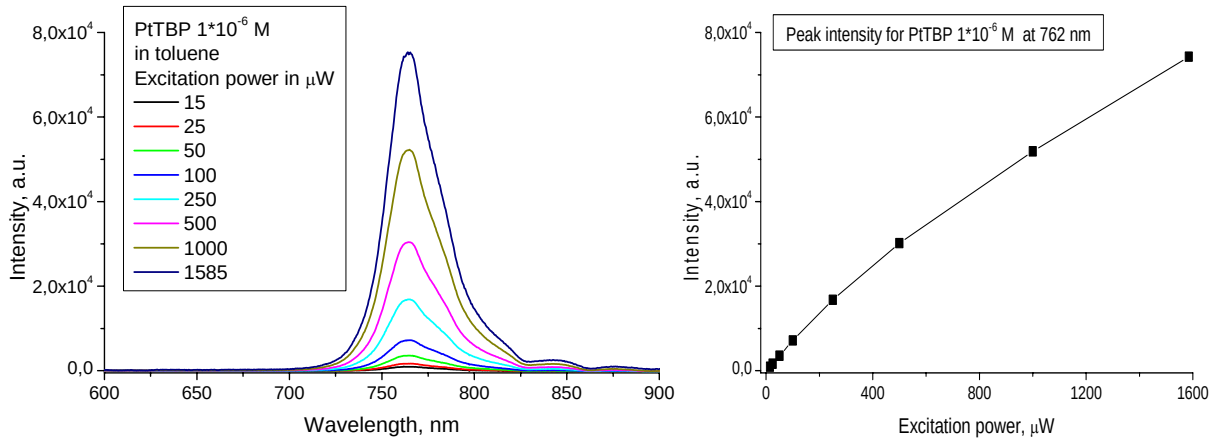

Figure 5.3 The measured spectra of phosphorescence (left) and their peak intensity (right) in dependence on excitation power for PtTBP sensitizer.

5.2 Perylene as emitter for tetrabenzoporphyrins

The chemical structure of perylene was presented earlier in Figure 4.7. Its characteristic spectra are shown in Figure 5.4. As it seen, the absorption is located in the region 350-450 nm with the corresponding fluorescence, which takes place with a small Stokes shift mainly in the blue region of spectra (430-530 nm).

The TTA – UC in combination both with Pt(II) and with Pd(II) TBP was shown earlier. Unfortunately, as it can be seen in Figure 5.5, in the case of PdTBP the perylene goes partially in contradiction with the requirement (2.8) postulated on page 6. The main maximum of the perylene emission overlaps with the maximum of the absorption of the Soret-band of PdTBP. Especially at the high concentrations of PdTBP it will lead to a strong decrease in UC efficiency because of the reabsorption of generated photons.

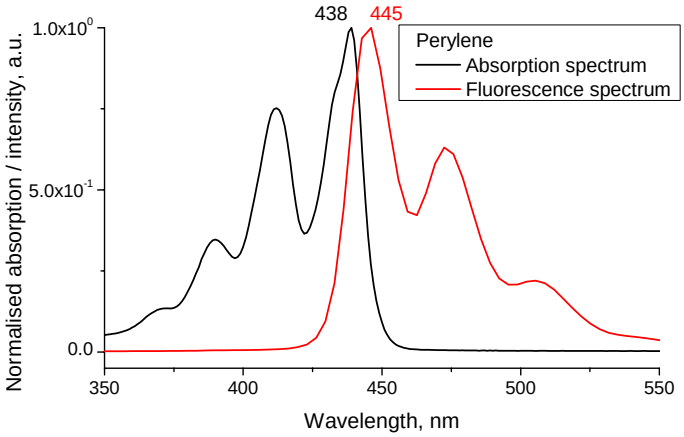

Figure 5.4 Absorption (black) and fluorescence (red) spectra of perylene in toluene.

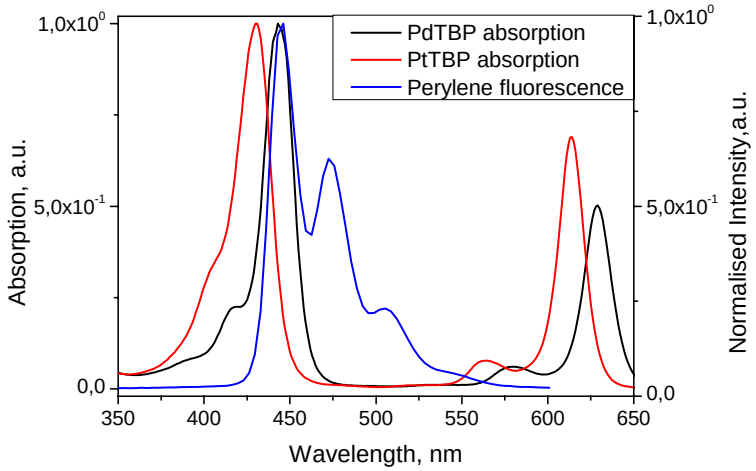

Figure 5.5 Absorptions of PdTBP and PtTBP sensitizers and fluorescence spectrum of perylene emission.

To increase the probability of TTT and TTA processes the concentration of emitter molecules in solution should be at least an order higher than concentration of sensitizer molecules. For the first measurements the ratio 1 to 10 was chosen and the corresponding concentrations were equal to $1 \cdot 10^{-6}$ M for the sensitizer and $1 \cdot 10^{-5}$ M for the emitter. Under the excitation by the red radiation with a wavelength 633 nm the generated UC signal in the mixture of PdTBP and perylene was detected in all range of excitation powers (shown in the left side of Figure 5.6). As it seen, the UC emission from perylene at the low excitation levels is comparable with the phosphorescence from PdTBP and at the high excitation powers becomes even higher. At the high irradiation level the UC emission from the mixture was clearly seen even with a naked eye.

The presence of the phosphorescence and its saturation at the higher excitation levels (red line in the right part of Figure 5.6) can be explained as a following. At low dye concentrations the probability of interaction between triplet acceptors (emitter molecules) with triplet energy donors (sensitizer molecules) is low. Therefore the preferable process of the energy relaxation from the sensitizer's triplet state is the phosphorescence, whereas the TTT process is not efficient. The long-time storage of energy in the triplet states of the sensitizer leads to a lower absorption of the sample in total and is expressed in the saturation of phosphorescent signal.

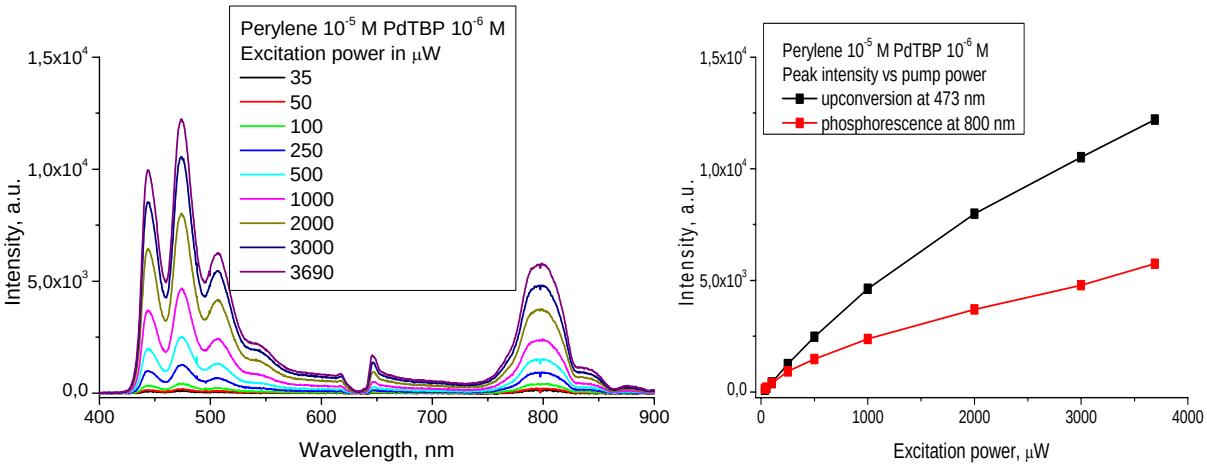

Figure 5.6 Spectra (left) and peak intensity (right) dependence of generated UC and residual phosphorescence signals in dependence on excitation power for the mixture of perylene ($1 \cdot 10^{-5}$ M) and PdTBP ($1 \cdot 10^{-6}$ M) in toluene.

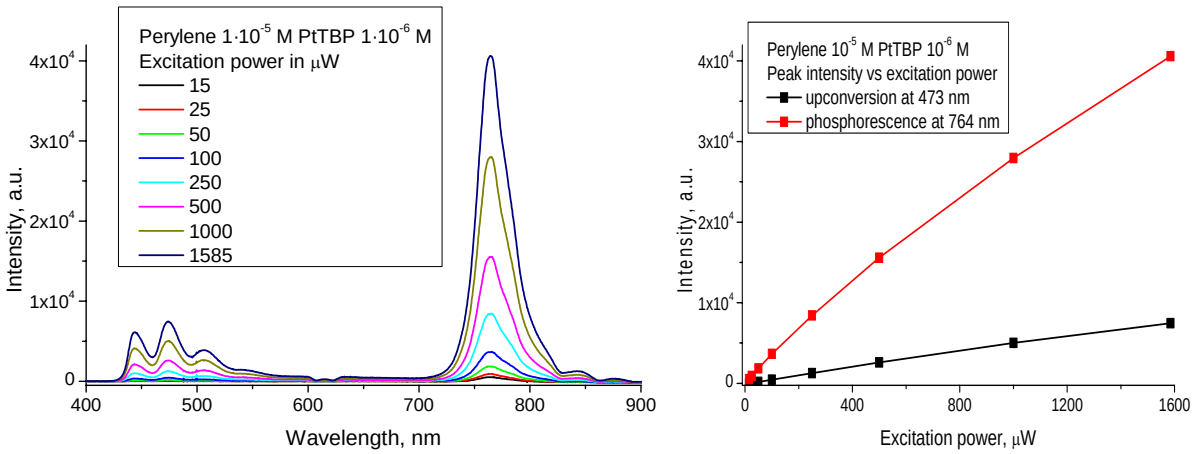

Figure 5.7 Spectra (left) and peak intensity (right) dependence of generated UC and residual phosphorescence signals in dependence on excitation power for the mixture of perylene ($1 \cdot 10^{-5}$ M) and PtTBP ($1 \cdot 10^{-6}$ M) in toluene.

For the mixture of perylene with PtTBP sensitizer the efficient UC photons generation was also observed (see Figure 5.7). Despite of the huge residual phosphorescence signal the efficiency of the UC generation is comparable with those for PdTBP sensitizer. The peak intensity dependence of the phosphorescence signal is still tending to saturation with increase of the excitation beam power, but with much lesser rate, than for the pure sensitizer solution.

During these measurements the fluorescent standard was used for the evaluation of the Q.Y. value. The deoxygenated in glovebox solution of perylene with a concentration $1 \cdot 10^{-4}$ M was sealed in the same vitrotube as the measured samples and served as the standard. The fluorescence of the standard was excited by the laser radiation (418 nm) and detected in the same conditions as for the investigated solutions. It should be also noted that all the investigated emitters were proved to not fluoresce under irradiation by the light used for excitation of sensitizers.

At the maximal levels of the excitation the values of Q.Y. of UC were evaluated to be 2% for the PdTBP and 2.2% for the PtTBP. It should be noted, that the Q.Y. values were calculated using absorption data, obtained in UV-spectrometer (please see part 3.3) in stationary conditions at low intensities of the excitation. It can lead to a mistake in the Q.Y. estimation because of the noted previously saturation of the phosphorescence. The real absorptivity of the sample at a high excitation level can be correspondingly lower than calculated one and, therefore, the real value of the Q.Y. should be higher, than calculated.

5.3 3-(4-*tert*-butylphenyl)perylene or Y-794

For the first modification of the perylene 4-*tert*-butylphenyl group was chosen as the substituent group. The structure of the resulting molecule named Y-794 is shown in Figure 5.8 (to avoid the incomprehension one should note that the numbers in the dye's name are not correlated with their photophysical properties). The application of this substituent shifts the absorption of the dye bathochromically by only 10 nm, so the maximum of the absorption is placed at 448 nm, whereas the fluorescence spectrum shifts on 20 nm up to 466 nm (see Figure 5.9).

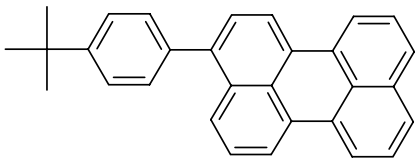

Figure 5.8 Chemical structure of Y-794 (3-(4-*tert*-butylphenyl)perylene).

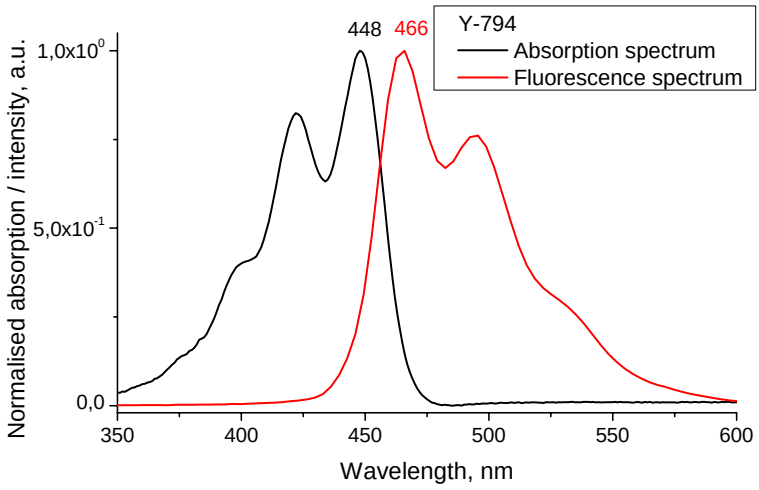

Figure 5.9 Absorption (black) and fluorescence (red) spectra of Y-794 dye in toluene.

As it is seen (Figure 5.10 (left)), UC signal in combination of Y-794 with the PdTBP sensitizer was obtained for all the range of the excitation powers. The efficiency of UC, calculated at the maximal excitation level, was slightly higher than for perylene and was estimated to reach 2.8%. For the case of PtTBP as sensitizer (Figure 5.10 (right)) the efficiency was almost the same like for perylene and the external Q.Y. of the sample at the maximal excitation level was as high as 2.4%.

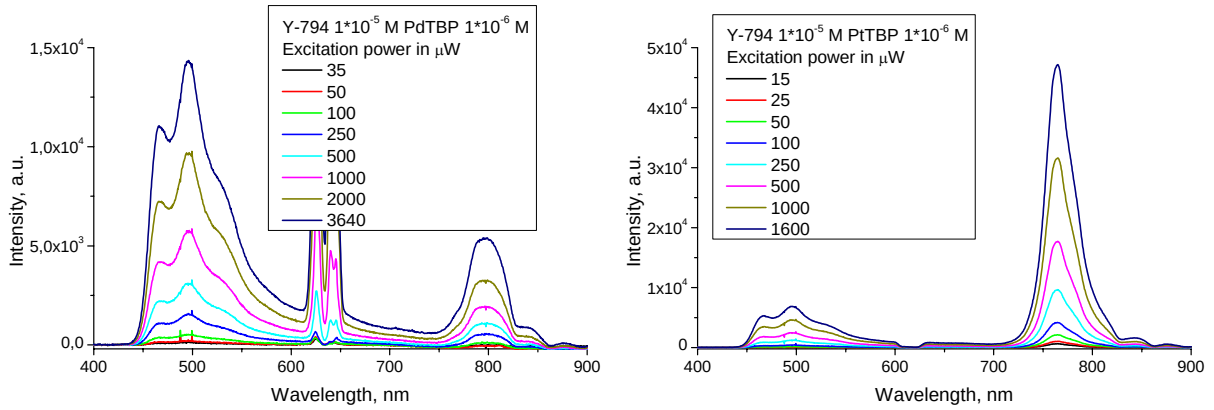

Figure 5.10 Spectra of generated UC and residual phosphorescence in dependence on excitation power for the emitter Y-794 ($1 \cdot 10^{-5}$ M) and sensitizers PdTBP ($1 \cdot 10^{-6}$ M) (left) and PtTBP ($1 \cdot 10^{-6}$ M) (right) dissolved in toluene.

5.4 3,10-bis(4-*tert*-butylphenyl)perylene or Y-635

As a logical continuation, the perylene structure was modified by connection of two *tert*-butylphenyl groups to the opposite sides of the molecule. The structure of the dye is shown in Figure 5.11. This modification allows shifting the maxima of the characteristic spectra in a higher degree than using one substituent group. The absorption and the emission were shifted in the longer wavelength range on 22 nm and 40 nm, respectively (shown in Figure 5.12). It allows to come out from the region of the absorption of the PdTBP sensitizer and to move into the transparency window of both PdTBP and PtTBP sensitizers.

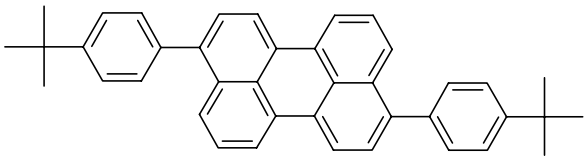

Figure 5.11 Chemical structure of Y-635 (3,10-bis(4-*tert*-butylphenyl)perylene).

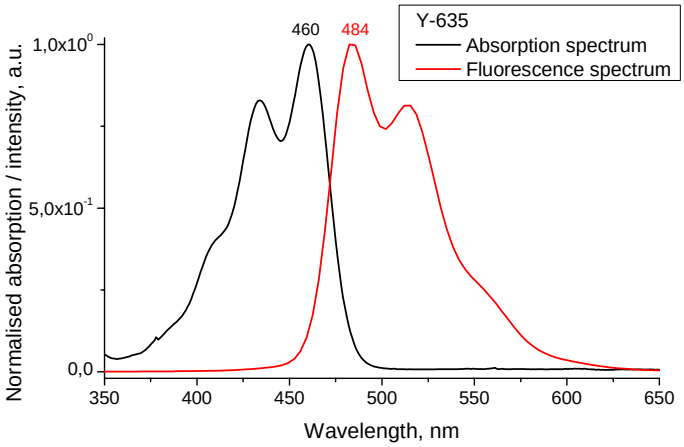

Figure 5.12 Absorption (black) and fluorescence (red) spectra of Y-635 dye in toluene.

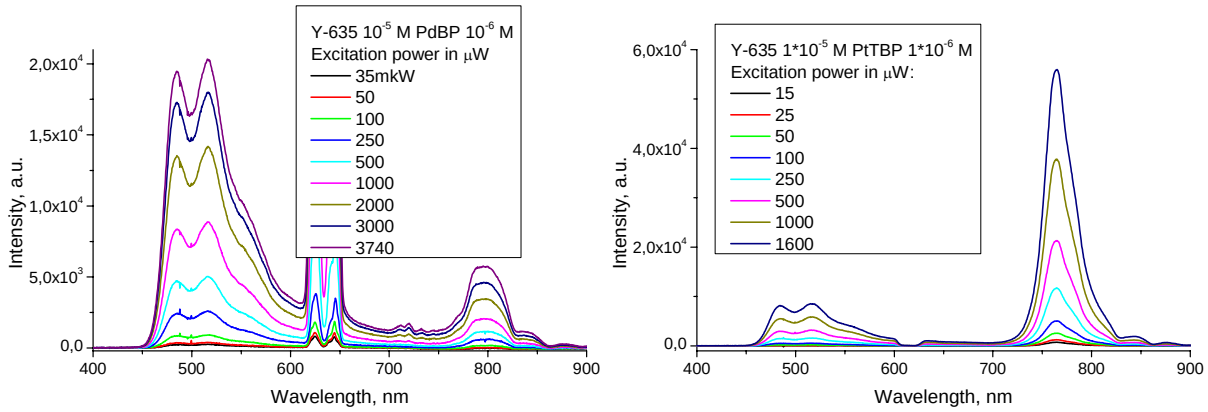

Figure 5.13 Spectra of generated UC and residual phosphorescence in dependence on excitation power for the emitter Y-635 ($1 \cdot 10^{-5}$ M) and sensitizers PdTBP ($1 \cdot 10^{-6}$ M) (left) and PtTBP ($1 \cdot 10^{-6}$ M) (right) dissolved in toluene.

The efficiency of the UC generation in the combination with PdTBP sensitizer (spectra are shown in Figure 5.13 (left)) increased twice in compare to the perylene and was estimated to reach 4% (at the maximal excitation power), whereas for the combination with the PtTBP sensitizer (see Figure 5.13 (right)) the increase of the efficiency was not so significant and the external Q.Y. was as high as 3.1%.

5.5 3-(Hex-1-ynyl)perylene or Y-792

The next kind of a substituent to be investigated was hexynyl group. The accordingly monosubstituted molecule became a short name Y-792 (see Figure 2.1). The maximum of its absorption strongly shifted in the same degree as for Y-635 molecule, namely up to 459 nm, but the maximum of the emission spectrum moved in a lesser extend and is similar to Y-794 molecule with the maximum of the emission at 466 nm. The obtained molecule, thereby, has a small Stokes shift and will be stronger subjected to the reabsorption effect at the higher concentrations.

The obtained UC generation in a combination of Y-792 with both sensitizers was one of the most efficient among all the investigated sensitizer-emitter pairs. Thus, for PdTBP the Q.Y. reached 4% (spectra is shown in Figure 5.16 (left)), whereas for PtTBP (see Figure 5.16 (right)) the Q.Y. value was equal to 2.9%.

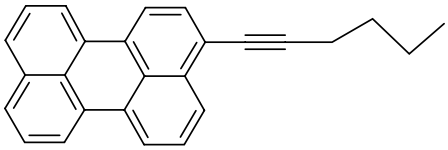

Figure 5.14 Chemical structure of 3-(Hex-1-ynyl)perylene (Y-792).

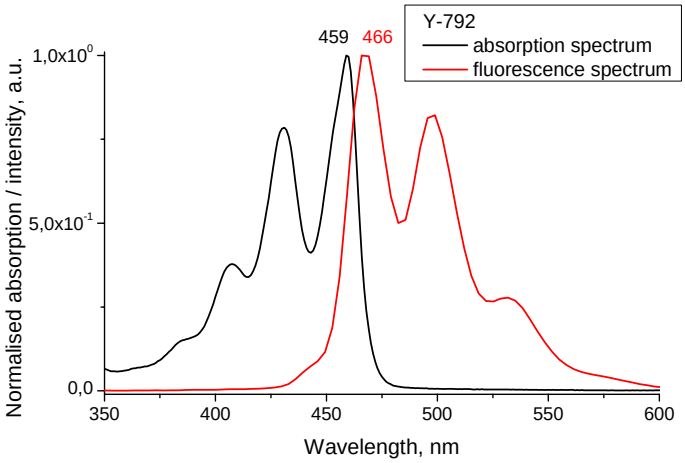

Figure 5.15 Absorption (black) and fluorescence (red) spectra of Y-792 dye in toluene.

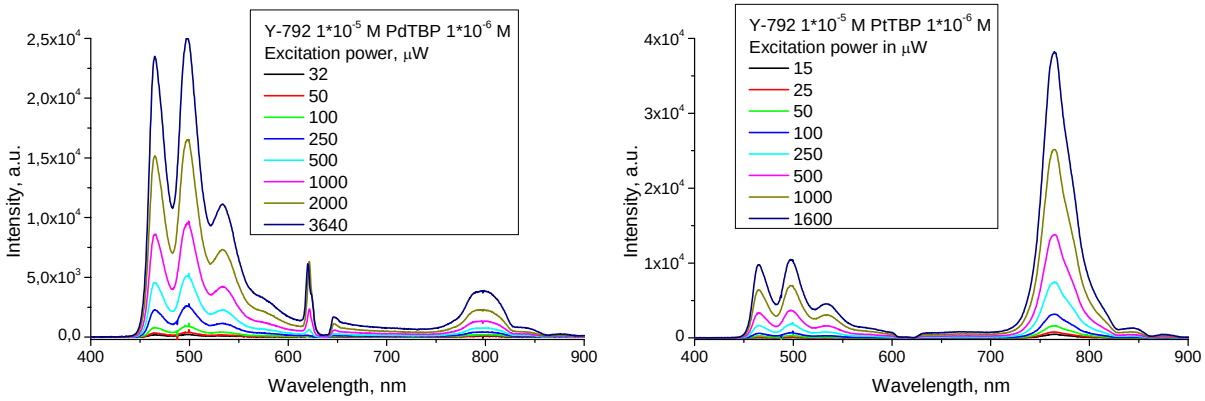

Figure 5.16 Spectra of generated UC and residual phosphorescence in dependence on excitation power for the emitter Y-792 with the concentration $1 \cdot 10^{-5}$ M and sensitizers PdTBP ($1 \cdot 10^{-6}$ M) (left) and PtTBP ($1 \cdot 10^{-6}$ M) (right) dissolved in toluene.

5.6 3,10-Di(hex-1-ynyl)perylene or Y-793

The molecule with two hexynyl substituents was also investigated. The resulting chemical structure of the modified perylene, which was named Y-793, is shown in Figure 5.17. The extremely strong shift of both absorption and fluorescent emission was obtained on around 40 nm, resulting in the emission maxima movement in the green region of spectra with the corresponding 479 nm for the absorption and 487 nm for the fluorescence spectra.

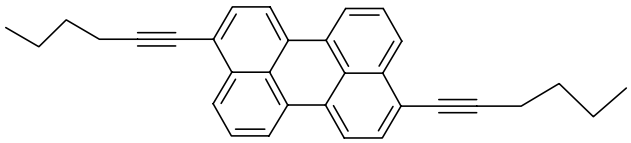

Figure 5.17 Chemical structure of 3,10-Di(hex-1-ynyl)perylene (short name Y-793).

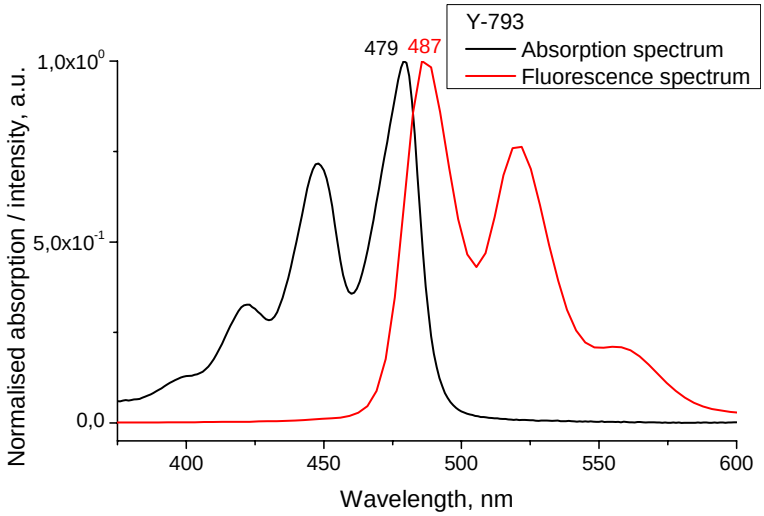

Figure 5.18 Absorption (black) and fluorescence (red) spectra of Y-793 dye in toluene.

The efficiency of UC generation by this molecule with the PdTBP as the sensitizer (the spectra are shown in Figure 5.19 (left)) had the small increase in comparison with the perylene-PdTBP pair and reached 2.3%, but for the combination of Y-793 with the PtTBP sensitizer (see Figure 5.19 (right)) the efficiency was even lesser than those for perylene and was not higher than 1.85% at 1 mW of excitation power. At the maximal excitation power (2.9 mW) it was even less and was equal to 1.6%.

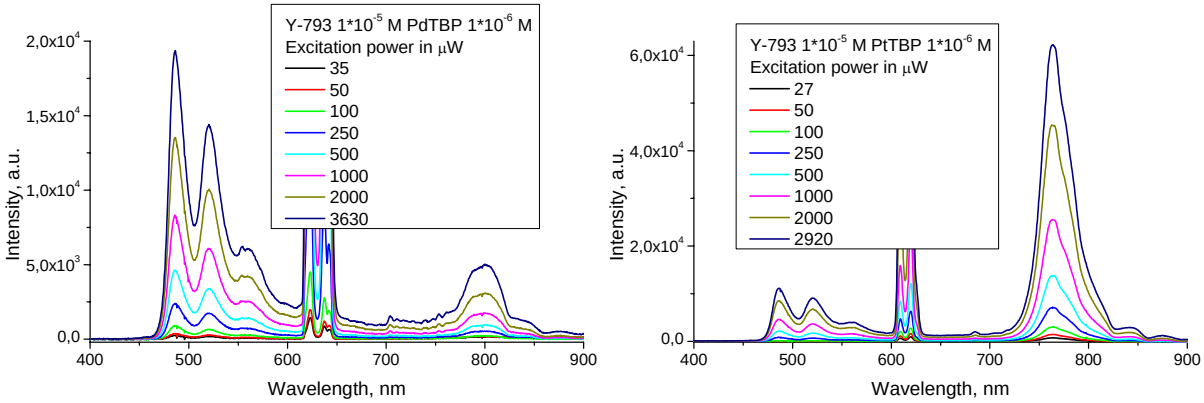

Figure 5.19 Spectra of generated UC and residual phosphorescence in dependence on excitation power for the combination of emitter Y-793 with the concentration $1 \cdot 10^{-5}$ M and sensitizers PdTBP ($1 \cdot 10^{-6}$ M) (left) and PtTBP ($1 \cdot 10^{-6}$ M) (right) dissolved in toluene.

5.7 3-(3,3-Dimethylbutyn-1-yl)perylene or Y-824

The further shift at one substituent application can be obtained by using of 3,3-dimethylbutynyl group. This perylene modification (named Y-824, the molecule structure is shown in Figure 5.20) has the same brutto-formula as the previously investigated Y-792. The difference in the structures (linear butyl vs. tert-butyl group) even does not influence on the absorption and emission spectra (maxima of absorption (459 nm) and emission spectra (467 nm) (see Figure 5.21) are the same). However, the bulky tert-butyl groups provide a better solubility and avoid the π–stacking of the perylene moieties stronger than the linear n-butyl groups. Additionally, the suppression of the aggregation of the fluorophore molecules in the solution usually leads to the increase of the Q.Y. of fluorescence. Such a phenomenon can also explain the higher efficiency of Y-824 in the UC measurements as compared to Y-792.

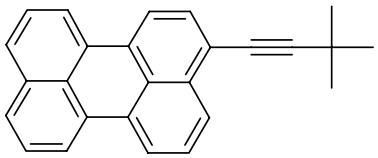

Figure 5.20 Chemical structure of 3-(3,3-Dimethylbutyn-1-yl)perylene (named Y-824).

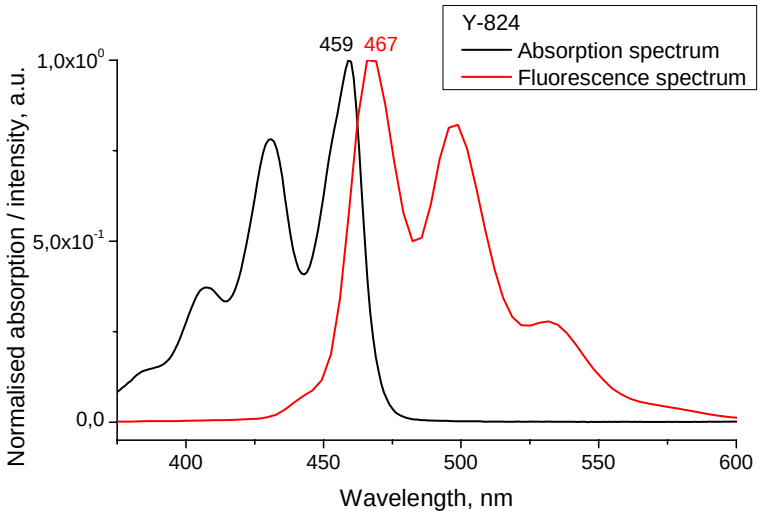

Figure 5.21 Absorption (black) and fluorescence (red) spectra of Y-824 dye in toluene.

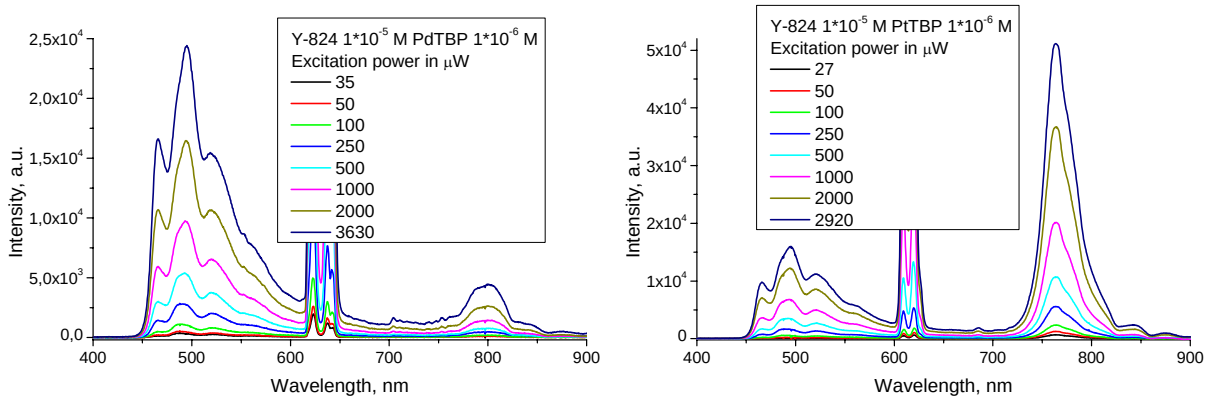

Figure 5.22 Spectra of generated UC and residual phosphorescence in dependence on excitation power for the combination of emitter Y-824 with the concentration $1 \cdot 10^{-5}$ M and sensitizers PdTBP ($1 \cdot 10^{-6}$ M) (left) and PtTBP ($1 \cdot 10^{-6}$ M) (right) dissolved in toluene.

Thus, the use of 3,3-dimethylbutynyl as the substituent for perylene molecule has the highest influence on the increase of the efficiency of the triplet energy transfer and annihilation processes among all the modified perylenes. For the combination of Y-824 having concentration $1 \cdot 10^{-5}$ M with the sensitizer PdTBP being in concentration $1 \cdot 10^{-6}$ M the efficiency closes to 5.1% (the spectra of the generated in sample emission are shown in the left side of Figure 5.22). For the combination with the platinum sensitizer the resulting efficiency was high as well and reached 3% (measured UC spectra are presented in Figure 5.22(right)).

5.8 3,10-bis(3,3-Dimethylbutyn-1-yl)perylene or Y-805

Perylene molecule substituted by two 3,3-dimethylbutynyl groups was named Y-805 (Figure 5.23). The comparable with Y-793 shifts of absorption and fluorescence spectra were achieved (see Figure 5.24). The corresponding maxima are located at 472 nm and 486 nm for the absorption and emission, respectively.

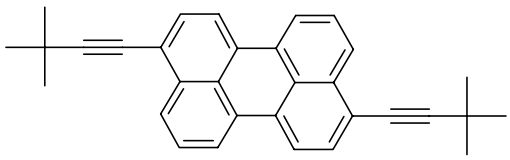

Figure 5.23 Chemical structure of 3,10-bis(3,3-Dimethylbutyn-1-yl)perylene (the short name is Y-805).

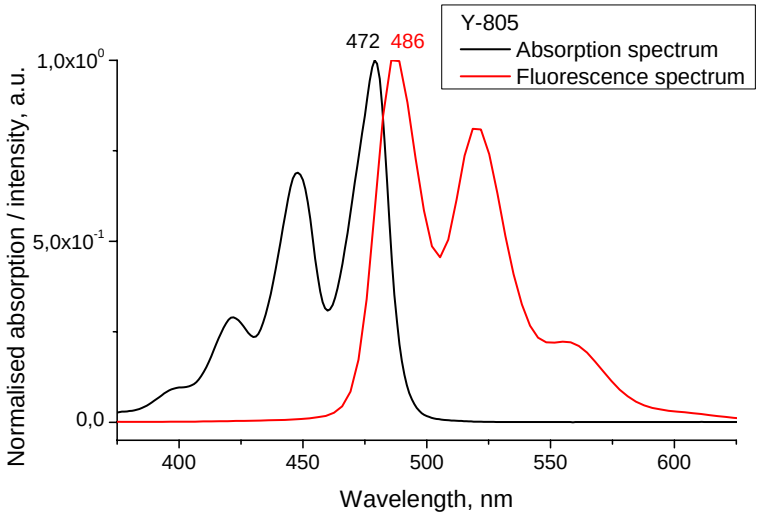

Figure 5.24 Absorption (black) and fluorescence (red) spectra of Y-805 dye in toluene.

The main emission of UC photons takes place in the region 500-600 nm. The moderate efficiency in 3.2% was obtained for the combination of the emitter with the PdTBP. For the mixture with the PtTBP the efficiency was comparable with the efficiency of perylene-PtTBP pair and reached 2.1%.

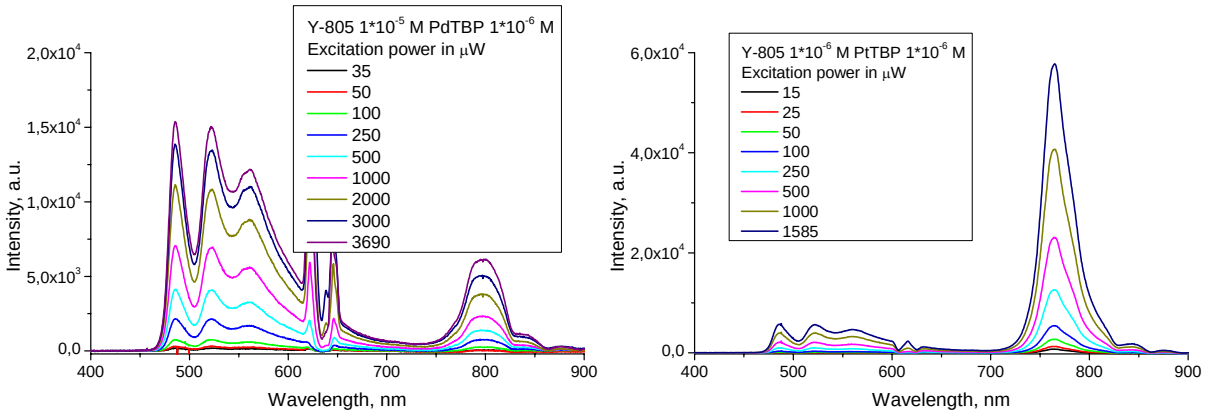

Figure 5.25 Spectra of generated UC and residual phosphorescence in dependence on excitation power for the combination of emitter Y-805 with the concentration 1·10^{-5} M and sensitizers PdTBP (1·10^{-6} M) (left) and PtTBP (1·10^{-6} M) (right) dissolved in toluene.

5.9 3-((4-*tert*-butylphenyl)ethynyl)perylene or Y-796

The biggest substituent we used for the modification of perylene core was (4-*tert*-butylphenyl)ethynyl group (the resulting molecule named Y-796 is shown in Figure 5.26). The addition of ethynyl to the 4-t*ert*-butylphenyl group increased the overall effect of the substituent on the shift of the singlet state of perylene, which in result has the same order as the two 4-t*ert*-butylphenyl groups (in Y-635 molecule). Thus, the absorption spectrum was shifted on 30 nm from the perylene maximum and the fluorescent emission on 37 nm.

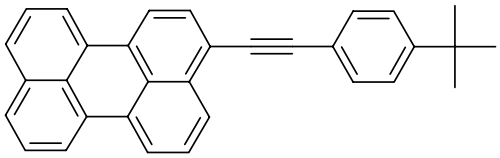

Figure 5.26 Chemical structure of molecule 3-((4-*tert*-butylphenyl)ethynyl)perylene (short name Y-796).

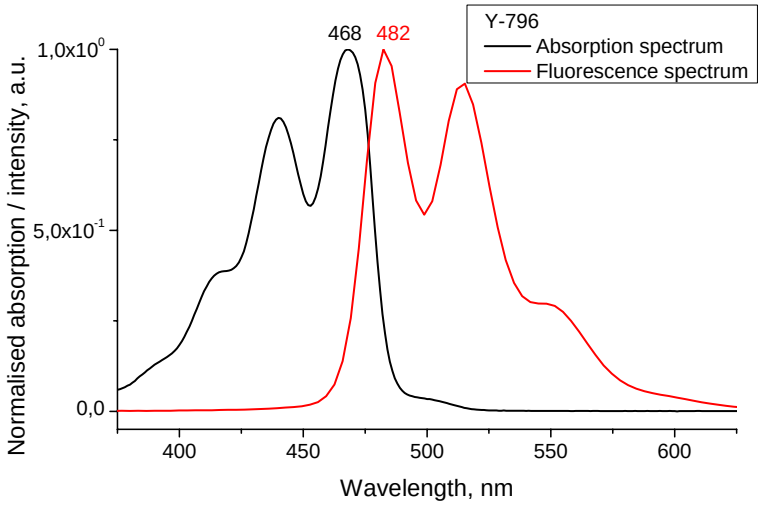

Figure 5.27 Absorption (black) and fluorescence (red) spectra of Y-796 dye in toluene.

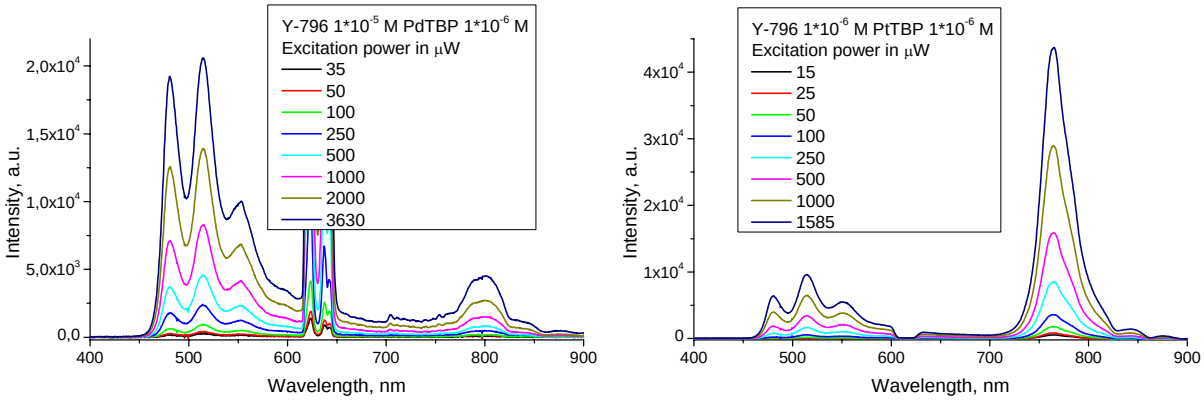

Figure 5.28 Spectra of generated UC and residual phosphorescence in dependence on excitation power for the combination of emitter Y-796 with the concentration $1 \cdot 10^{-5}$ M and sensitizers PdTBP ($1 \cdot 10^{-6}$ M) (left) and PtTBP ($1 \cdot 10^{-6}$ M) (right) dissolved in toluene.

The achieved UC generation efficiency in the mixture with PdTBP was definitely lower than those for Y-635 and reached only 3.1%. The effect on the generation of UC in the case of PtTBP was at the moderate level and the efficiency was estimated to be 2.7%.

5.10 3,10-bis((4-*tert*-butylphenyl)ethynyl)perylene or Y-795

The usage of two (4-*tert*-butylphenyl)ethynyl groups resulted in the biggest shift of the absorption and emission spectra among all the modified perylene molecules. The resulting molecule Y-795 is shown in Figure 5.29. Its absorption spectrum maximum is placed at 500 nm with the corresponding maximum of emission at 515 nm.

Despite of so big shift of the singlet state the efficiency of UC generation with PdTBP sensitizer (Figure 5.31) was still higher than for the perylene and reached 3%. In the combination with PtTBP, however, the lowest efficiency among all the investigated perylene-based molecules was measured and reached only 1.6%.

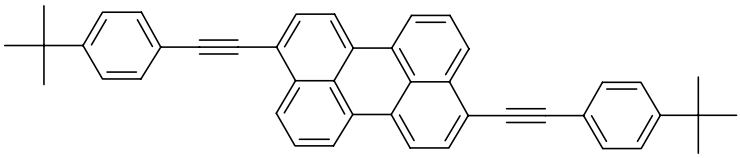

Figure 5.29 Chemical structure of the molecule 3,10-bis((4-*tert*-butylphenyl)ethynyl)perylene (given short name Y-795).

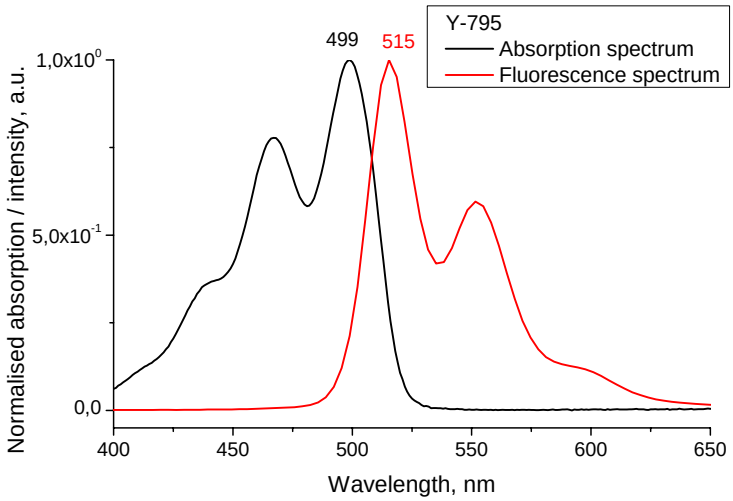

Figure 5.30 Absorption (black) and fluorescence (red) spectra of Y-795 dye in toluene.

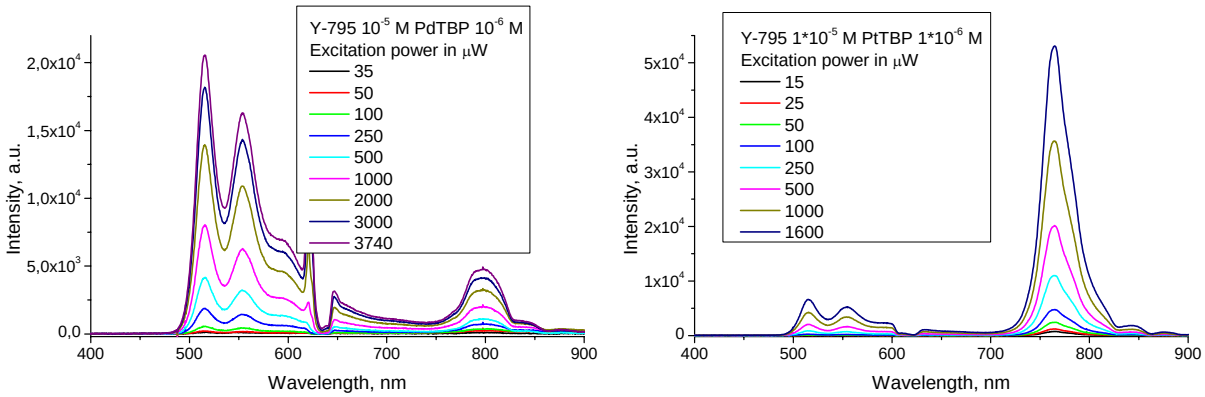

Figure 5.31 Spectra of generated UC and residual phosphorescence in dependence on excitation power for the combination of emitter Y-795 with the concentration $1 \cdot 10^{-5}$ M and sensitizers PdTBP ($1 \cdot 10^{-6}$ M) (left) and PtTBP ($1 \cdot 10^{-6}$ M) (right) dissolved in toluene.

5.11 Summary for new perylene based emitters

The new dyes, based on the modification of the perylene, were synthesized in our department and tested in the combination with TBP sensitizers for the application in the TTA –UC process. The effective emitters for the blue, green and yellow regions of spectra were found, that is especially important for the development and creation of all-organic transparent color display systems [18].

The efficient UC was successfully obtained for all modified molecules (the ratio between the sensitizer (PdTBP) and emitter of 1 to 10 and the corresponding concentrations $1 \cdot 10^{-6}$ M and $1 \cdot 10^{-5}$ M). The results of the Q.Y. determination for the combination of emitters with PdTBP and PtTBP sensitizers are summarized in Table 5.1. In comparison to perylene emitter, used as the reference sample, the maximal obtained efficiency increases by 2.6 times for the Y-824 molecule and PdTBP sensitizer. For PtTBP an increase of 1.4 times was observed in combination with Y-635 and Y-824 emitters.

The presence of a large amount of residual phosphorescence of the sensitizer and its tendency to saturate at the high excitation levels indicates unoptimised conditions for TTT and TTA processes.

Table 5.1 Quantum yields and emission parameters for different emitters ($1 \cdot 10^{-5}$ M) in UC systems with PdTBP ($1 \cdot 10^{-6}$ M) and PtTBP ($1 \cdot 10^{-6}$ M) sensitizers.

Emitter	Range of emission, nm	Maximum of emission, nm	Q. Y. of upconversion with PdTBP, %	Q. Y. of upconversion with PtTBP, %
Perylene	440 - 515	473	2	2.2
Y-794	450 - 550	497	2.8	2.4
Y-635	470 - 560	517	4	3.1
Y-792	460 - 540	498	4	2.9
Y-793	475 - 565	487	2.3	1.85
Y-824	460 - 545	496	5.1	3
Y-805	480 - 605	487, 522	3.2	2.1
Y-796	475 - 560	515	3.1	2.7
Y-795	504 - 575	515	3	1.6

6 Conditions for the efficient TTA – UC observation

There are many parameters that can be varied during an investigation of the TTA – UC process: sensitizer and emitter molecules, where the mutual arrangement of the singlet and triplet states plays the crucial role, concentrations of the dyes and their mutual ratio, the viscosity parameters of a used solvent, the concentration of the residual oxygen in the solution, the temperature of the surroundings, the characteristics of the excitation radiation and its intensity.

It is clear that it is impossible to investigate all the factors and their influence on the TTA – UC process, so one should fix some factors and vary the others. In this work the following parameters were stated to be constant:

- The ambient temperature was close to 22 ºC.
- The oxygen concentration of surrounding atmosphere could not be measured for each sample individually, because it was determined by the total oxygen level in glovebox during a sample preparation time. Additionally, the influence of the oxygen amount on the efficiency of the UC generation is dependent on the dye concentration. Thus, the lower is the dye concentration – the larger the influence of the oxygen. The upper limit of the oxygen concentration was chosen to be 5 ppm. All the samples were sealed only when the oxygen level in glovebox did not overcome this value.
- The choice of the solvent is not a trivial task. The solubility of the dyes and their energy levels positions are dependent on the solvent. To restrict the experimental parameters, toluene (sealed under argon, extra dry) was used as standard solvent for the most part of the samples.

The optimization of the following parameters will be considered in this part: the excitation intensity and the sample irradiation parameters, the dye concentrations from the point of view maximal Q.Y. value achievement, the dependence of the triplet state energy utilization from the ratio between the relative quantity of emitter molecules to sensitizer molecules, and the assignment of different functions to the different parts of the molecule for the UC efficiency increase.

6.1 Dependence of TTA – UC process on excitation beam diameter

As it was explained earlier, the TTA – UC process is based on the long-lived triplet states. For sensitizers, where the ISC process probability between the singlet and triplet state is strongly enhanced, the lifetimes of excited triplet state in the absence of a quencher can be as high as hundreds of microseconds. For a highly fluorescent emitter molecule, which received the energy from a sensitizer through TTT process, the decay time of the triplet state can be several orders longer.

The simple 2D-illustration for the following discussion is presented in Figure 6.1.At the sample irradiation by the focused light, the excitation of sensitizer molecules into the triplet state takes place only in the region of irradiation. During the triplet state lifetime the molecules (or the triplet state energies), which are on the edge of the region of excitation, can escape from the main excited region into a non-excited one. Without consideration of the TTA between the sensitizer molecules, the probability for the excited sensitizer molecule to meet there the unexcited emitter and to transfer the triplet state energy should be even higher than in the main excitation region, while the concentration of not excited emitters is higher there. From the other side, the probability of the excited emitter to meet another emitter molecule in the excited state and to annihilate with a photon creation is significantly lower than in the main excited region. It is evident that the smaller the diameter of the excitation spot is, the higher is the ratio between the number of molecules, which are on the border, to the total amount of the excited molecules. In the same time, the smaller is the excited region area, the smaller is the distance that should be overcame to leave the main excitation region.

From this consideration follows that the energy migration should depend on the velocity of molecules movement and, therefore, on the viscosity of the solvent. The following experiment was devoted to the investigation of the triplet-state energy migration rate and the determination of the optimal parameters for the spot diameter of UC samples excitation.

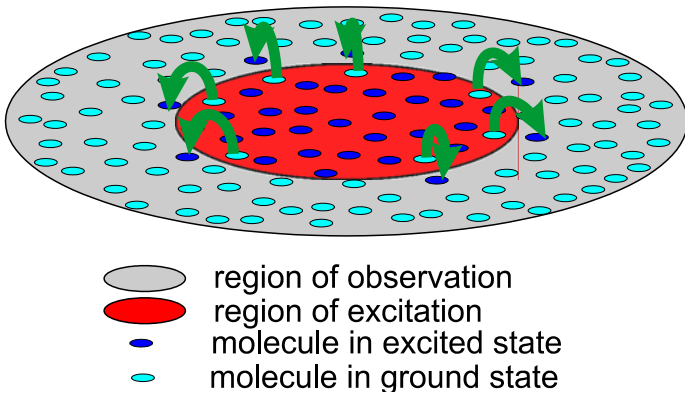

Figure 6.1 Illustration of the process of energy migration from the region of excitation.

Two media with a different viscosity were chosen: the toluene and more viscous oligo-styrene (PS400). The set of the samples with a different ratio emitter to sensitizer was prepared both in toluene and in oligo-styrene. The concentration of the sensitizer was equal to $2 \cdot 10^{-5}$ M for all the samples. The concentration of the emitter was varied to be 5, 10, 20 and 40 times higher than those for the sensitizer and was equal $1 \cdot 10^{-4}$ M, $2 \cdot 10^{-4}$ M, $4 \cdot 10^{-4}$ M and $8 \cdot 10^{-4}$ M, correspondingly.

By the movement of the rear lens in the spatial filter (shown on the experimental scheme in Figure 3.2) the diameter of the excitation spot on the sample can be varied from 35 μm up to 420 μm (seen in Figure 3.5). The detection area on the sample is determined by a relation between the focal distances of the emission collecting lens (100 mm), fiber coupler (25 mm) and the fiber core diameter (μm) and is around 2 mm in diameter.

For each value of the spot diameter the excitation power was attenuated in order to keep the excitation intensity (ratio of the incident power on the excited region area) on the constant level, which was chosen to be equal to 1.28 W·cm^{-2}. The constant intensity should provide in the excitation region the equal concentration of excited states for each sample with the same sensitizer concentration. In this way, the excitation conditions for all samples will be kept constant during the variation of the beam size.

In the Figure 6.2 the Q.Y. of UC in dependence on the excitation beam diameter for the toluene samples is shown. It is seen that in the region of diameters 40 – 200 μm the Q.Y. of UC strongly depends on the beam size. At the minimal possible diameter (40 μm) the efficiency of all samples is extremely low. The Q.Y. is growing up with the beam size increase and this tendency is stronger for the lower emitter to sensitizer ratios.

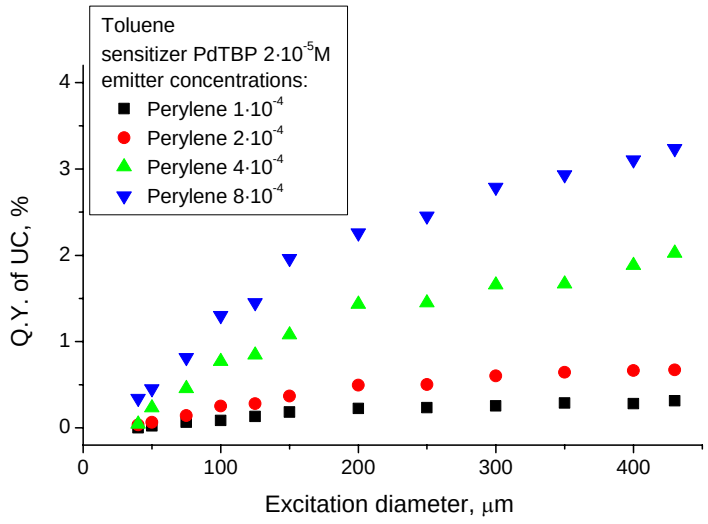

Figure 6.2 Dependence of the Q.Y. of UC on the excitation beam diameter at the constant intensity of excitation (1.28 W·cm^{-2}) for the samples prepared in toluene.

Thus, the increase in the efficiency at a beam diameter increase from 50 μm up to 200 μm amounted 9, 7.6, 6 and 5 times for the samples with 5, 10, 20 and 40 ratios of concentrations. For the beam sizes higher than 200 μm the dependence slowly tends to the highest value of Q.Y. and in the range of diameters 200 – 430 μm increases in near 1.4 times for all the samples.

In the viscous oligo-styrene PS400 this dependency is not so pronounced (see Figure 6.3). Even at the lower beam diameter the efficiency is quite high and reaches 1 - 1.5%. It is seen, that the increase of the ratio between the sensitizer and emitter concentrations almost not influences on the character of the dependence. Nevertheless, the Q.Y. grows up in around 2.5 times at the beam size increase from 40 μm up to 200 μm and almost not changes (the increase is only 10%) at the further excitation spot magnification.

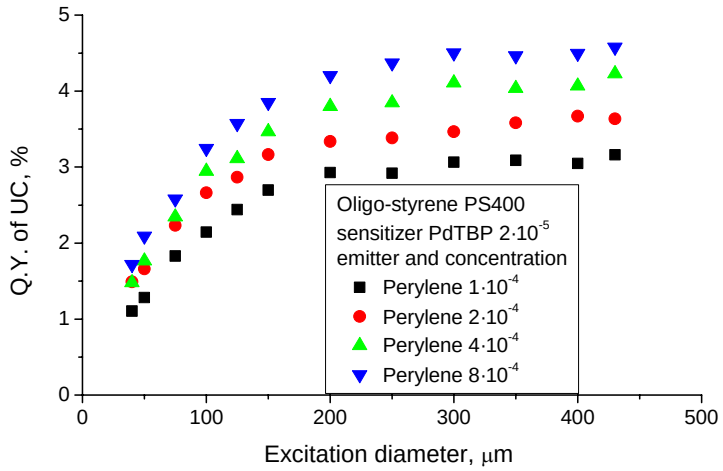

Figure 6.3 Dependence of the Q.Y. of UC on the excitation beam diameter at the constant intensity of excitation (1.28 W·cm^{-2}) for the samples prepared in oligo-styrene.

Comparing the data from both experiments one can evaluate the rate of the triplet state migration. Thus, taking for the migration distance for the volatile solvent (toluene) of 100 μm and for the average decay time of the excited triplet state of emitter at least 100 μs (it is equal to the decay time of the delayed fluorescence; the value is taken from the experimental data reported in the part 7), the estimated value of the energy migration velocity is approximately equal to 1 m·s^{-1}, that is orders higher than the velocity of the molecular mass transport [98]. It means that the intermolecular triplet energy transfer is very effective. However, in the same time the viscosity of the media strongly influences the energy migration and, therefore, the transfer mechanism is also related to the local mobility and orientation of the participating molecular species.

As a conclusion, if the detection area is not restricted by the used optical scheme, the measurements of Q.Y. of UC should be conducted with a highest possible diameter of the excitation spot. If the region of observation is limited, the sizes of excitation beam at least 200 μm are strongly advised.

6.2 TTA – UC process dependence on excitation intensity

For all nonlinear UC processes the excitation intensity plays a critical role. As it was previously mentioned, due to its origin the TTA – UC can be obtained even at extremely low intensities of irradiation. Thus, the successful TTA – UC of non-coherent sun-light (focused up to intensity of 0.1 – 1 W·cm^{-2}) was previously reported [13, 14, 80].

In order to investigate the dependence of the TTA – UC generation on the excitation intensity the following experiment was conducted. The sample, containing perylene (5·10^{-4} M) and PdTBP (5·10^{-5} M) in toluene, was prepared in glovebox and sealed in vitrotube. It was irradiated by the CW emission of the laser diode having the wavelength 635 nm. The emission was focused into the area of nearly 0.1 mm^2 (beam spot diameter is 350 μm). By the use of neutral filters and a reflective attenuator the excitation power was varied from 0.6 μW up to 6 mW that corresponds to the excitation intensities variation from 0.64 mW·cm^{-2} up to 6.4 W·cm^{-2} (four orders of change of the excitation intensity). The spectra of the UC and the residual phosphorescence were detected by the CCD spectrometer at different accumulation times. At an accumulation time setting change the signal was detected at both accumulation times in order to prove the scaling factor. The spectra were correspondingly recalculated after the measurements.

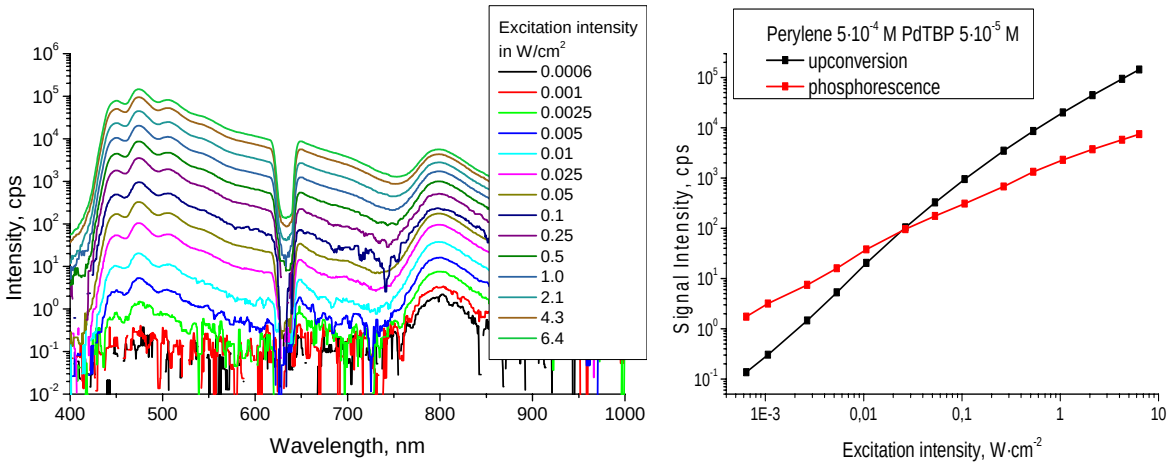

Figure 6.4 Spectra (left, logarithmic scale) and peak intensity (right) of UC and residual phosphorescence signals in dependence on the excitation intensity for the sample containing perylene (5·10^{-4} M) and PdTBP (5·10^{-5} M) dissolved in toluene.

The experimentally detected spectra plotted in the logarithmic scale are shown in Figure 6.4 (left). The emission of perylene is presented in range 440 nm – 550 nm, and the residual phosphorescence of PdTBP is centered at 800 nm. It is seen that even at extremely low excitation levels the UC photons are created (perylene emission spectrum is clearly distinguished from the noise even at excitation intensity in order of 2.5 $mW \cdot cm^{-2}$).

The higher the intensity of excitation, the more triplet states are created in the excitation area and, therefore, the higher the probabilities of the TTT and the subsequent TTA processes are. These arguments are proven by the experimental data. Thus, the slope of growth of the UC signal at the lowest irradiation levels was equal to 1.85, at the moderate irradiation – 1.5 and becomes almost linear (the slope, fitted for the last three points on the graph, reached 1.07). It should be noted, that the UC pair perylene – PdTBP has the moderate efficiency and for the measured sample the Q.Y. is equal to only 2.5%. With an increase of the UC pair efficiency the intensity dependence tends to linear even at the lowest excitation levels.

The observation of a sublinear dependency of the UC signal on the excitation intensity was published at the very beginning of the UC investigations [70]. However, almost a decade some authors held the positions of the classical theory of the intermolecular interaction, predicted the square dependence for the bimolecular processes [99] (that is actually valid only for extremely low concentrations of the molecules in excited triplet state regarding the molecules in ground state). As a result, many articles contain the dependencies of an experimental signal to an excitation intensity which were evidently wrong fitted (the example is shown in Figure 6.5) because of the erroneous background theory.

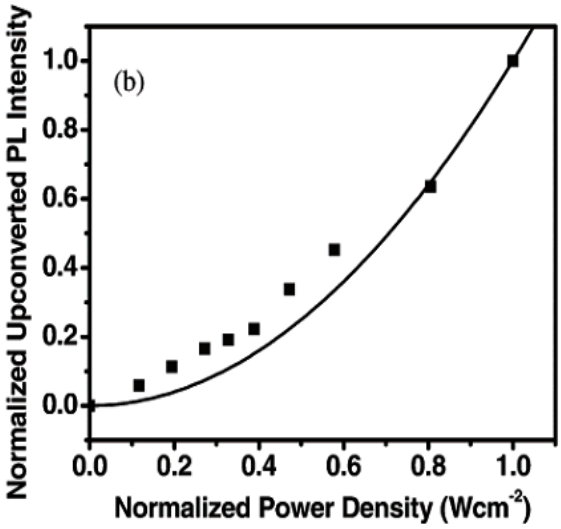

Figure 6.5 The example of the obviously erroneous conducted data fitting. Reprinted with permission from [89]. Copyright © 2008, American Chemical Society.

Newly published articles [26, 100] were devoted to the calculation of the multimolecular kinetic equations applied to the TTA – UC process. The progressive transfer from the almost quadratic up to the linear dependence at the certain conditions was shown. The interplay between velocities of an energy usage by molecules plays a crucial role. Thus, when the probability of the dissipation of the excited triplet state energy in a single-molecule process (like the phosphorescence and the nonradiative energy dissipation for the cases both sensitizer and emitter) is much higher than those for the bimolecular TTA process, the final dependence will tend to the quadratic behaviour. From the other side, when the energy is fast transferred to the emitter and the TTA process is effective, the dependence will tend to the linear relation between the numbers of emitted and absorbed photons. The efficient TTT process and long-living emitter triplet states were claimed to be the main points in efficient TTA – UC in the noted publication [100] and fully overlap with the postulated by us requirements (2.5)-(2.8).

For the relatively small concentration of the PdTBP sensitizer ($5 \cdot 10^{-6}$ M) it was prepared the set of the samples, containing different amounts of emitter (perylene). The ratio between the concentrations of the emitter and the sensitizer matched the values 1 (2, 5, 10, 20 and 50) to 1 (logarithmic concentration chain). As it seen in Figure 6.6 (left), the detected UC signal is growing for all the samples with increase of the excitation intensity. The corresponding slope (Figure 6.6 (right)) is changing from 1.6-1.7 down to 1.15 for most of the dependencies at an excitation intensity increase. For the small emitter to sensitizer concentrations ratios the slope value is bigger, than for the higher ratios. It indicates the less effective energy transfer and the TTA process in these samples.

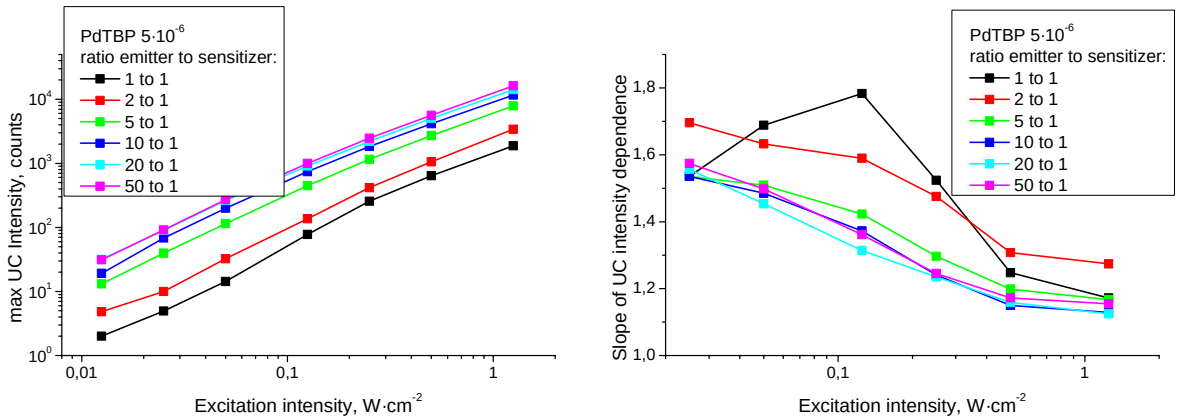

Figure 6.6 The dependence of the maxima of the UC signal on the excitation intensity (left) and the corresponding slope (right) (first derivative) of the dependencies for the set of the samples containing perylene as emitter (concentrations are $5 \cdot 10^{-6}$ M – $2.5 \cdot 10^{-4}$ M) and PdTBP concentration of $5 \cdot 10^{-6}$ M as the sensitizer.

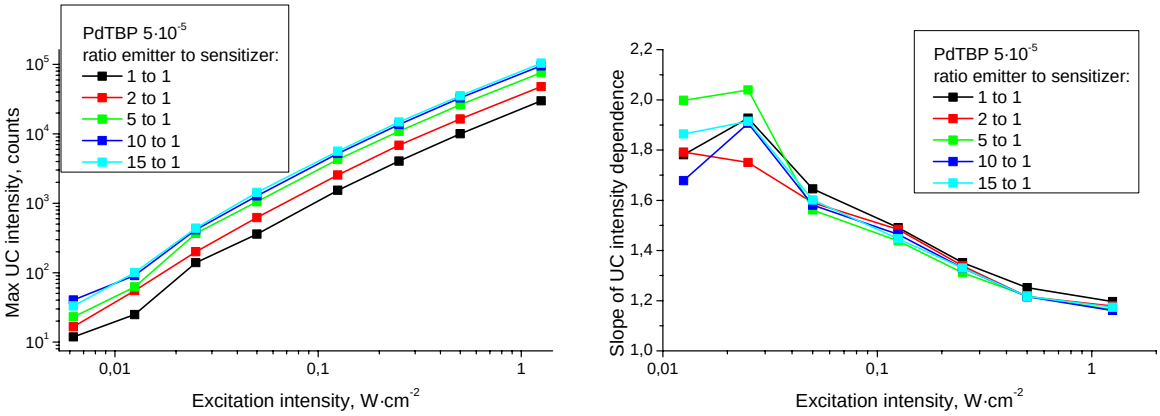

Figure 6.7 The dependence of the maxima of the UC signal on the excitation intensity (left) and the corresponding slope (right) (first derivative) of the dependencies for the set of the samples containing perylene as emitter (concentrations are $5\cdot10^{-5}$ M – $7.5\cdot10^{-4}$ M) and PdTBP concentration of $5\cdot10^{-5}$ M as the sensitizer.

For an order higher concentration of the sensitizer (PdTBP), namely $5\cdot10^{-5}$ M, the similar set of the samples was prepared. The corresponding emitter (perylene) concentrations match the ratio 1 (2, 5, 10 and 15) to 1 part of the sensitizer and were in the region from $5\cdot10^{-5}$ M up to $7.5\cdot10^{-4}$ M. The higher ratios were not accessible, because the limit of the perylene solubility in the base toluene solution was reached (the highest obtained perylene concentration in toluene of $1\cdot10^{-3}$ M was achieved).

In opposite to the previous case, no strong dependence of the ratio between the emitter and the sensitizer on the resulting slope value was detected. As it seen in Figure 6.7, the corresponding slopes of dependencies become almost equal at the moderate excitation levels and tend to the same value of around 1.16 at the further excitation intensity increase. The absence of this dependence is explained by the high total concentrations of the molecules of both types and, as a result, the efficient TTT and the TTA processes are happening.

It should be noted, that the oxygen, as an extremely efficient triplet states quencher, plays the crucial role in this behavior. It interacts both with the sensitizer and the emitter molecules, consuming the triplet state energy, and is not involved in the process of the TTA. As a result, in the first approximation its presence is equivalent to the increase of the energy dissipation in the single-molecule process and, therefore, pushes the UC intensity dependence to the square behavior.

Obviously, the excitation intensity can be easily increased to enlarge the overall efficiency of the process. However, for the case of a investigation of the TTA –UC process, devoted to a direct sun-light conversion or to an enhancement of the efficiency of organic solar cells, one should set the experiment conditions approaching to the real. It means that the maximal excitation light intensity should stay on the low level and not exceed the conditions corresponding to the low sun-light concentration (up to 100 times, that corresponds to the intensities of an order 0.1 $W \cdot cm^{-2}$).

6.3 The dependence of TTA – UC on the dyes concentration

It was already shown that the concentration of the used emitter and sensitizer and especially the ratio between them is extremely important for the process of the energy transfer and the triplet states annihilation. Thus, a high concentration of the sensitizer molecule provides a high absorption of the excitation photons, and, as a result, increases the amount of the excited triplet states, which could serve as donors of the energy for the emitter molecules. The high concentration of the emitter will result in the high concentration of the energy acceptors around the excited sensitizer molecule and, subsequently, to the higher probability of the triplet energy transfer and the consequent TTA process. Additionally, the increase of absolute dye's concentrations will lead to a decrease of the average distances between the molecules (proportionally to the cube-root from a concentration) that will increase the probability of their interaction. Nevertheless, evident drawbacks of the high dye concentrations are: the collisional deactivation of the excited states with the consequent nonradiative energy dissipation, and the change of the spectrum of the generated emission because of the reabsorption effect.

To investigate the influence of the dyes concentration on the process of TTA – UC the following samples were prepared. For each of the four concentrations of the sensitizer starting from $5 \cdot 10^{-6}$ M and ending with $5 \cdot 10^{-5}$ M, the set of the samples with a varied emitter concentration was prepared. It was already mentioned, that the concentration of the stoke solution of the perylene was limited by the solubility in toluene and was equal to $1 \cdot 10^{-3}$ M. Therefore the samples with ratios between emitter and sensitizer higher than 50 to 1 were not prepared. The full list of the samples and the corresponding concentrations of the dyes are presented in the Table 6.1. For each sample the absorption measurements were done for a further Q.Y. calculation. The samples were excited by the CW radiation of the laser diode (635 nm), focused on the sample at the area of 0.4 mm^2. The deoxygenated in glovebox solution of perylene with the concentration of $5 \cdot 10^{-5}$ M was used as the standard for comparative Q.Y. determination. Its fluorescence spectrum at the known excitation power, as well as the spectrum of the excitation radiation, was measured. The Q.Y. of the UC generation was determined at the maximal excitation intensity, which has reached 1.25 $W \cdot cm^{-2}$.

Table 6.1 Samples for the TTA – UC dependence on dye's concentration and the corresponding quantum efficiency. The excitation intensity is equal to 1.25 W·cm^{-2}.

Sample name	Concentration of sensitizer (PdTBP), M	Concentration of emitter (perylene), M	Ratio between emitter and sensitizer concentrations	Quantum yield of upconversion, %
s121	$5\cdot10^{-6}$	$5\cdot10^{-6}$	1 : 1	0.5
s122	$5\cdot10^{-6}$	$1\cdot10^{-5}$	2 : 1	0.9
s123	$5\cdot10^{-6}$	$2.5\cdot10^{-5}$	5 : 1	1.8
s124	$5\cdot10^{-6}$	$5\cdot10^{-5}$	10 : 1	2.7
s125	$5\cdot10^{-6}$	$1\cdot10^{-4}$	20 : 1	3.1
s126	$5\cdot10^{-6}$	$2.5\cdot10^{-4}$	50 : 1	3.5
s131	$1\cdot10^{-5}$	$1\cdot10^{-5}$	1 : 1	0.7
s132	$1\cdot10^{-5}$	$2\cdot10^{-5}$	2 : 1	1.2
s133	$1\cdot10^{-5}$	$5\cdot10^{-5}$	5 : 1	2.2
s134	$1\cdot10^{-5}$	$1\cdot10^{-4}$	10 : 1	2.7
s135	$1\cdot10^{-5}$	$2\cdot10^{-4}$	20 : 1	3.4
s136	$1\cdot10^{-5}$	$5\cdot10^{-4}$	50 : 1	3.7
s141	$2\cdot10^{-5}$	$2\cdot10^{-5}$	1 : 1	0.7
s142	$2\cdot10^{-5}$	$4\cdot10^{-5}$	2 : 1	1.3
s143	$2\cdot10^{-5}$	$1\cdot10^{-4}$	5 : 1	2.1
s144	$2\cdot10^{-5}$	$2\cdot10^{-4}$	10 : 1	2.7
s145	$2\cdot10^{-5}$	$4\cdot10^{-4}$	20 : 1	3.0
s146	$2\cdot10^{-5}$	$8\cdot10^{-4}$	40 : 1	3.4
s151	$5\cdot10^{-5}$	$5\cdot10^{-5}$	1 : 1	0.8
s152	$5\cdot10^{-5}$	$1\cdot10^{-4}$	2 : 1	1.2
s153	$5\cdot10^{-5}$	$2.5\cdot10^{-4}$	5 : 1	2.1
s154	$5\cdot10^{-5}$	$5\cdot10^{-4}$	10 : 1	2.4
s155	$5\cdot10^{-5}$	$7.5\cdot10^{-4}$	15 : 1	2.7

The results of the calculation of the Q.Y. for each sample are presented in the last column of the Table 6.1. For the better comparison the obtained data are graphically summarized in the Figure 6.8. It is clearly seen, that the increase of the emitter concentration normally leads to the increase of the UC generation efficiency. The start of the saturation of the dependencies is seen for the sensitizer concentrations $5\cdot10^{-6}$ M and $1\cdot10^{-5}$ M. The highest Q.Y. of the UC was obtained for the concentrations of $1\cdot10^{-5}$ M for sensitizer and $5\cdot10^{-4}$ M for emitter. IT should be noted that the sample with PdTBP at the concentration of about $1\cdot10^{-5}$ M, being sealed in the vitrotubes having thickness 400 μm, absorbs about 10% of the incoming radiation. Thus, the requirement for the correct Q.Y. determination procedure (given in part 3.4) on the small sample absorption (optically diluted solution) are nearly fulfilled.

Based on these experiments, for the further investigations of the efficiency in different sensitizer-emitter pairs the following concentrations were taken as standard: $1\cdot10^{-5}$ M for a sensitizer and $5\cdot10^{-4}$ M for an emitter.

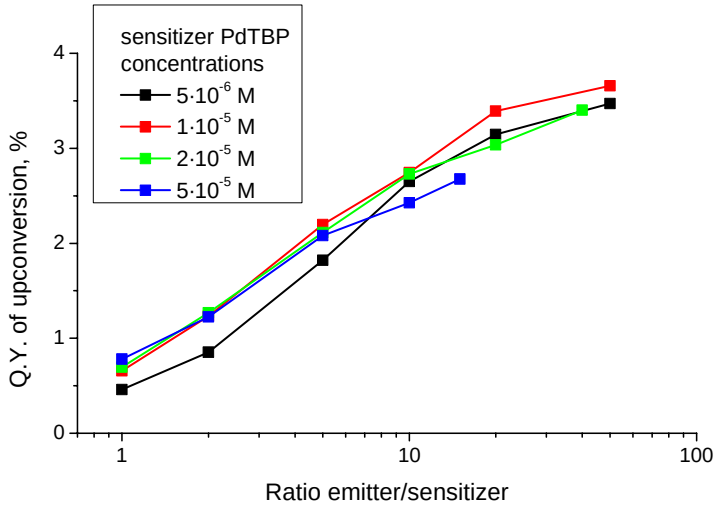

Figure 6.8 Dependence of the Q.Y. of UC on the ratio between emitter (perylene) and sensitizer (PdTBP) concentrations for the different sensitizer concentration.

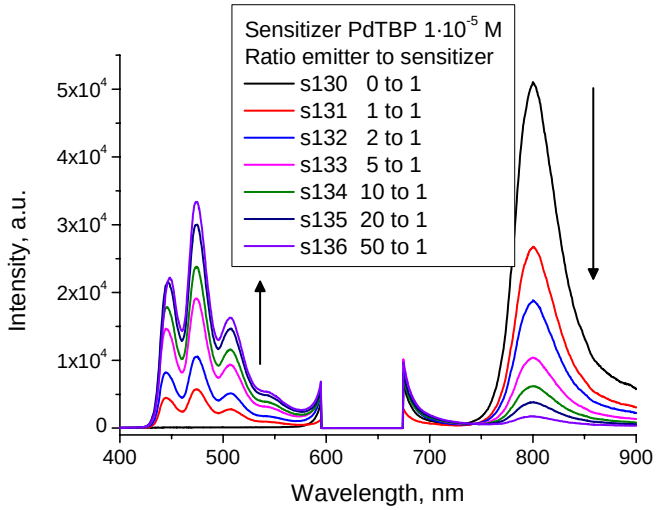

Figure 6.9 Spectra of generated UC and residual phosphorescence in dependence on the ratio between concentration of emitter and sensitizer. Sensitizer (PdTBP) concentration is equal to $1 \cdot 10^{-5}$ M, emitter (perylene) concentration is changed from 0 up to $5 \cdot 10^{-4}$ M. Excitation power is equal to 1.25 W·cm^{-2} for all the samples.

The efficiency of the processes involved in the TTA – UC could be also estimated by the spectra of sample emission and comparison of the relationship between the generated UC signal and the residual phosphorescence. Thus, with increase of the ratio between the emitter and sensitizer concentrations the phosphorescence of sensitizer is drastically decreases (shown in Figure 6.9), that is the result of effective TTT process, while UC signal is growing, indicating the efficient TTA process. As it seen in Figure 6.10, the ratio between signal of the generated UC and residual phosphorescence is almost linearly (the slope is around 1.15 for all the sensitizer concentrations) dependent on the emitter concentration. Shortly, the higher the emitter concentration, the better the sensitizer excited states are quenched and the higher the resulting UC signal should be.

In the same time, the increase of the emitter concentration in several times does not lead to the same increase of the luminosity (or the UC-photon flux) of the sample. Thus, as it seen in Figure 6.11 the dependence of the photon flux of the UC signal tend to saturate with an increase of the emitter concentration. From a point of view of practical application a balance between the desired photon flux and the materials consumption should be found.

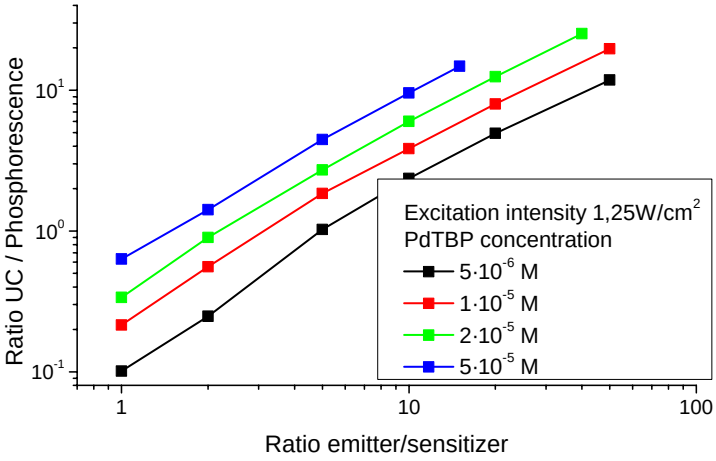

Figure 6.10 The dependence of the ratio between emitter delayed fluorescence and residual phosphorescence of the sensitizer as a function of relationship between dyes concentrations for different sensitizer concentrations.

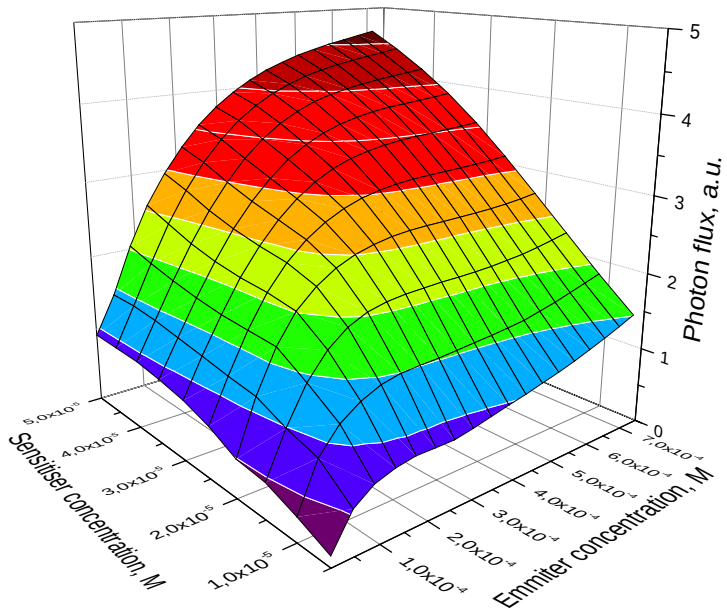

Figure 6.11 The dependence of the photon flux of generated UC on the sensitizer and emitter concentrations.

7 Synergetic effect in TTA – UC

The previously shown techniques on the increase of the Q.Y. of TTA – UC were based on modifications of an emitter or sensitizer molecules, the optimization of the relative and the absolute molar concentrations of the dyes. As it was shown during the creation of the library of new emitters, the efficiency of TTA – UC process can strongly vary even at a slight molecule modification. It was also previously described in the part 2.1 that TTA – UC consists from a many other processes, an efficiency of which can be also optimized. The main processes responsible for efficiency are TTT and TTA. It is essential to create a procedure for independent and simultaneous optimization of their efficiencies.

One of the ways is to use a multi-component system, where the process of energy transfer from a sensitizer is referred to one molecule, while another molecule will be responsible for the efficient energy utilization by the annihilation of the triplet states.

Let's imagine the system containing the sensitizer and two emitters, each of which works quite efficiently in a separate mixture with the sensitizer. In the mixture of all the dyes the concentrations of the excited triplet states of the both emitters are comparable, and, therefore, the probability of a hetero-interaction between different emitters should be comparable with the interaction between the identical emitter molecules. All possible interactions between the emitter molecules excited in the triplet states could be described by the following:

$$T^1_{emitter,i} + T^1_{emitter,j} \xrightarrow{TTA} S^1_{emitter,i} + S^0_{emitter,j} \longrightarrow$$

$$\longrightarrow S^0_{emitter,i} + S^0_{emitter,j} + h\nu_i, \quad i, j = 1,\ 2 \qquad (7.1)$$

where i and j are related to one of the molecules first or second type,

S and T – singlet and triplet states,

superscript 0 and 1 – the ground and first excited state (triplet or singlet).

If the excited singlet state of the first emitter has a lower energy than the second one, its state should be preferably populated during the hetero-TTA process. The consequent UC photon emission will take place from this energy state. In a dyad, where two emitters are linked by an intervening bridge or a molecular scaffold [101, 102], the fluorescence will always take place from the lowest energy state, whereas both components will serve as the triplet state acceptors independently.

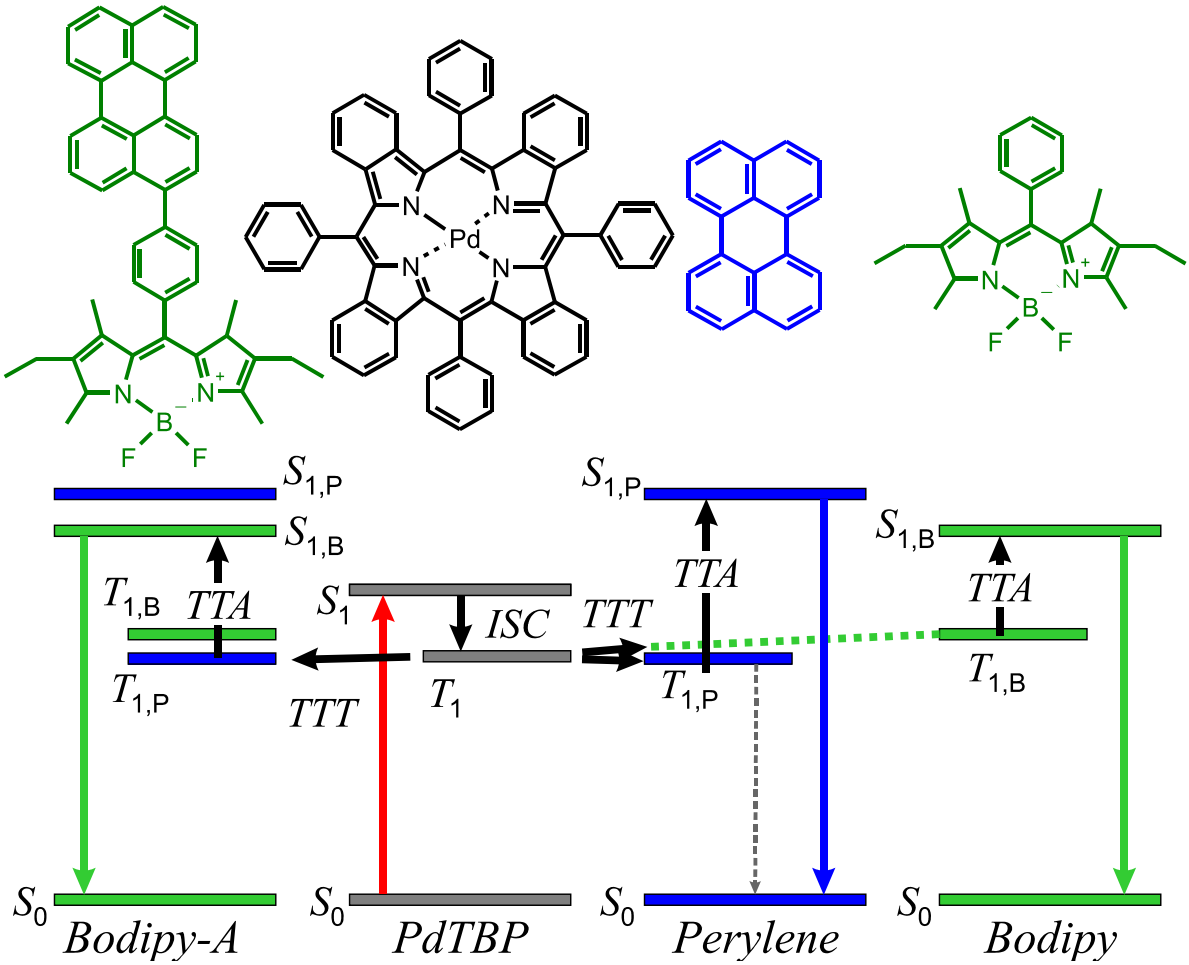

Figure 7.1 (top) Structures of the sensitizer (PdTBP) and emitters: perylene, 1,3,5,7-tetramethyl-8-phenyl-2,6-diethyl dipyrromethane•BF_2 (Bodipy) and dyad – 4-(perylene-3'-yl)-8-phenyl-1,3,5,7-tetramethyl -2,6-diethyl dipyrromethane•BF_2 (Bodipy-A). (bottom) Energetic scheme of the TTA − UC process in multi-component molecular system.

For the experimental proof of the above described idea two dyes were chosen to serve as emitters: perylene and Bodipy. Both of them are shown to be effective emitters in combination with TBP sensitizers [18, 34]. Corresponding dyad, named Bodipy-A, was synthesized in our laboratory by xxxxxxxxxxx and xxxxxxxxxxx. Chemical structures of all used compounds, as well as the corresponding energetic scheme of the TTA – UC process, are shown in Figure 7.1. The corresponding energies of the triplet and singlet states are known to be: for perylene 2.83 eV and 1.54 eV [90], for Bodipy – 2.35 eV and 1.64 eV [103], for PdTBP the triplet state energy is placed near 1.55 eV [37].

The comparison of these values shows, that for the perylene all the requirements for the efficient UC are matched: the triplet states are in the nearest proximity and the doubled energy of the triplet state is higher, than those needed to reach the excited singlet state, whereas for the Bodipy molecule one discrepancy is immediately evident: the triplet state has the higher energy, as those in PdTBP. The energy gap in 0.1 eV could be still overcome by

addition of thermal energy from surrounding [104], but it should strongly limit the efficiency of TTT process.

The samples containing perylene and Bodipy in molar concentrations $8 \cdot 10^{-5}$ M in the combination with $2 \cdot 10^{-6}$ M of PdTBP were prepared. All the experimental conditions like the temperature (room temperature, 22 ºC), the solvent (toluene), the excitation area (having diameter of 400 μm), and the excitation wavelength (635 nm) were kept constant for all samples and measurements. All samples were prepared and sealed in the nitrogen-glove box with the residual oxygen concentration less than 1 ppm.

As it seen in Figure 7.2, the highly efficient UC generation was obtained for the perylene. The chosen ratio of 1 to 40 between sensitizer and emitter concentrations provided the efficient TTT that resulted in almost absent phosphorescent signal.

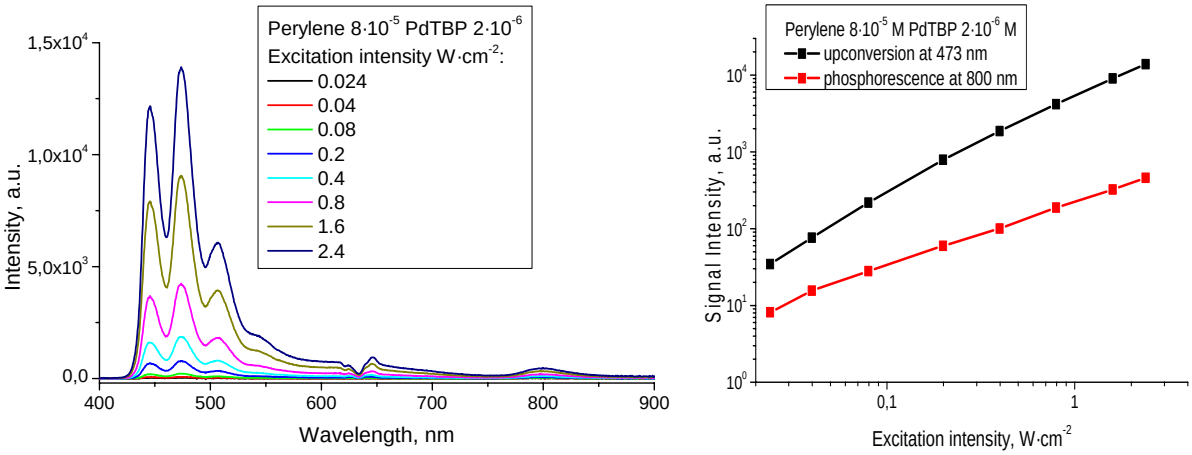

Figure 7.2 Spectra (left) and peak intensity (right) dependence of generated UC and residual phosphorescence signals in dependence on excitation intensity for the mixture of perylene ($8 \cdot 10^{-5}$ M) and PdTBP ($2 \cdot 10^{-6}$ M) in toluene.

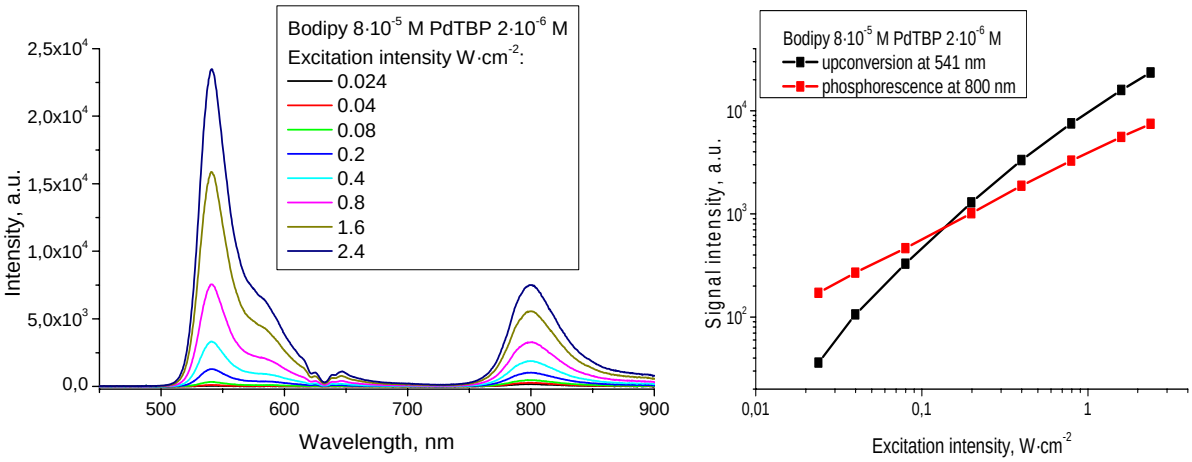

Figure 7.3 Spectra (left) and peak intensity (right) dependence of generated UC and residual phosphorescence signals in dependence on excitation intensity for the mixture of Bodipy ($8 \cdot 10^{-5}$ M) and PdTBP ($2 \cdot 10^{-6}$ M) in toluene.

The slope of the intensity dependence started from 1.5 at the low excitation levels and decreased down to 1.1 for the highest excitation intensity (2.4 $W \cdot cm^{-2}$). The overall efficiency of the UC was on the moderate level and was equal to 4.5%.

In contradiction with the perylene, the Bodipy seems to be the worse triplet acceptor. It is seen (Figure 7.3) that in the same conditions, as for the perylene, the residual phosphorescence signal was comparable with the generated UC signal and at the low excitation intensities was even higher. The intensity dependence at the lowest excitation levels had a slope of 1.8 that indicate the extremely low efficiency of the UC, and became almost linear (the slope factor is equal to 1.1) at the highest excitation intensities of 2.4 $W \cdot cm^{-2}$ (that nevertheless is extremely low from the point of view traditional nonlinear UC processes). Even with the huge amount of the not quenched phosphorescence the external Q.Y. of Bodipy – PdTBP pair was as high as 6% and is on one third more than for the perylene sample. It indicates an extremely high probability of TTA process, the efficiency of which compensates the weak triplet harvesting ability of the Bodipy.

To investigate the UC process and especially the efficiency of the constituent TTT and TTA processes, the experimental setup was additionally supplied by a temporal characteristics measurement unit (described in detail in part 3.1, the scheme of setup is shown in Figure 3.7). The radiation of the laser diode was modulated by an arbitrary pulse generator (TGA1244, *TTi Inc.*) with a caring frequency of 40 MHz. The created pulses had a rectangular shape with the pulse duration of 2 ms, pulse period of 10 ms and the rise- and decay slopes of less than 25 ns. The time-response function of the used PMTs is better than 50 ns which is much shorter than the characteristic times of the TTA and TTT processes (usually, in order of 10÷100 μs). The pulse duration (2 ms) was significantly long for the molecular system to reach the stationary conditions, while the time interval between the excitation pulses (8 ms) was large enough for the full relaxation of the excited molecules.

The comparison of the oscillograms, measured for the perylene and the Bodipy UC systems, shows that for the residual phosphorescence (left part of Figure 7.4) the remarkable distinctions are visible. Thus, the decay time (because of multi-exponential character of the dependence the level of 1/e is taken as specific one for all oscillograms) for the perylene is equal to 65 μs, whilst for Bodipy it is four times longer and equal to 266 μs. It is the clear a proof of the considerations above – the perylene is much better triplet state quencher for PdTBP than Bodipy. The longer in compare to perylene “shoulder” in the start of the UC decay (right part of Figure 7.4) for the Bodipy is the consequence of the weak TTT process and corresponding longer “income” of the energy from sensitizer.

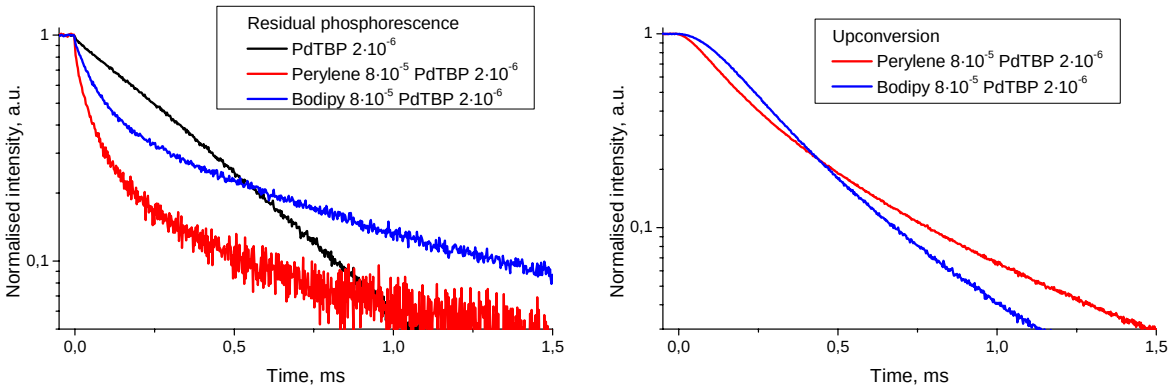

Figure 7.4 Oscillograms for residual phosphorescence (left) and UC (right) signals (in logarithmic scale) for neat solution of the sensitizer PdTBP ($2 \cdot 10^{-6}$ M), and for UC systems with perylene ($8 \cdot 10^{-5}$ M) and Bodipy ($8 \cdot 10^{-5}$ M) as emitters.

The perylene, in its turn, withdraw the energy from the sensitizer faster and utilize it quite efficient at the beginning. However, as it seen, at the longer time-scales the Bodipy better and therefore faster utilizes the energy, that indicates the higher probability of the triplet states annihilation.

In order to combine the properties of both molecules the dyad Bodipy-A was synthesized (the structure is shown in Figure 7.1). The initially presented in Bodipy molecule phenyl now serves as an energy bridge between the perylene and Bodipy parts of the combined molecule. With the aim to receive the same concentration of the fluorophores, the molar concentration of the dyad in the UC sample was reduced in two times and was equal to $4 \cdot 10^{-5}$ M, while the sensitizer have the same concentration as earlier - $2 \cdot 10^{-6}$ M.

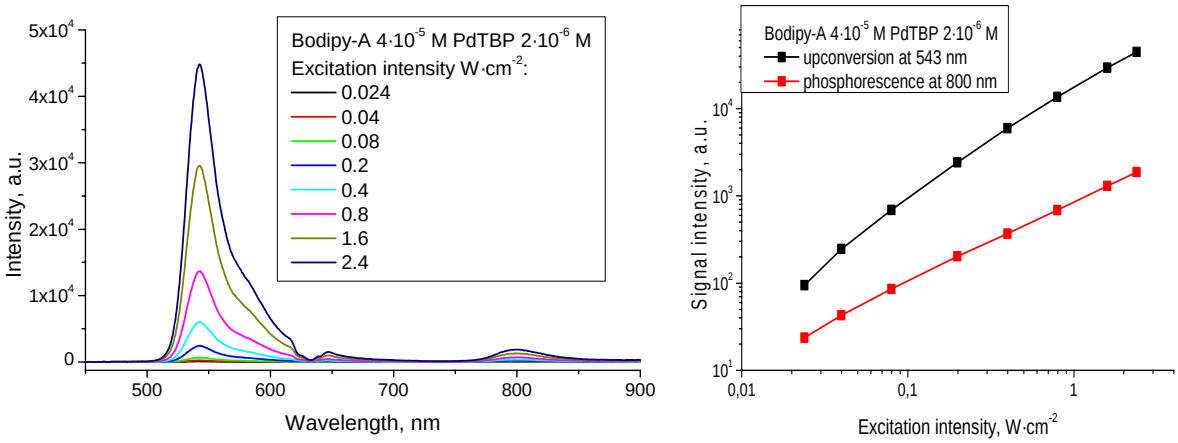

Figure 7.5 Spectra (left) and peak intensity (right) dependence of generated UC and residual phosphorescence signals on excitation intensity for the Bodipy-A dyad ($4 \cdot 10^{-5}$ M) and PdTBP ($2 \cdot 10^{-6}$ M) in toluene.

The extremely efficient UC generation was detected for the dyad (the UC spectra are shown in Figure 7.5). Despite two times lower molar concentration the UC signal was almost two times higher in compare to the Bodipy solution and three times higher than for the perylene. The slope of the intensity dependence is almost unity at the highest excitation intensities that indicate the extreme efficiency of the entire TTA – UC process. The external Q.Y. is as high as 11.3% that is one of the highest reported nowadays values.

In order to prove that namely the combination of two dyes in one molecule, but not the mixture of them is responsible for such a high result, the sample contained the mechanical mixture of the same amount of fluorophores (perylene ($4 \cdot 10^{-5}$ M), Bodipy ($4 \cdot 10^{-5}$ M) and PdTBP ($2 \cdot 10^{-6}$ M)) was prepared. The generated UC is represented by the ultrabroad spectrum of emission of both emitters, simultaneously working in the combination with one sensitizer. The Q.Y. for the mechanical mixture was calculated to be 5.9% that is slightly higher than for each emitter working separately, but still twice less, than for Bodipy-A dyad.

The summary oscillograms for all the samples are presented in Figure 7.7. It is seen, that in the mixture of two emitters namely the perylene is responsible for the efficient triplet-triplet transfer, because the decay curves are almost identical with the only perylene sample and the characteristic decay time is equal to 69 μs. A relatively high intensity of the Bodipy fluorescence in a mixture (Figure 7.6) could be a result of the hetero-TTA process described above.

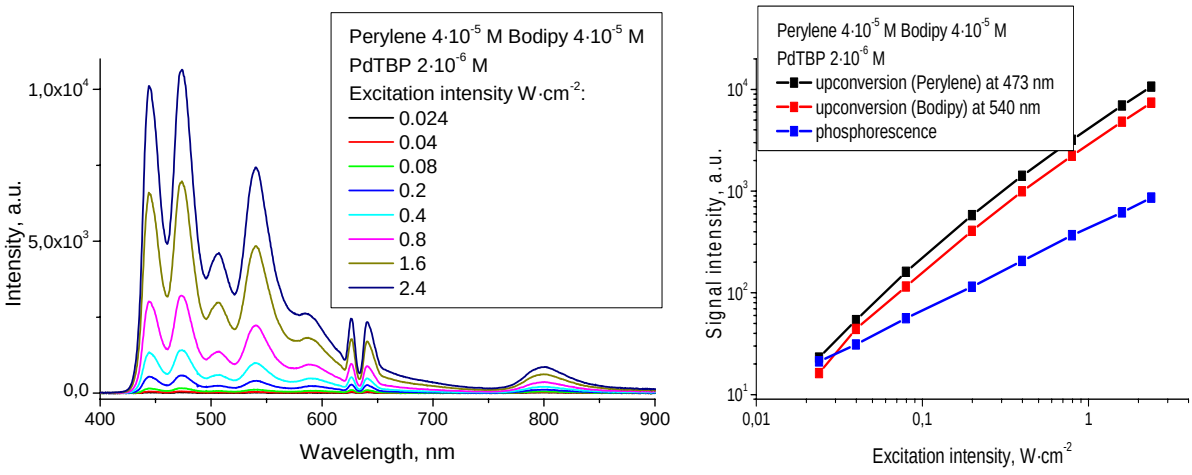

Figure 7.6 Spectra (left) and peak intensity (right) dependence of generated UC and residual phosphorescence signals in dependence on excitation intensity for the mechanical mixture of perylene ($4 \cdot 10^{-5}$ M), Bodipy ($4 \cdot 10^{-5}$ M) and PdTBP ($2 \cdot 10^{-6}$ M) in toluene.

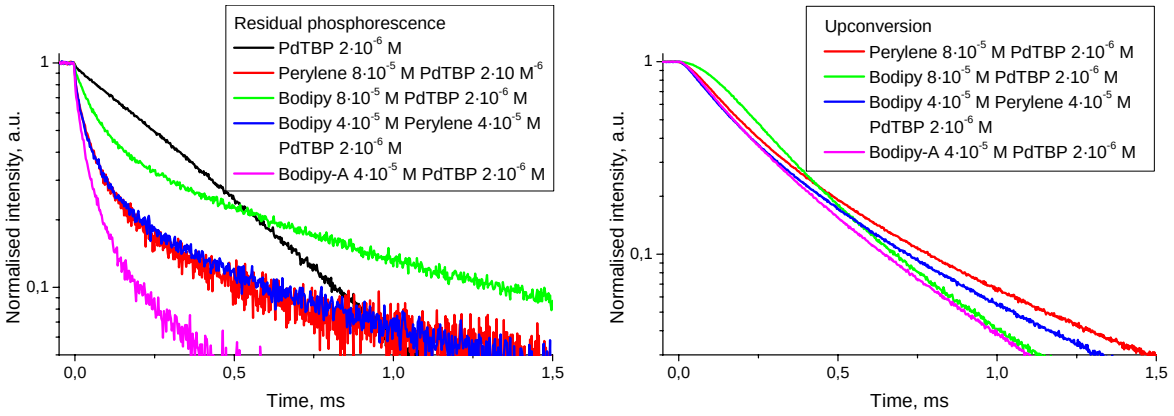

Figure 7.7 Oscillograms for residual phosphorescence (left) and UC (right) signals (in logarithmic scale) for neat solution of the sensitizer PdTBP ($2 \cdot 10^{-6}$ M), UC systems with perylene ($8 \cdot 10^{-5}$ M), Bodipy ($8 \cdot 10^{-5}$ M), mixture of perylene and Bodipy ($4 \cdot 10^{-5}$ M each), and dyad Bodipy-A ($4 \cdot 10^{-5}$ M) as emitters.

Extremely fast decay of the residual phosphorescence for the dyad was observed (violet line in Figure 7.7). The decay time is at least two times shorter than for any of the emitters and was equal to 36 μs that indicates the strongly efficient triplet energy transfer from the sensitizer to the dyad. The decay of the UC signal for the dyad not differs significantly from other UC systems, but still is the shortest one.

As it seen in Figure 7.8 (left graph), the absorptivity of the created dyad has the evident difference from the absorptivity of the perylene and almost replicate the Bodipy part of the spectrum. It could be a result caused by the perylene substitution with the phenyl group that leads to the according influence on its photophysical properties. To be fully sure that the discovered synergetic effect is not a mistake and the efficiency increase was not a result of the perylene modification by the bridge phenyl group, the closest to the phenyl-perylene molecule – previously described in part 5.3 3-(4-*tert*-butylphenyl)perylene (named Y-794) dye was taken. As it seen (Figure 7.8 right graph), its spectrum perfectly matches to the dyads absorptivity.

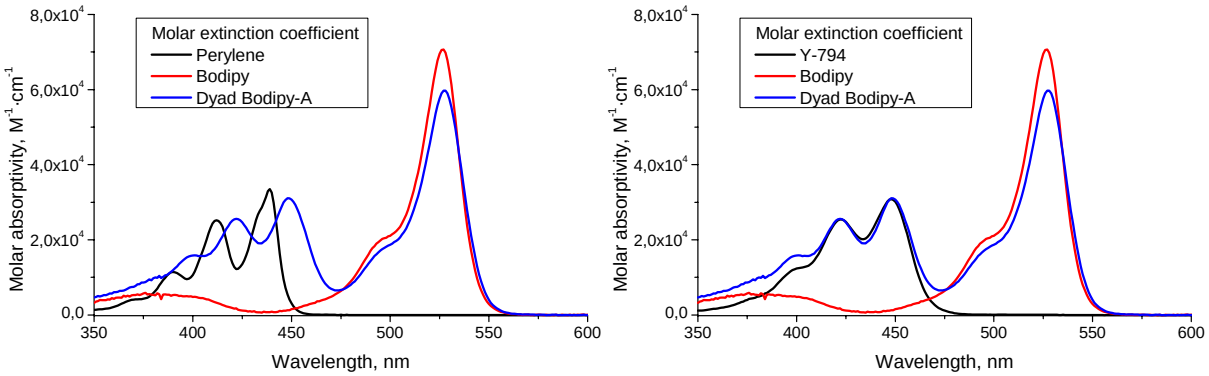

Figure 7.8 Molar absorptivity for perylene, Bodipy and dyad Bodipy-A (left); and Y-794, Bodipy and dyad Bodipy-A (right).

The samples containing PdTBP as the sensitizer ($2 \cdot 10^{-6}$ M), Y-794 in concentration of $8 \cdot 10^{-5}$ M, and mixture Y-794 with Bodipy ($4 \cdot 10^{-5}$ M each) were prepared and measured at the same conditions as previously described. The efficient UC generation was detected in both cases (spectra shown in Figure 7.9). The Q.Y. values for single Y-794 emitter and in mixture with Bodipy were calculated to be equal 6.6% and 7.6%, respectively. It is higher than for the similar samples using perylene as emitter, but is still significantly lower than the quantum yield for the dyad.

The combined spectra for both series of experiments are presented in Figure 7.10. The main photophysical parameters like the decay time of the phosphorescence and UC, and the Q.Y. of UC are presented in the Table 7.1.

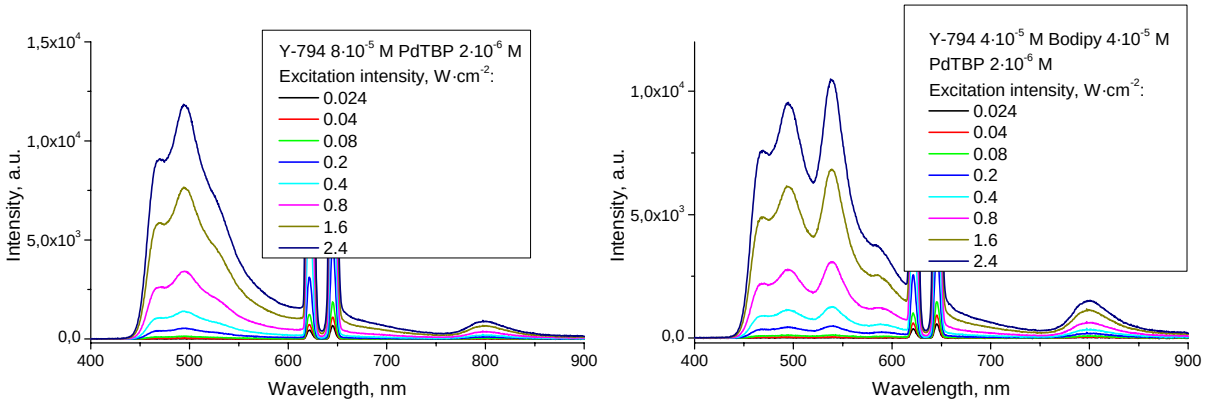

Figure 7.9 Spectra of generated UC and residual phosphorescence signals in dependence on excitation intensity for sensitizer PdTBP ($2 \cdot 10^{-6}$ M) with emitters Y-794 ($8 \cdot 10^{-5}$ M) (left) and mechanical mixture of Y-794 ($4 \cdot 10^{-5}$ M) and Bodipy ($4 \cdot 10^{-5}$ M) (right) in toluene.

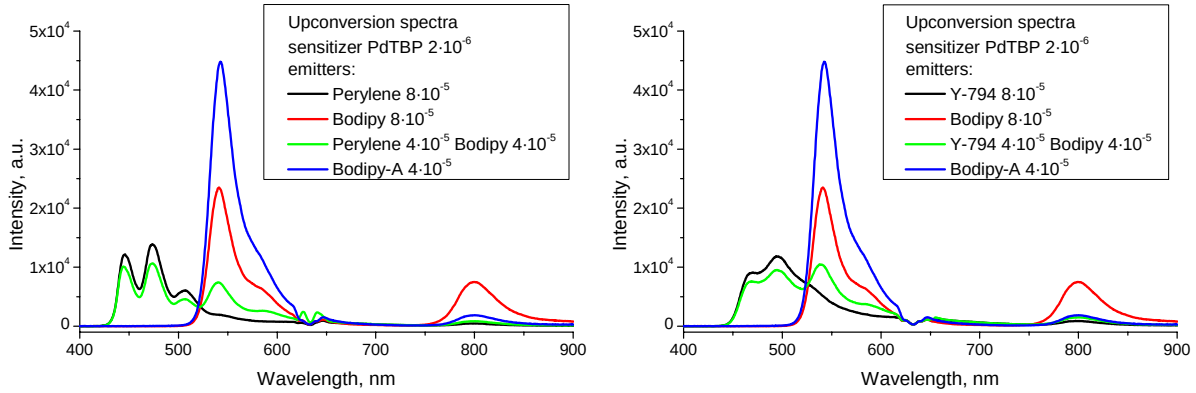

Figure 7.10 Spectra of generated UC and residual phosphorescence for the series of experiments with perylene (left) and Y-794 (right). Concentration of fluorophores for all the emitter dyes is equal to $8 \cdot 10^{-5}$ fluorophors·L^{-1}, the concentration of sensitizer PdTBP is equal to $2 \cdot 10^{-6}$ M.

Table 7.1 Photophysical parameters of the studied UC systems.

Emitter	Perylene	Mixture Perylene+Bodipy	Y-794	Mixture Y-794+Bodipy	Bodipy	Dyad Bodipy-A
Phosphorescence decay time, μs	**65**	**69**	**45**	**56**	**266**	**36**
Upconversion decay time, μs	**281**	**259**	**328**	**363**	**368**	**251**
Quantum yield of upconversion, %	**4.5**	**5.9**	**6.6**	**7.6**	**6**	**11.3**

As a summary, the process of TTA – UC was performed on the multi-component molecular system and high Q.Y. of UC generation, as high as 11%, was achieved. For the first time, the functions of two emitter molecules were attributed to the different processes, namely the emitter molecule with a lower triplet state energy was used as the effective quencher of the sensitizer triplet state, while the emitter molecule with the appropriately situated singlet state was used for the efficient TTA process. The demonstrated strategy for the increase of the Q.Y. of TTA – UC based on the independent optimization of the processes of the TTT and the TTA is not restricted to the species presented herein and can be applied to the various UC molecular systems.

8 Highly efficient TTA – UC with different sensitizer-emitter pairs

During the investigations devoted to the search of the optimal conditions for the TTA –UC process, the investigations of the influence of the dyes absolute and relative concentrations on the Q.Y. of UC generation was done. It was shown that the external Q.Y. of the UC samples can be noticeably higher with an increase of the UC dyes concentrations. The experiments in the new standardized conditions were conducted for the created perylene-based emitters, previously measured at the low concentrations of the dyes. The obtained results for TBP sensitizers, as well as the investigations devoted to other effective sensitizer-emitter UC pairs, are reported in this part.

8.1 Highly efficient TTA – UC with tetrabenzoporphyrins

Almost every bio-research oriented equipment like confocal microscopes and Fluorescence-Activated Cell Sorting (FACS) stations for a bio-materials imaging and a flow cytometry are equipped with cheap and commercially available lasers like Helium-Neon laser or laser diodes having the wavelength of radiation of 635 nm. The absorption of the PdTBP, one of the molecules serving as the sensitizers in our experiments, has the absorption spectrum, which maximum perfectly matches to this wavelength. From the point of view of expansion of the regions of the application of the TTA – UC, highly efficient emitters for this sensitizer in different regions of spectra should be found.

All molecules from the created perylene-based library, reported in part 4, were newly tested. All experiments were done for the concentrations of dyes, found in part 6.3 to be optimal. Thus, in all investigated samples the molar concentration of the sensitizer was kept to be $1 \cdot 10^{-5}$ M and of the emitter $5 \cdot 10^{-4}$ M. The Q.Y. values were calculated relative to two standards – perylene in toluene at the concentration $5 \cdot 10^{-6}$ M and Rhodamine-123 in ethanol at $1 \cdot 10^{-5}$ M. Both dyes were deoxygenated in glovebox and sealed in vitrotubes. The comparison with both standards gave similar results for all investigated UC solutions.

The spectra of the UC generation for all the samples, excited by the laser radiation (635 nm) with excitation intensity of 2.4 $W \cdot cm^{-2}$ are combined in Figure 8.1. The phosphorescence spectrum of the neat solution of the PdTBP at the concentration of $1 \cdot 10^{-5}$ M is presented for comparison (red in top left graph in Figure 8.1).

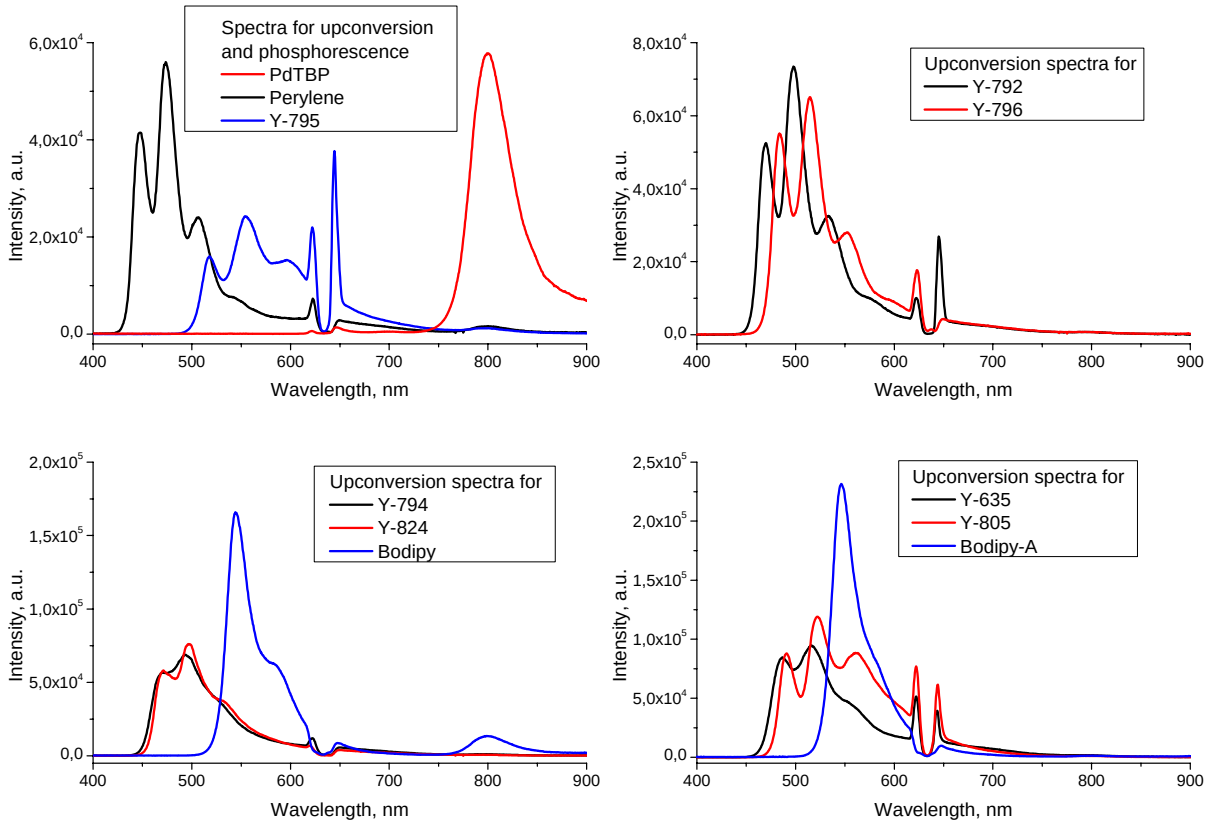

Figure 8.1 Spectra of UC and residual phosphorescence for the neat solution of sensitizer PdTBP ($1 \cdot 10^{-5}$ M) (top left graph) and UC systems with emitters ($5 \cdot 10^{-4}$ M): top left graph – Y-795 and perylene, top right graph – Y-796 and Y-792, bottom left graph – Y-794, Y-824 and Bodipy, bottom right graph – the emitters with a highest Q.Y. – Y-635, Y-805 and Bodipy-A. Excitation intensity ~ 2.4 W·cm^{-2}.

It is seen, that for all the dyes (except of Bodipy) the sensitizer's phosphorescence is highly suppressed that indicates the efficient triplet state energy transfer from the sensitizer to the emitter molecules. The efficient UC light generation was successfully obtained in blue, green and yellow regions of visible spectrum.

The results of the Q.Y. values calculation and other photophysical characteristics of the UC radiation generated by the investigated emitters are summarised in the Table 8.1. The table is sorted in respect to the increase of the UC generation efficiency. It is seen, that almost all sensitizer-emitter pairs have the Q.Y. of the UC more than 5%. The maximal Q.Y. of the UC was detected for Y-805 dye and reached 13.4%. The UC systems with the dyad Bodipy-A and double substituted perylene Y-635 also have the Q.Y. higher than 10% and in certain circumstances can be used on a par with the conventional fluorescent dyes.

Table 8.1 Quantum yields and emission parameters for different emitters in UC systems containing $5 \cdot 10^{-4}$ M of emitter and $1 \cdot 10^{-5}$ M of sensitizer. Excitation intensity 2.4 W·cm^{-2}.

Emitter	Range of emission, nm	Maximum of emission, nm	Quantum yield of upconversion, %
Y-795	510 - 630	555	2.1
Perylene	440 - 515	473	4.5
Y-796	475 - 560	515	5.6
Y-792	460 - 540	498	6
Y-824	465 - 545	496	7
Y-794	460 - 540	497	7.4
Bodipy	530 - 590	544	8.9
Y-635	470 - 560	517	10.1
Bodipy-A	530 - 575	547	11.6
Y-805	480 - 605	522	13.4

Based on the results obtained at low dyes concentrations, only the most promising emitters were checked in the combination with PtTBP sensitizer, which Q-band of the absorption placed at 615 nm.. Despite a much lower lifetime of the triplet state of PtTBP (50 μs [105]) than for PdTBP (286 μs) the efficient TTT process with successive UC generation was observed. The spectra of the obtained phosphorescence signal for the neat solution of PtTBP (taken at the concentration $1 \cdot 10^{-5}$ M) and the spectra of the generated UC at PtTBP combination with the different emitters are summarized in Figure 8.2. The excitation intensity was kept on the level of 2.4 W·cm^{-2}.

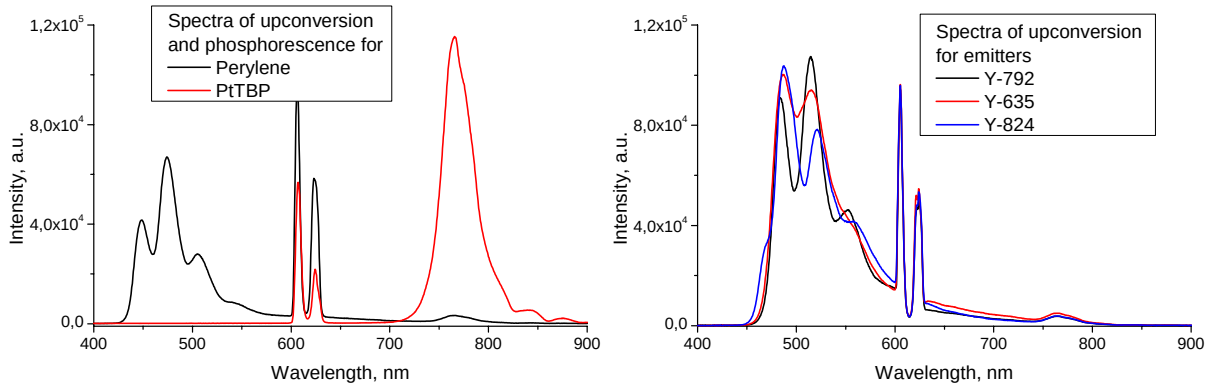

Figure 8.2 Spectra of UC and residual phosphorescence at the excitation intensity 2.4 W·cm^{-2} for the neat solution of sensitizer PtTBP ($1 \cdot 10^{-5}$ M) (left graph) and UC systems with emitters ($5 \cdot 10^{-4}$ M): left graph – perylene, right graph – Y-792, Y-824 and Y-635.

Table 8.2 Quantum yields and emission parameters for different emitters in UC systems containing $5 \cdot 10^{-4}$ M of emitter and $1 \cdot 10^{-5}$ M of sensitizer. Excitation intensity 2.4 W·cm^{-2}.

Emitter	Range of emission, nm	Maximum of emission, nm	Quantum yield of upconversion, %
Perylene	440 - 515	473	4.9
Y-792	460 - 540	498	8.9
Y-824	465 - 545	496	9.2
Y-635	470 - 560	517	9.7

The calculated values of the Q.Y. characteristics of the emitters' emission are summarized in the Table 8.2. The highest obtained efficiency was obtained with emitter Y-635 and was equal to 9.7%.

8.2 New efficient UC emitters for tetranaphtoporphyrins

As known, biological tissues strongly absorb the radiation in the region of wavelengths shorter than 600 nm Oxyhemoglobin and deoxyhemoglobin absorptions and a strong scattering rising from many substances with different refraction coefficients complicate the light transfer within the biological tissue. In order to bring an optical radiation deep inside a biological matter without a loss of its power and to avoid the heating of the surrounding parts of a body, one should use a radiation with the wavelength matched to the so-called tissue transparency window (shown in Figure 8.3). As it seen, for the wavelengths higher than 615 nm the factors influencing on the available depth of the light penetration are strongly decreased.

Tetranaphtoporphyrin (TNP) was shown to be the efficient sensitizer for the TTA – UC [80]. This sensitizer absorbs in the deep-red region of spectra (700 nm) that is very promising for biological oriented applications. Up to now the following emitters used in combination with PdTNP were reported – the rubrene and 9,10-bis(phenylethynyl)naphthacene [14, 80]. The main aim for this part of the dissertation is to find new effective emitters for the metallated TNP sensitizers.

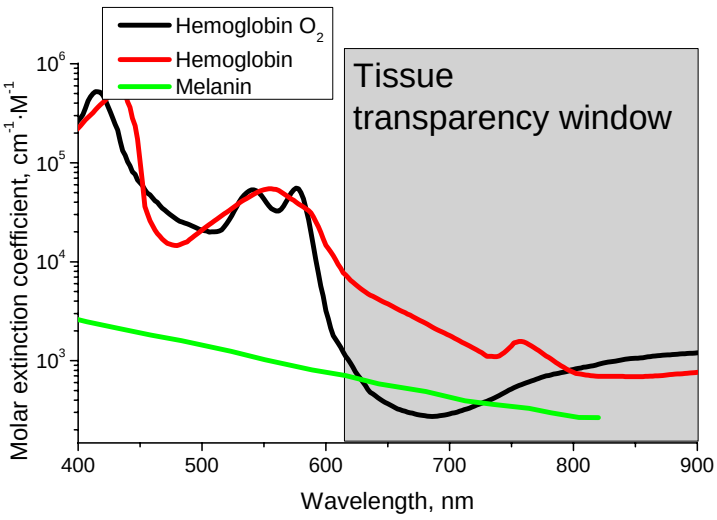

Figure 8.3 Tissue transparency window in visible and near infra-red regions of spectra [106, 107].

8.2.1 Platinum tetranaphtoporphyrin (PtTNP)

The chemical structure of the TNP sensitizers used in the following experiments was slightly different from the published (structure of the PdTNP from [14, 80] is shown earlier in Figure 4.10). The PtTNP, synthesized in our group by xxxxxxxxxxx, has no butoxy groups (Figure 8.4). The main maxima of Q-band of absorption of PtTNP measured in toluene is placed at 689 nm. The wavelength of excitation radiation was chosen by 4f-monochromator from the SC radiation of Fianium laser in order to obtain maximum level of emitted signal (match of absorption spectra and excitation radiation spectrum is shown in Figure 8.4).

Being excited, PtTNP emits the phosphorescent signal having the maximum at 892 nm (shown in Figure 8.4). For the efficient UC, suitable emitters should have a singlet state located at 445 nm (corresponding energy near 2.8 eV) and longer. In the same time, in order to suit in “transparency window” of the sensitizer, the emitter fluorescence should take place in the range 450-670 nm.

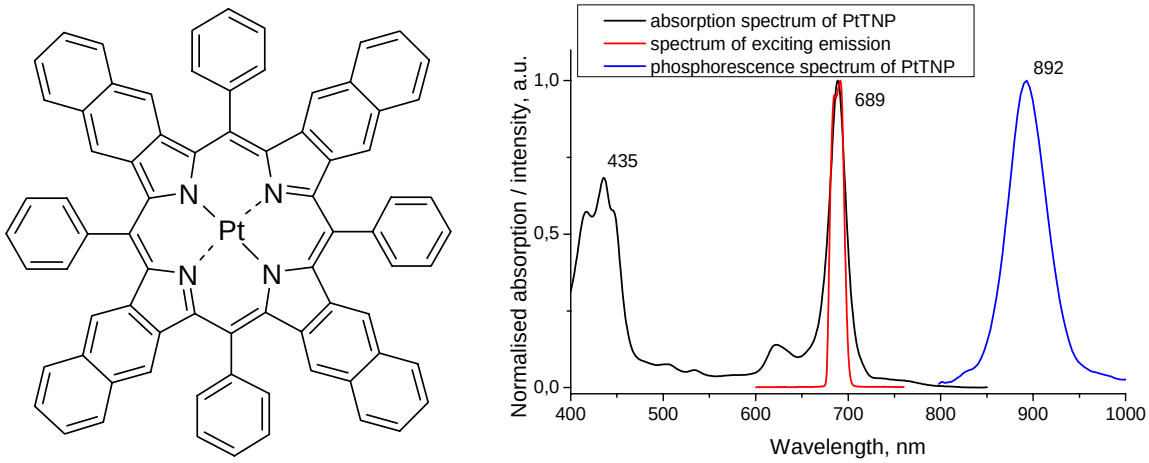

Figure 8.4 The chemical structure, absorption (black), emission (phosphorescence) (blue) spectra and spectrum of corresponding excitation radiation (red) for (Pt)tetraphenyltetranaphtoporphyrin (PtTNP).

The following dyes were suggested to be efficient emitters for the TTA – UC in the combination with PtTNP: the dye Y-795, previously described in the part 5.10, which have the biggest batochromic shift from all modified perylenes, and new red emitters from a Bodipy and a perylene-monoimide (PMI) families. The reason for the choice of latter was the high fluorescent ability of PMI-based molecules; relatively ease of their modification and corresponding huge variation of optical properties [108, 109]. The perylene core played the important role in our choice as well. We assume that it mainly determines a triplet state position of the molecule. The influence of substituents on the original molecule, and,

correspondingly, on its singlet and triplet state energies should also correlate with our earlier investigations devoted to perylene-based dyes.

The chemical structures and the characteristic photophysical spectra of the PMI dye used in experiment are presented in Figure 8.5. The emission of the PMI takes place in green-yellow region of spectra with a maximum located at 532 nm.

Two dyads, named PMI-Bodipy and Bodipy-A2, were synthesized in our department by xxxxxxxxxxx and xxxxxxxxxxx. The chemical structures and photophysical spectra of the compounds are shown in Figure 8.6 and Figure 8.7. In both cases the Bodipy part is responsible for the emission of a created photon. Thus, the maximum of emission of the PMI-Bodipy dyad is placed at 595 nm, whereas for Bodipy-A2 dyad – at 545 nm.

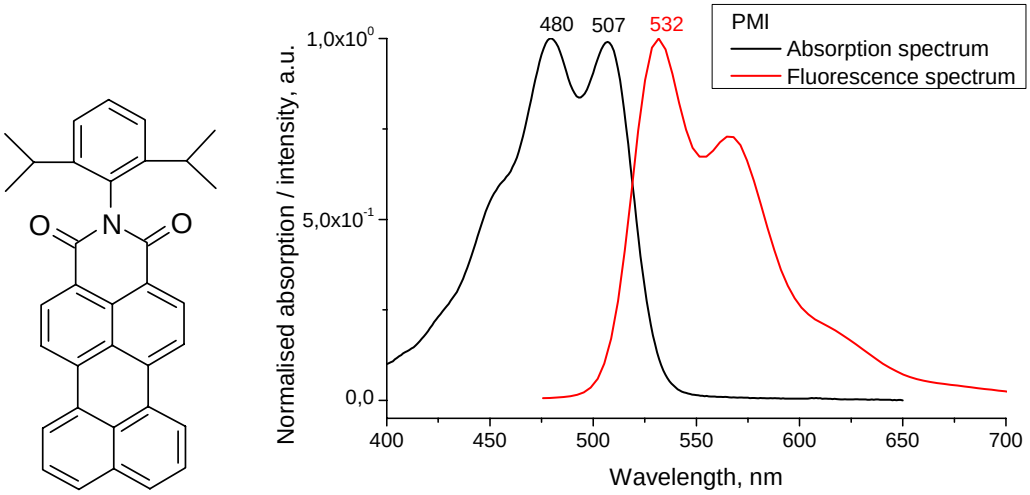

Figure 8.5 Chemical structure (left), absorption and fluorescence spectra (right) of N-(2,6-diisopropylphenyl)perylene-3,4:9,10-perylenedicarboximide (or shortly PMI).

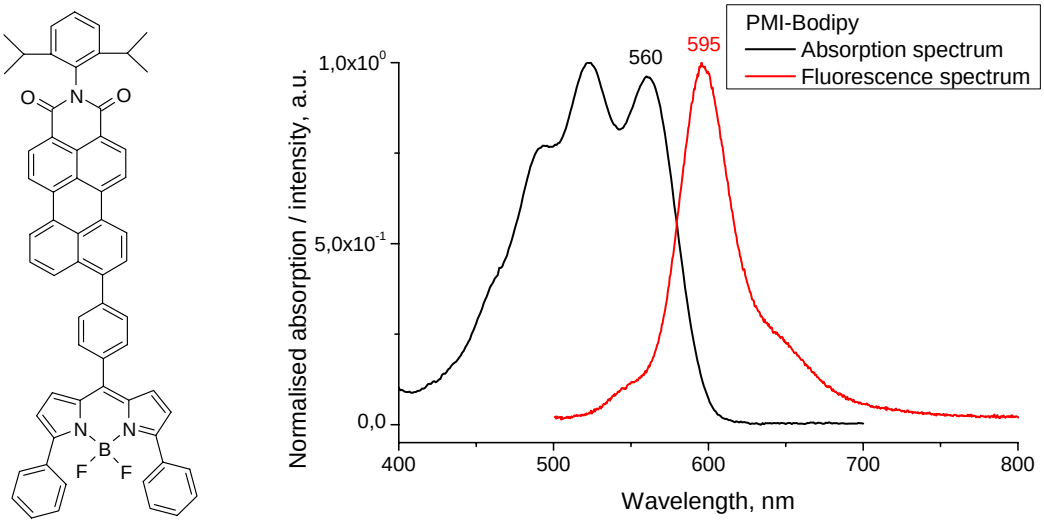

Figure 8.6 Chemical structure (left), absorption and fluorescence spectra (right) of (N-(2,6-diisopropylphenyl)perylene-3,4:9,10-perylenedicarboximide-yl)-8-phenyl-1,3,5,7-tetramethyl-2,6-diethyl dipyrromethane•BF_2 (dyad PMI-Bodipy).

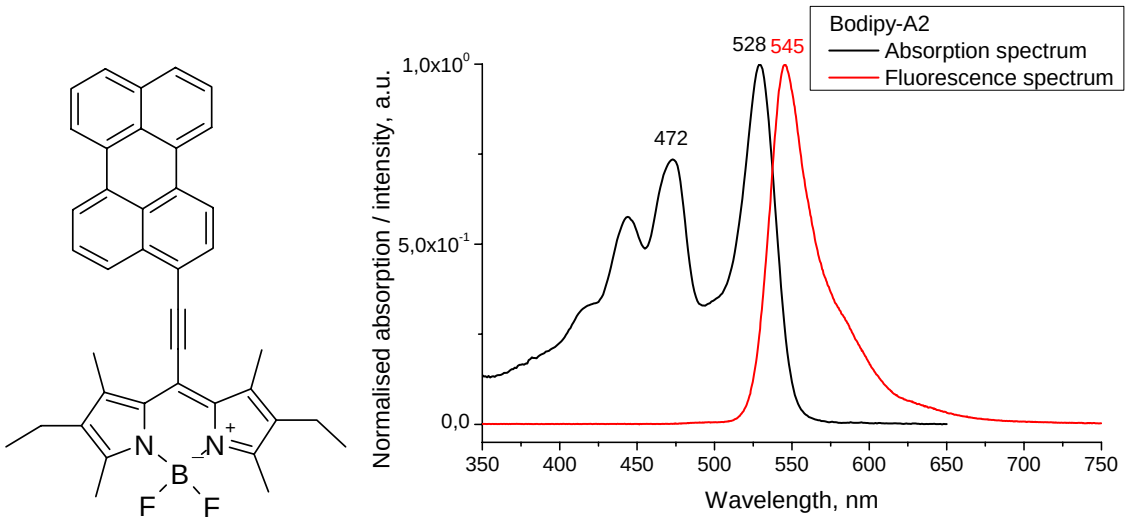

Figure 8.7 Chemical structure (left), absorption and fluorescence spectra (right) of (4-(perylene-3'-yl)ethynyl-8-phenyl-1,3,5,7-tetramethyl- -2,6-dipyrromethane•BF2) (dyad Bodipy-A2).

UC samples were prepared in accordance to the conditions, taken as standard after the optimization of the conditions of the UC process ($1 \cdot 10^{-5}$ M for the sensitizer (PtTNP) and $5 \cdot 10^{-4}$ M for the emitter dyes). The excitation beam diameter was equal to 400 μm and the corresponding excitation intensity reached 2.4 $W \cdot cm^{-2}$. The usage of the short-pass filter SP01-633RS-25 to block the scattered and reflected excitation radiation gave an unexpected advantage – the filter was partially transparent at the wavelengths higher than 800 nm. This allows the observation of a slightly spectrally deformed signal of the residual sensitizer's phosphorescence and the further evaluation of a degree of its suppression by the emitter molecules.

The results of the UC generation for the combination of the PtTNP and the emitters are combined in Figure 8.8. The most efficient UC generation was observed with the PMI emitter (Q.Y. reached 2.2%), although the quenching of the sensitizer triplet states energy (and therefore most efficient TTT process) was in 5 times better with the Y-795 emitter, the Q.Y. of the UC for which was calculated to be only 1.1%. The same behavior was observed for Y-795 emitter with PdTBP sensitizer. The TTT process was quite efficient, but for some reasons the efficiency of TTA process was the lowest among all the investigated emitters. Both synthesized dyads in combination with PtTNP sensitizer show extremely low efficiency of TTT process (high residual phosphorescence signal obtained) and, as a result, obtained external Q.Y. values were only 0.3% for Bodipy-A2 and 0.4% for PMI-Bodipy dyad.

The reason of such a low efficiency of TTT process could be the fast decay of the triplet state of PtTNP sensitizer – the value for toluene solution was reported to be near 12.7 μs [110] that is 20 times less in compare to the PdTBP (286 μs).

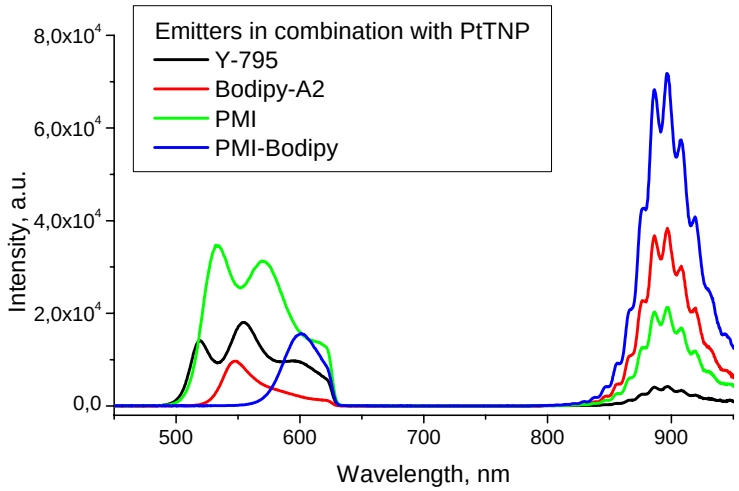

Figure 8.8 Spectra of UC and residual phosphorescence for the combination of PtTNP (at concentration $1 \cdot 10^{-5}$ M) as sensitizer and emitters Y-795, Bodipy-A2, PMI and PMI-Bodipy (concentration is $5 \cdot 10^{-4}$ M for every case). Excitation intensity 2.4 W·cm^{-2}.

8.2.2 Palladium tetranaphtoporphyrin (PdTNP)

It is known from the literature, that TNP metallated by palladium possess near 5 times longer lifetime of the triplet state (65 μs [111]) than metallated by platinum (12.7 μs). The longer lifetime should positively influence on the probability of the TTT process. The chemical structure of the PdTNP, synthesized in our group, is shown in Figure 8.9. It is known that palladium shifts the spectrum of the free-base porphyrines in a lesser extent in compare to platinum. Thus, the maximum of absorption of the Q-band of PdTNP is placed at 705 nm (black line in Figure 8.9) that is on 16 nm more than for PtTNP. In the deoxygenated solution of toluene, the PdTNP emits the phosphorescence with a maximum placed at 939 nm (shown blue in Figure 8.9).

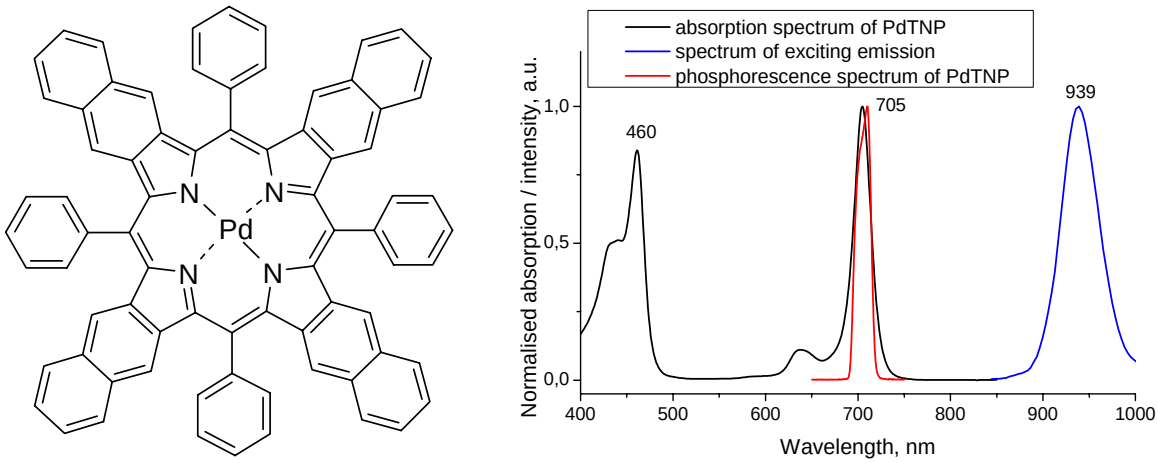

Figure 8.9 The chemical structure, absorption (black), emission (phosphorescence) (blue) spectra and spectrum of corresponding excitation radiation (red) for (Pd)tetraphenyltetranaphtoporphyrin (PdTNP).

The radiation for the excitation of the PdTNP was chosen by the use of 4f-monochromator from SC emission of the Fianium laser to fit the maximum of dye absorption. The excitation radiation spectrum used in the experiments and its matching to the absorption spectrum of the PdTNP is shown in Figure 8.9 (red line).

Based on the good result of the combination PMI emitter with PtTNP, two other emitter dyes were synthesized by the decoration of the initial PMI molecule with *tert*-butylphenyl group (the resulting molecule structure is shown in Figure 8.10, short name of the molecule is Y-895) and with 3,3-dimethylbutynyl (shown in Figure 8.11, named Y-896). As a result of the modification, the absorption spectrum of the PMI dye was shifted on 18 nm and 23 nm for Y-896 and Y-895 dye, respectively (the spectra of absorption and emission of the dyes are shown in Figure 8.10 and Figure 8.11).

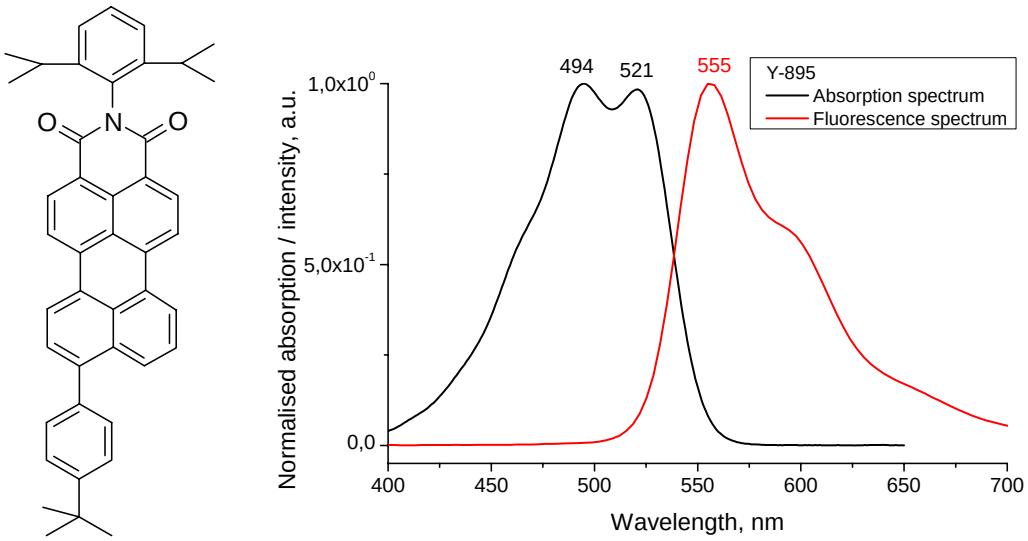

Figure 8.10 Chemical structure, absorption and fluorescence spectra of 9-(4-tert-butylphenyl)-N-(2,6-diisopropylphenyl)perylene-3,4-perylenedicarboximide (shortly Y-895).

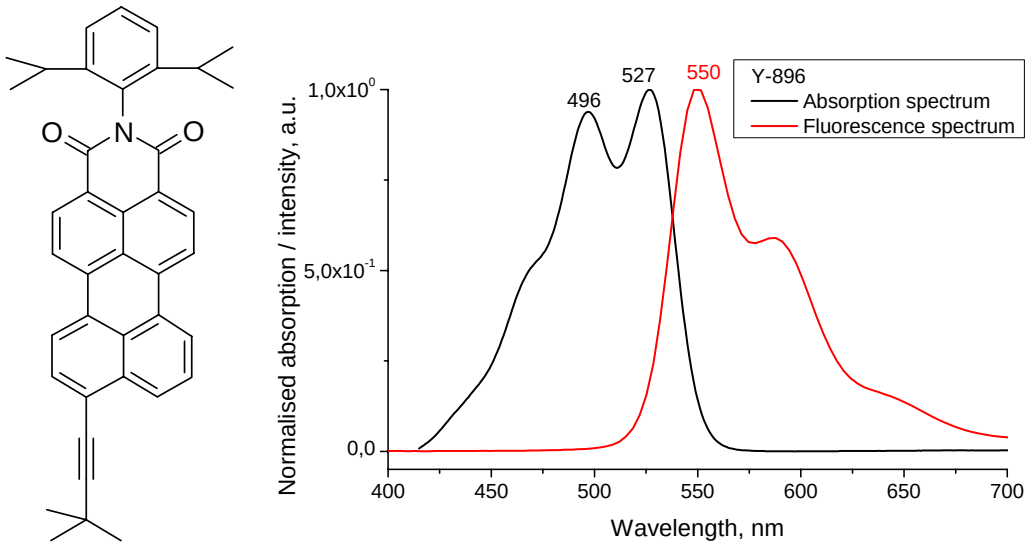

Figure 8.11 Chemical structure, absorption and fluorescence spectra of 9-(3,3'-Dimethylbutynyl)-N-(2,6-diisopropylphenyl)perylene-3,4-perylenedicarboximide (shortly Y-896).

Additionally, the dye Y-805 (described in part 5.8), which shows the best result in the combination with PdTBP sensitizer, was supposed to be tried as emitter for PdTNP as well.

The same concentrations of the dyes for the samples, as for PtTNP sensitizer, were used for the UC samples with PtTNP ($1 \cdot 10^{-5}$ M for sensitizer, $5 \cdot 10^{-4}$ M for emitter). The suppression of the excitation radiation was done by the short-pass filter FF01-694/SP-25 (Semrock Inc.). Excitation beam diameter was set to be 400 μm. The maximal excitation power reached 3 mW that leads to the excitation intensity of 2.4 W·cm^{-2}. Unfortunately, there was no suitable filter for the simultaneous excitation radiation suppression and the observation of the UC and phosphorescence signals.

The results of the UC generation for the different emitters with the PdTNP sensitizer are shown in Figure 8.12. For the Y-795 emitter the obtained Q.Y. was close to that obtained in the combination with the PtTNP sensitizer and reached 1.4%, whilst for the PMI the result was lower and reached only 1.5%.

From the other side, the modified PMI dyes were more than twice more efficient in comparison to the parent PMI dye. The Q.Y. of the UC generation for both emitters were almost equal and amounted 3.5% and 3.6% for Y-895 and Y-896 dyes, respectively.

The emitter Y-805, having the record of 13.4% in the combination with PdTBP, have only moderate efficiency with the PdTNP. The calculated external Q.Y. was as high as 2.4%. Nevertheless, it should be noted that its emission spectrum has the shortest part among other used emitters and, therefore, the UC photons with the highest energy shift ($\Delta E = 0.83$ eV) relatively to the excitation photons (E = 1.75 eV) were created by this UC pair.

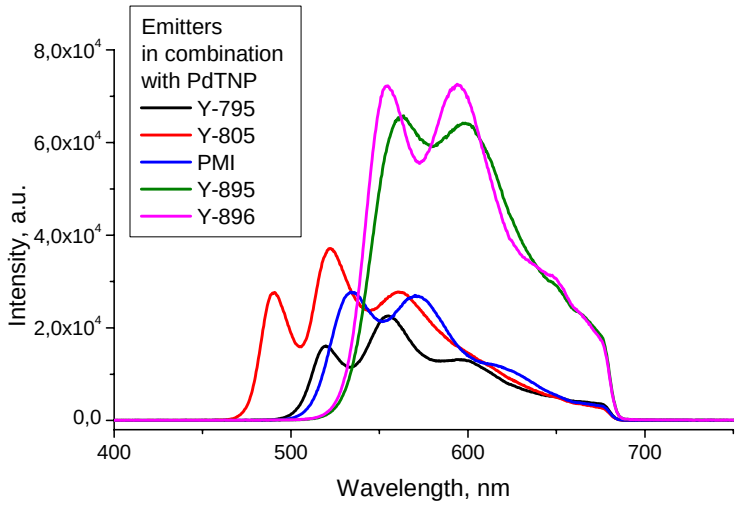

Figure 8.12 Spectra of UC and residual phosphorescence for the combination of PtTNP (at concentration $1 \cdot 10^{-5}$ M) as sensitizer and emitters Y-795, Bodipy-A2, PMI and PMI-Bodipy (concentration is $5 \cdot 10^{-4}$ M for every case). Excitation intensity 2.4 W·cm^{-2}.

8.2.3 Summary on new emitters for TNP sensitizers

The effective UC generation with the TNP sensitizers was observed. The values of the Q.Y. for PtTNP and PdTNP in the combination with different emitters are summarized in Table 8.3. The maximal UC efficiency was obtained for the combination of Y-896 emitter with PdTNP sensitizer with a resulting Q.Y. of 3.6%. The highest among reported nowadays anti-Stokes shifts obtained in the TTA – UC process, namely $\Delta E = 0.83$ eV, was achieved in the combination of PdTNP as the sensitizer and the Y-805 as the emitter (the total external Q.Y. for this UC pair reached 2.4%).

Table 8.3 Quantum yields of UC and emission parameters for different emitters with TNP sensitizers. Concentrations for emitters are $5 \cdot 10^{-4}$ M, for sensitizer $1 \cdot 10^{-5}$ M. Excitation intensity 2.4 W·cm^{-2}.

Sensitizer	Emitter	Range of emission, nm	Maximum of emission, nm	Quantum yield of upconversion, %
PtTNP	Bodipy-A2	535 - 575	548	0.3
	PMI-Bodipy	580 - 630	600	0.4
	Y-795	510 - 620	554	1.1
	PMI	520 - 600	532	2.2
PdTNP	Y-795	510 - 620	554	1.4
	PMI	520 - 600	532	1.5
	Y-805	480 - 605	496	2.4
	Y-895	540 - 650	563	3.5
	Y-896	545 - 650	554	3.6

9 Efficient TTA – UC in water environment

Up to now all the experiments on the TTA – UC were conducted in different organic media: volatile and non-volatile organic solvents [13, 35, 56], oligomer and polymer matrices [7, 18, 72, 73, 82]. The TTA – UC in the water environment was first shown in 2010 [112] but the efficiency of the UC generation was two orders less in comparison to the UC in organic media. Recently, embedding of the UC system consisted from hydrophobic dyes and an organic media in polymer-shell nanocapsules was shown [77]. The efficiency of the generation of the UC light photons was comparable to that obtained in an organic media and estimated to be approximately 0.5%. The living HeLa cells were stained by the nanocapsules and successfully imaged in the UC regime by a confocal scanning microscopy.

Further studies on organic media replacement by the aqueous medium would enable an application of the TTA – UC in other fields of the material science and the life science.

9.1 TTA – UC with water soluble dyes

As a first attempt to transfer the UC system in the water environment a chemical modification of already existing dyes was proposed. PdTBP and one of our most effective perylene-based dyes, namely Y-635, were chemically modified to be soluble in water. The corresponding structures of the molecules and the characteristic photophysical spectra are shown in Figure 9.1 and Figure 9.2.

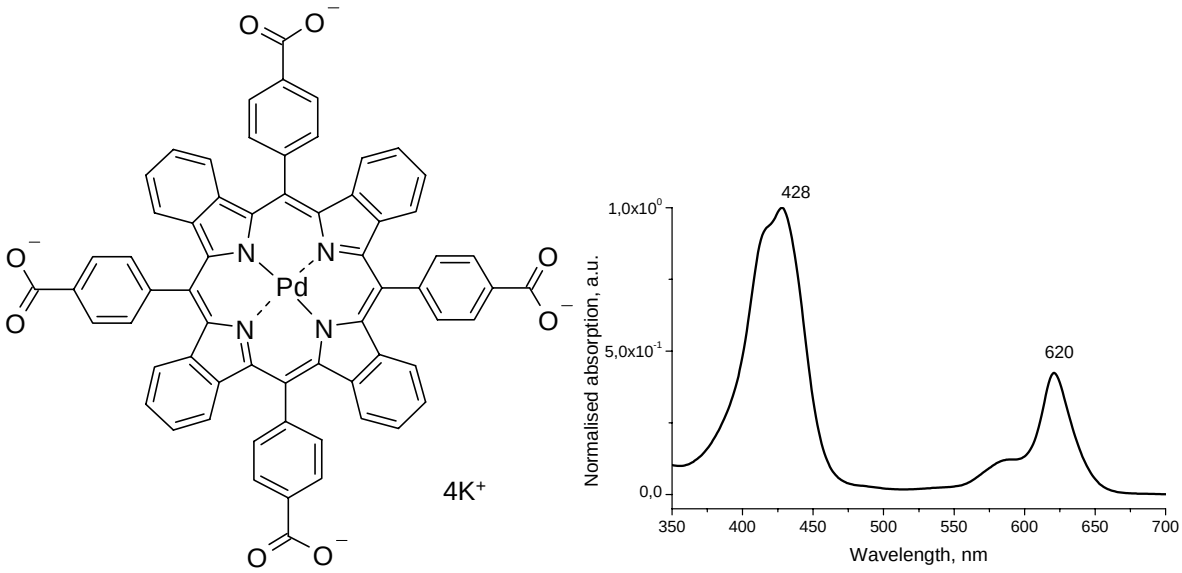

Figure 9.1 Chemical structure (left) and absorption spectrum (right) of water soluble sensitizer Pd-tetra(4-carboxyphenyl)tetrabenzoporphyrin potassium salt (short name PdTBP-W)

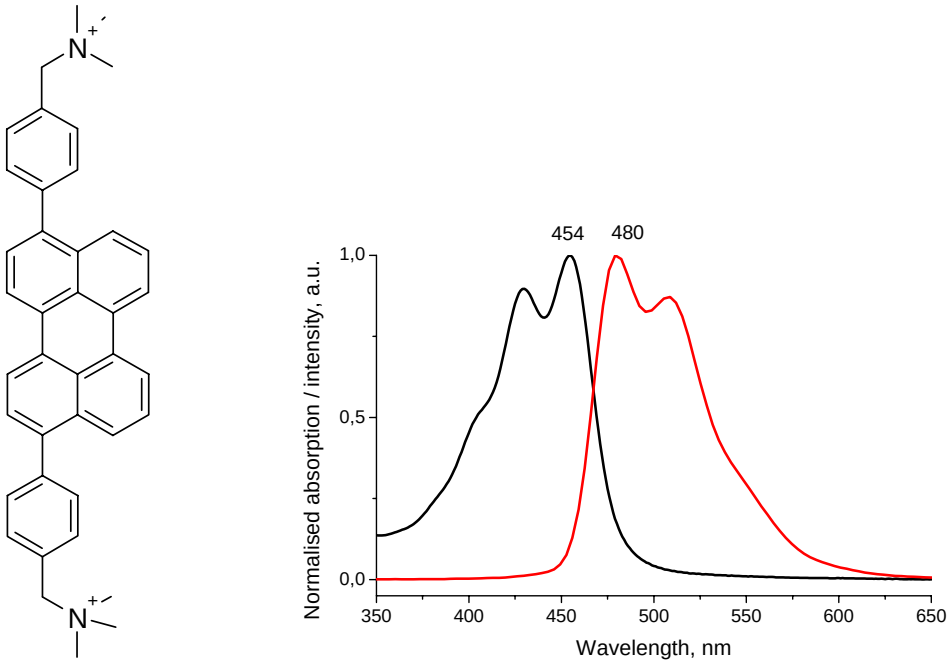

Figure 9.2 Chemical structure (left) and characteristic spectra (right) of water soluble emitter 1,1'-(4,4'-(perylene-3,10-diyl)bis(4,1-phenylene))bis(N,N',-trimethylmethanaminium) iodide (named Y-789-W).

The samples, containing $1 \cdot 10^{-6}$ M of PdTBP-W sensitizer and $2 \cdot 10^{-5}$ M of Y-789-W as the emitter were dissolved in the milli-Q water at the ambient conditions and deoxygenated in the glovebox overnight. First experiment on the UC in the water environment showed the total absence both phosphorescence of the sensitizer and the delayed fluorescence from the emitter. The experiment on the direct excitation of the emitter by the UV light (wavelength of excitation was 420 nm) shows the total quenching of the fluorescent emission of the emitter molecules in the presence of the sensitizer dye. The possible reason is an insufficient solubility of the dyes in water environment and a resulting aggregation of the molecules.

In order to avoid the possible aggregation of the dyes, the water-THF solution in the ratio 1:1 was proposed to be tested instead of the pure water. As it seen in Figure 9.3, under the excitation by the low-intensive radiation at 620 nm the signal of the delayed fluorescence has almost the same intensity as the signal of the phosphorescence from the sensitizer. The Q.Y. of the UC generation in the sample was comparable with obtained in a pure organic solvent and was estimated to reach 1%.

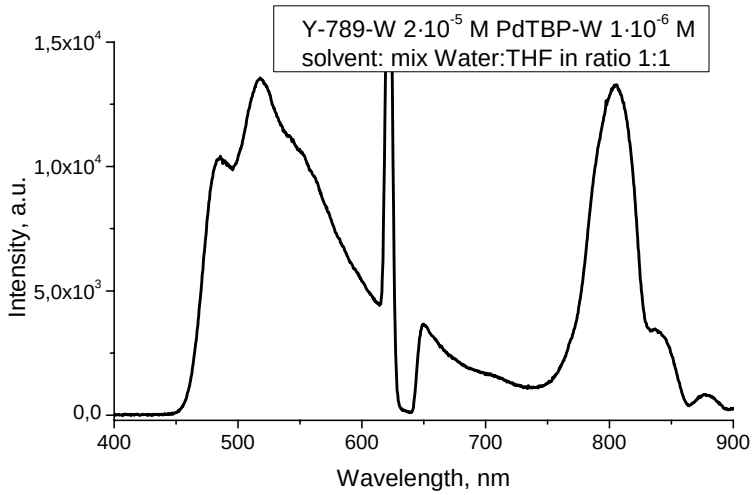

Figure 9.3 Spectrum of generated emission in $1 \cdot 10^{-6}$ M of PdTBP-W sensitizer and $2 \cdot 10^{-5}$ M of Y-789-W dissolved in water:THF (ratio 1:1) mixture.

In order to substitute the toxic water:THF mixture by a bio-compatible medium, the solvent medium was changed by the mixtures of water with 10% of ethanol, 5% of buffer solution and 25% of DMF. In all created media the total absence of any signal was detected even at extremely long accumulation times.

From the same propulsive reason the nonionic surfactant Triton X-100 (the chemical structure is shown in Figure 9.4), used in molecular biology, was chosen. The dyes at the same concentrations ($1 \cdot 10^{-6}$ M of PdTBP-W sensitizer and $2 \cdot 10^{-5}$ M of Y-789-W) were dissolved in the water solution containing 1 wt% of the Triton X-100 surfactant. At the excitation of the sample by the laser radiation with the wavelength near 620 nm the strong phosphorescent signal was detected (shown in Figure 9.5). The direct excitation of the solution by the laser radiation with the wavelength 420 nm showed a strong fluorescent signal corresponding to the emitter dye. It refuted the hypothesis about the fluorescence quenching caused by the molecules aggregation, like in the case of pure water solvent, described above. There was no any evident reason found why the UC generation was not obtained in these conditions. The answer was found two years after these experiments and will be described in part 9.3.

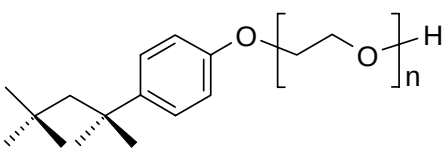

Figure 9.4 Chemical structure of polyoxyethylene octyl phenyl ether (Triton X-100). n = 9 - 10.

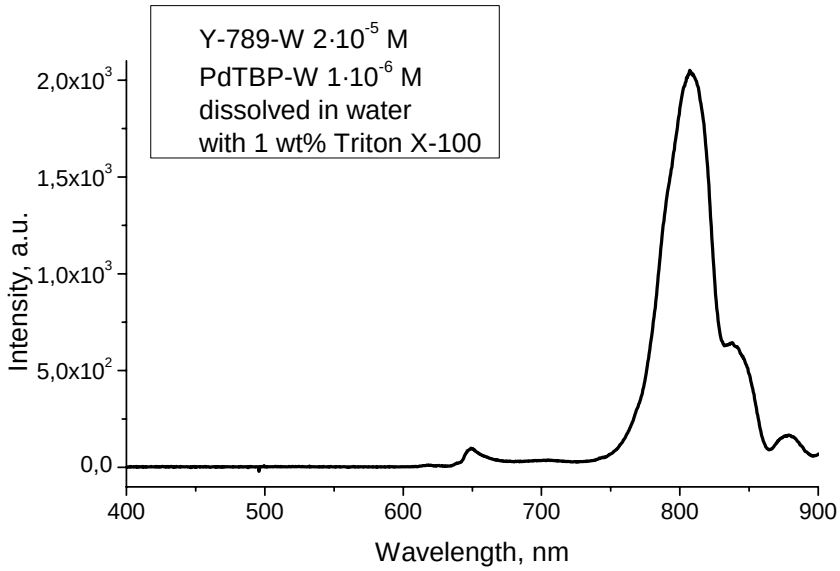

Figure 9.5 Spectrum of generated emission in sample containing $1 \cdot 10^{-6}$ M of PdTBP-W sensitizer and $2 \cdot 10^{-5}$ M of Y-789-W, dissolved in water with 1 wt% of Triton X-100.

As a conclusion, despite of the successful observation of the efficient UC generation by the synthesized water-soluble UC dyes in the mixture of water with organic solvent (THF), no successful UC generation in any investigated bio-compatible media was achieved.

9.2 Encapsulation of TTA – UC system in micelles

The second attempt to transfer the UC system into the water environment was dedicated to an encapsulation of hydrophobic UC dyes in micelles created by the non-ionic surfactant. The micelle carriers are known to be widely used for a delivery and a controlled release of bioactive hydrophobic components [113, 114]. The efficient solubilization of substances with low solubility in the water was demonstrated by the use of a amphiphilic block-copolymer from the family of polyoxyethanyl-tocopheryl sebacate (PTS) [115] (the structure of the surfactant is shown in Figure 9.6). It was shown that the PTS surfactant forms the spherical micelles with the diameter of 20 nm having the non polar core, where hydrophobic organic molecules can accumulate.

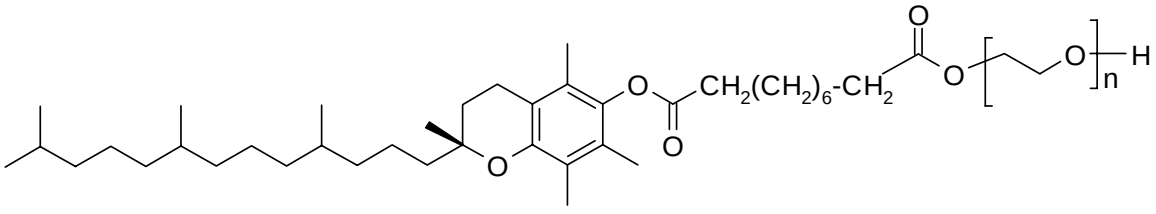

Figure 9.6 Chemical structure of polyoxyethanyl α-tocopheryl sebacate (PTS).

For the PTS micelles a high capability of the core loading is specific. Thus, a highly water insoluble Q10 coenzyme was successfully solubilized by the use of the PTS micelles and delivered into a human body [116]. The molar ratio between the PTS and the coenzyme was in the range of 2:1 that with a 5 wt% of the PTS corresponds to the solubilization of nearly 1.8 wt% (or $2.1 \cdot 10^{-3}$ M) of Q10. Therefore, the high solubilization levels are achievable. Starting from these, we estimated the maximal micelles loading by UC dyes to be in a range 10^{-4} – 10^{-2} M. Taking into account an order increased concentration of the dyes in the micelles core and the investigations reported in the part 6.3, it should be sufficient to observe an effective TTA – UC process.

The PTS micelles were also used as nanoreactors, where chemical transformations such as Heck and Suzuki coupling, an olefin metathesis and a ring-closing metathesis were conducted with a good yield in the ambient conditions [117-120]. For such types of the chemical reactions relatively high mobility of the reactants is required. A high efficiency of the conducted experiments indicates the liquid-like nature of the micelle core. The results of our experiments show that for an efficient UC generation the participating in the TTA – UC process molecules should have a high local mobility. Therefore the PTS micelles seem to be the perfect candidates to be used for transferring of the TTA – UC process from organic solvents into the bio-compatible aqueous environment.

The standard sensitizer emitter pair, PdTBP and perylene, was used as a model UC system. The samples were prepared at the ambient atmosphere conditions, deoxygenated and afterward sealed in vitrotubes in the nitrogen-filled glovebox. The THF (spectroscopic grade) and the deionized water were used for the solubilization. In order to create the stock solutions, perylene and PdTBP were dissolved in THF in the concentrations 10^{-3} M and 10^{-4} M, respectively. To achieve the desired concentrations of the UC dyes, the necessary amounts of the stock solutions were mixed with 15 wt% solution of the PTS in the water. The water was slowly added while stirring the main solution. The THF was removed by a rotor evaporation (overnight, at 200 mbar and temperature of 45 ºC). An additional amount of water was added to compensate the water loss during the evaporation.

To prove the efficiency of the THF evaporation and its absence in the resulting solution a control experiment was performed. In 6 ml of heavy water (D_2O) 100 µl of THF was added. Then, THF was evaporated by the same procedure described above. After the evaporation in order to estimate the residual concentration of THF a fixed concentration of tert-butanol (5 ppm) was added and H-NMR spectra were recorded (^{1}H NMR 300 MHz). The signal from 9H of methyl groups (1.24 ppm) was clearly observed.

Figure 9.7 Photo of obtained micelles solution. Blue UC emission is visible even with a naked eye at ambient light conditions.

The measurements of the size of the created structures was done by a photon cross correlation spectroscopy (PCCS) using a Nanophox (SimpaTec). The size of the micelles loaded with the UC system was estimated to be of approximately 30-35 nm and stays in the same level for a wide diapason of the PTS concentrations. So small size of the created structures results in a negligible light scattering of the solution and the high transparency of obtained solutions (shown in Figure 9.7). It should be noted that at the PTS concentrations lower than 2.5 wt% the size of the micelles strongly altered. At the concentration of 0.5 wt% the size of micelles increased up to 100 nm and the solution becomes turbid. Additionally, the amount of a solubilized dye strongly lowers at the PTS concentration decrease that was proven by absorption measurements. It is seen (Figure 9.8) that with increase of the micelles size the optical density of solution in the region of perylene absorption is correspondingly reduced. For further investigations the concentrations of PTS higher than 2.5 wt% were used.

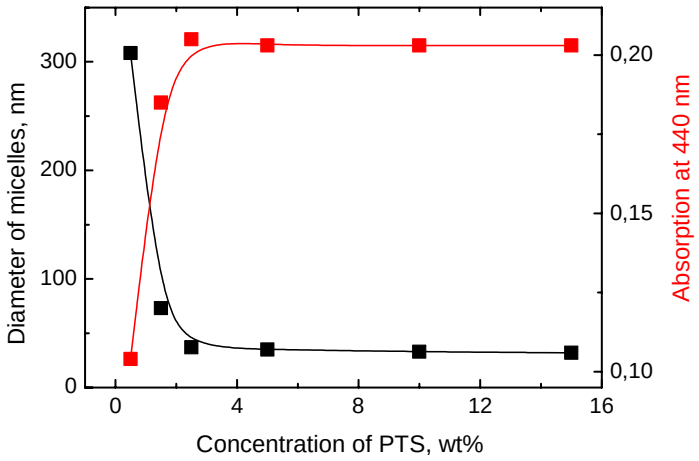

Figure 9.8 Sample absorption at 440 nm and micelles size in dependence on PTS concentration. Concentration of perylene during the sample preparation was kept $5 \cdot 10^{-5}$ M.

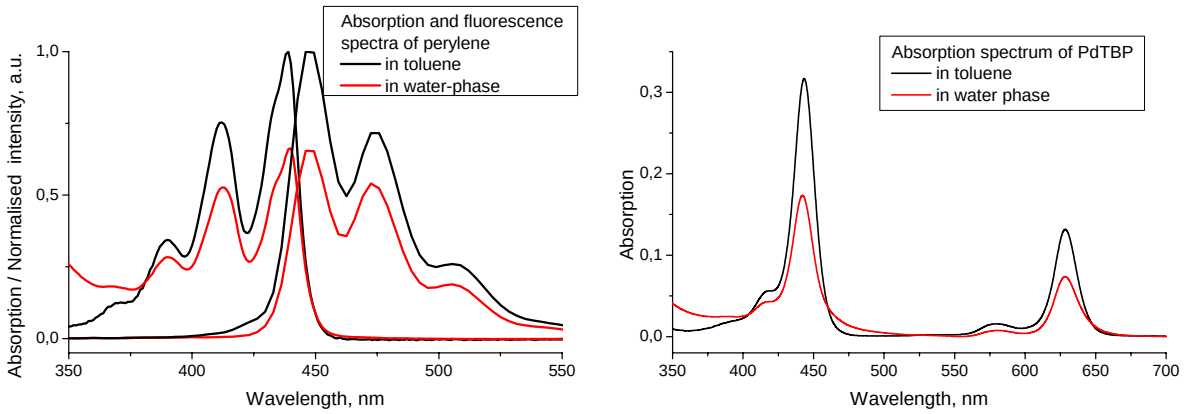

Figure 9.9 Absorption and fluorescence spectra for perylene (left) (dye concentration $5 \cdot 10^{-5}$ M, concentration of PTS in water phase sample 2.5 wt%) and PdTBP (right) (dye concentration $1 \cdot 10^{-6}$ M, concentration of PTS in water phase sample 2.5 wt%) in toluene (black line) and water phase (red line).

As mentioned above, the concentration of the dyes inside the micelles is higher than averaged over all the volume of the solution. Taking into account that the hydrophobic dyes are soluble only in the inner part of the micelles and that water solution contain around 5 wt% of PTS, the local concentration of the dyes in the core should be at least 20 times higher than the average concentration. Anyway, the form of the absorption spectra of perylene and PdTBP in the water-phase did not differ from those taken at the same concentration of dyes in toluene (shown in Figure 9.9). The fluorescence spectra of the perylene, excited by the UV-light in both media, did not show any excimer formation. Nevertheless, in the water phase the absorption, as well as the corresponding emission, was lower than in the organic medium. We explain it by increased polarity of the surrounding in the case of water solution.

The typical UC spectra dependence on the excitation intensity, observed from the micelles solutions, is seen in Figure 9.10. There is no evident difference in a behavior of the water-phase sample in compare to any UC system dissolved in an organic solvent.

The spectra, obtained at the maximal excitation intensity (26.5 $W \cdot cm^{-2}$) for the micelles solution and the equal UC system but in the organic solvent (toluene), are shown in Figure 9.11. As it seen, the intensity of the UC signal for the water-phase sample is about 4 times less than for the toluene sample. Taking into account the mentioned earlier decrease of the absorptivity of the sensitizer in the water-phase sample, the external Q.Y. of the UC generation in the water phase was estimated to reach 2.4 %. In the only paper [112], devoted to the TTA – UC generation in the water environment, the reported efficiency was as high as 0.06%, that is two orders less, than the Q.Y. of our system.

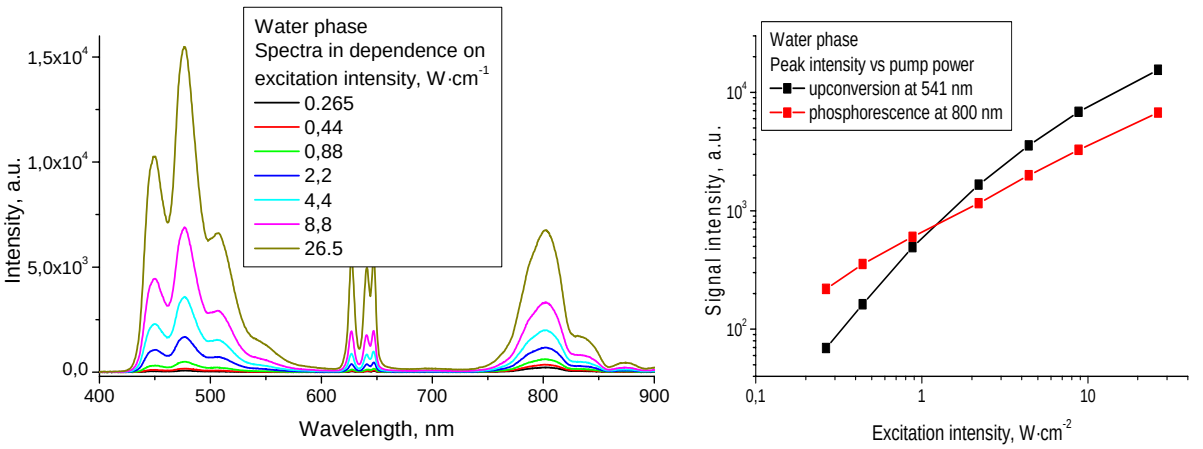

Figure 9.10 Spectra of generated UC and residual phosphorescence signals in dependence on excitation intensity for the sample containing perylene ($4 \cdot 10^{-4}$ M) and PdTBP ($2 \cdot 10^{-5}$ M), solubilized in PTS/water solution (PTS concentration 5 wt%).

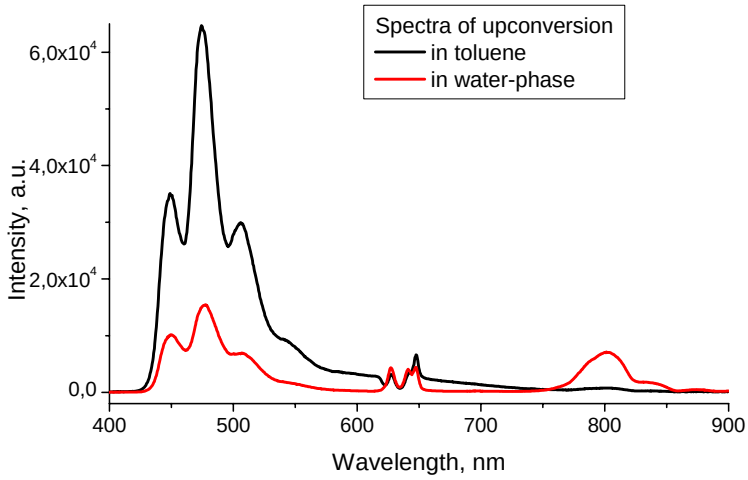

Figure 9.11 The emission spectrum for the samples containing perylene ($4 \cdot 10^{-4}$ M) and PdTBP $2 \cdot 10^{-5}$ M, dissolved in PTS/water solution (PTS concentration 5 wt%) (red line) and in toluene (black line). Excitation wavelength 633 nm.

The higher signal of the residual phosphorescence of the sensitizer in the water-phase in comparison to the toluene sample indicates the reduced efficiency of the TTT process. The reason for it is the crucial change of the surrounding. Thus, the local surround parameters like a viscosity of the "solvent" and a subsequent mobility of the dyes in the micelle core can strongly differ from those in the organic solvent, resulting in a decreased probability of molecules interaction leading to the reduced energy transmission.

In order to increase the obtained maximal efficiency of UC generation, the optimization of the experimental conditions, namely the volume concentration of the surfactant, the molar concentrations of the sensitizer and the emitter dyes and the ratio between them was conducted.

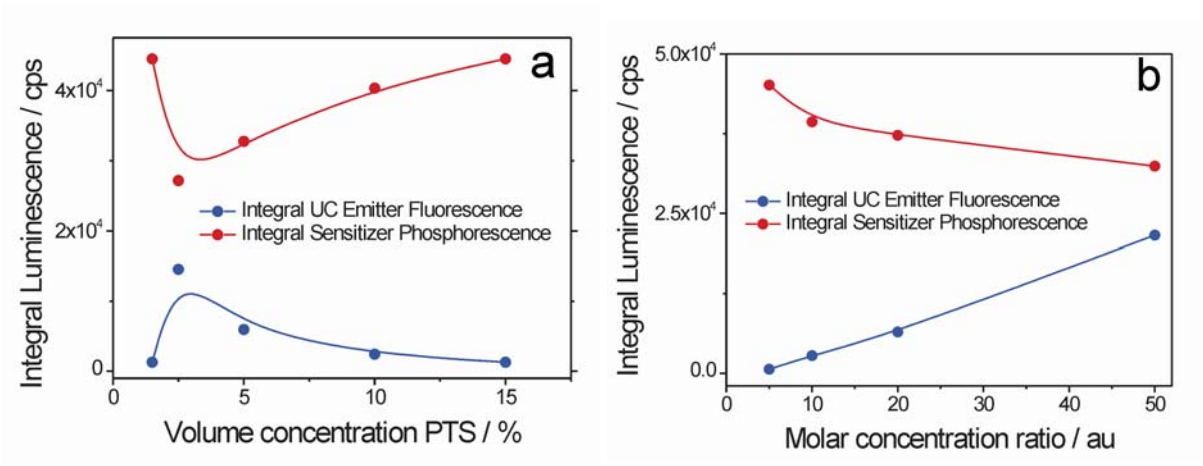

Figure 9.12 Dependence of the integral UC fluorescence and the integral sensitizer phosphorescence on the concentration of PTS (concentrations of the dyes are $1 \cdot 10^{-6}$ M for PdTBP and $5 \cdot 10^{-5}$ M for perylene.) (left) and on the ratio between concentrations of perylene and PdTBP (right) (concentration of PdTBP is $1 \cdot 10^{-6}$ M, perylene concentrations are varied from $5 \cdot 10^{-6}$ M up to $5 \cdot 10^{-5}$ M, PTS concentration 2.5 wt%).

For the sample containing $1 \cdot 10^{-6}$ M of PdTBP and $5 \cdot 10^{-5}$ M of perylene the PTS concentration was increased from 1.5 wt% up to 15 wt%. The results are shown in Figure 9.12. As it was previously mentioned, at the lowest concentration the micelles grew drastically and their loading capacity strongly decreased. The maximal UC was observed at 2.5 wt% of the PTS. The further increase of the PTS concentration led to the UC signal decrease, whilst the phosphorescence signal grew.

For the optimal concentration of the PTS (2.5 wt%) the concentration of the sensitizer of $1 \cdot 10^{-6}$ M was kept constant, whereas the emitter concentration was varied from $5 \cdot 10^{-6}$ M up to $5 \cdot 10^{-4}$ M that correspond to the ratio from 1:5 up to 1:500 between the sensitizer and emitter concentrations. However, it was observed, that the maximal loading capacity of the micelles is limited. Thus, for every PTS concentration the critical concentration of the loading dye exists, above which the micelles solution become unstable. For example, for the PTS concentration of 2.5 wt% the maximal reached concentration of perylene was only $5 \cdot 10^{-5}$ M, that limited further increase of the emitter concentration. After increase of the PTS concentration up to 5 wt% the critical perylene concentration grew up to $5 \cdot 10^{-4}$ M. The results on emitter concentration increase for the PTS concentration of 2.5 wt% are shown in the right graph of Figure 9.12 and Figure 9.13. The monotonous increase of the UC signal is seen. Nevertheless, even at the relative concentration of 1:50 the residual phosphorescence was higher than the UC signal. After the increase of the PTS concentration, the UC generation efficiency dropped down in more than 3 times, but grew significantly up to 2.4% at further emitter concentration raise (blue in Figure 9.13).

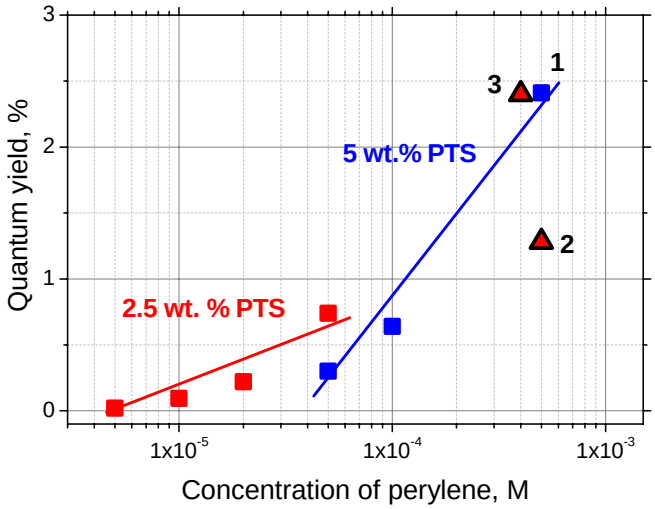

Figure 9.13 Dependence of the Q.Y. of UC for the PdTBP-perylene pair dissolved in PTS-water mixture on the emitter molar concentration at different PTS concentrations: red – 2.5 wt%, blue – 5 wt%. Points 2 and 3 are for the sensitizer concentrations $1 \cdot 10^{-5}$ M and $2 \cdot 10^{-5}$ M, correspondingly.

Increase of sensitizer concentration up to the value of $1 \cdot 10^{-5}$ M led to decrease of Q.Y. of UC down to 1.3% (for the sample with $5 \cdot 10^{-4}$ M of perylene) (point 2 in Figure 9.13), but rose again with twice increased sensitizer concentration and reached 2.4% ($2 \cdot 10^{-5}$ M of PdTBP and $4 \cdot 10^{-4}$ M of perylene) (point 3 in Figure 9.13). PTS concentration was kept at 5 wt% for these samples.

In summary, an energetically conjoined TTA – UC was successfully transferred into the water environment by the use of PTS surfactant. One of the main benefits of the hydrophobic dyes embedding in the micellar structures is the increase of the local molar concentration of the UC dyes. It enables to obtain the UC in the aqueous environment with the generation efficiency of 2.4 % that is similar to that in the volatile organic solvent. An extremely low light excitation intensity (UC signal was detected even at 10 $mW \cdot cm^{-2}$) was sufficient to generate the UC photons. Should be also noted that the used for solubilization of the hydrophobic species PTS surfactant has an outstanding biocompatibility.

9.3 Temperature sensitive TTA – UC in water phase

The dependence of the phosphorescence emission or its decay time is known to be used for a thermal sensing [121]. Commonly, for metallated porphyrins a strong decrease of the phosphorescent signal at the sample temperature increase is observed [122]. Recently the thermal distribution sensing method, operating by this effect, was patented [123]. The principle is based on the use of a ratiometric parameter, showing a proportion between the phosphorescence and the fluorescence of PdOEP at a temperature variation. Thus, at the increase of the temperature, the phosphorescence of PdOEP strongly decreases, whereas the delayed fluorescence, which is the result of the TTA between PdOEP molecules, rises [124]. Recently, the temperature dependence of the TTA – UC system in rigid matrices was reported [75]. At an increase of the temperature the rise of the UC signal was observed, but the cause for such behavior was not discussed. From our knowledge, the only reason is the reduced viscosity of the polymer films at the heating and the successive increased mobility of the sensitizer and emitter molecules.

On the other hand, it has long been known that a micelles phase structure and characteristics like the shape [125], the critical micelle concentration [126, 127], the size [128] and the viscosity [129] are strongly dependent on the temperature. For example, the increase of Triton X-100 micelles size in 2 times at the temperature raise from 10 ºC up to 50 ºCwas observed [128].

We assumed that a change of the size of the micelle at the temperature increase can influence on the local viscosity and the intrinsic diffusion coefficient of the micelle. Together with a temperature sensitive porphyrin it should result in a strong dependence of the TTA – UC efficiency on the temperature.

For the UC sample temperature variation the conventional sample holder was changed by a microscope thermostabilised stage (LINKAM). According to the stage design a sample is closed in a chamber in order to isolate it from the ambient atmosphere influence, and is located on a silver plate, which could be fast heated or cooled. The sample can be excited by the optical radiation through the optical window. The plate has the opening to let the excitation beam go through. For the exact temperature control a cooling system should be assembled. The combination of the simultaneous cooling by a coolant and the heating by the electrical heater the temperature of the silver plate can be controlled with the accuracy of 0.1°C in the range from -190°C (for a case of cooling by a vapor of liquid nitrogen) up to 120°C. The heater current is controlled by the driver, keeping the temperature at the given

level. The cool water from the supply system was used as a coolant for these experiments. Therefore, the lowest achievable temperature in the chamber was limited to 15°C.

To avoid a thermal shock of the sample, the temperature was increased with a rate of 10°C·min^{-1}. The temperature step used for the measurements was equal to 3°C. The measurements of the UC spectra were done after 30 seconds behind the necessary temperature level reached. This time was given for an additional sample's characteristics stabilization.

The emission with the central wavelength 633 nm and the maximal power of 2.5 mW was used for the UC excitation. The excitation beam was focused on the sample with a resulting spot having diameter of 400 μm. Thus, the calculated maximal excitation intensity reached 2 W·cm^{-2}.

One can choose the initial ratio between the phosphorescence and the UC signals by a variation of the absolute and the relative concentrations of the UC dyes. In order to increase the phosphorescence signal, not optimized concentrations of the dyes (PdTBP as the sensitizer at the concentration of $1 \cdot 10^{-5}$ M and perylene as emitter at $2 \cdot 10^{-4}$ M) were solubilized in the milli-Q water by 5 wt% of non-ionic PTS surfactant according to the preparation method described in part 9.2. The ready sample solution was deoxygenated in the glovebox and sealed by the two-component epoxy in the vitrotubes having the thickness of 400 μm.

The measured UC spectra at the different temperatures are shown in Figure 9.14. The excitation intensity was kept constant at the level of 2 W·cm^{-2}. It is seen, that the increase of the sample temperature led to the UC signal raise, whereas the phosphorescence signal decreased. Thus, the change of the temperature from 20 ºC up to 41 ºC was accompanied by twice increased UC signal (and corresponding Q.Y.) and twice decreased phosphorescence signal from the sensitizer. The presence of two processes, having the opposite response, can increase the temporal sensitivity if a differential parameter is introduced. Thus, the ratiometric parameter changed in round 4 times (from 0.54 up to 2.1) (shown in bottom graph in Figure 9.14) at increase of temperature on 21 ºC, that correspond to the average sensitivity of 0.1·K^{-1} (growth of the ratiometric parameter on 10%·at increase of temperature on 1 K).

In order to investigate how the temperature variation influences on the temporal characteristics of the UC process in the micelles solution, the phosphorescence and the UC signal were registered in dependence on time. The same detection scheme was used, as the previously described in part 7. The UC in the sample was excited by the radiation of the diode laser, modulated by the pulse generator.

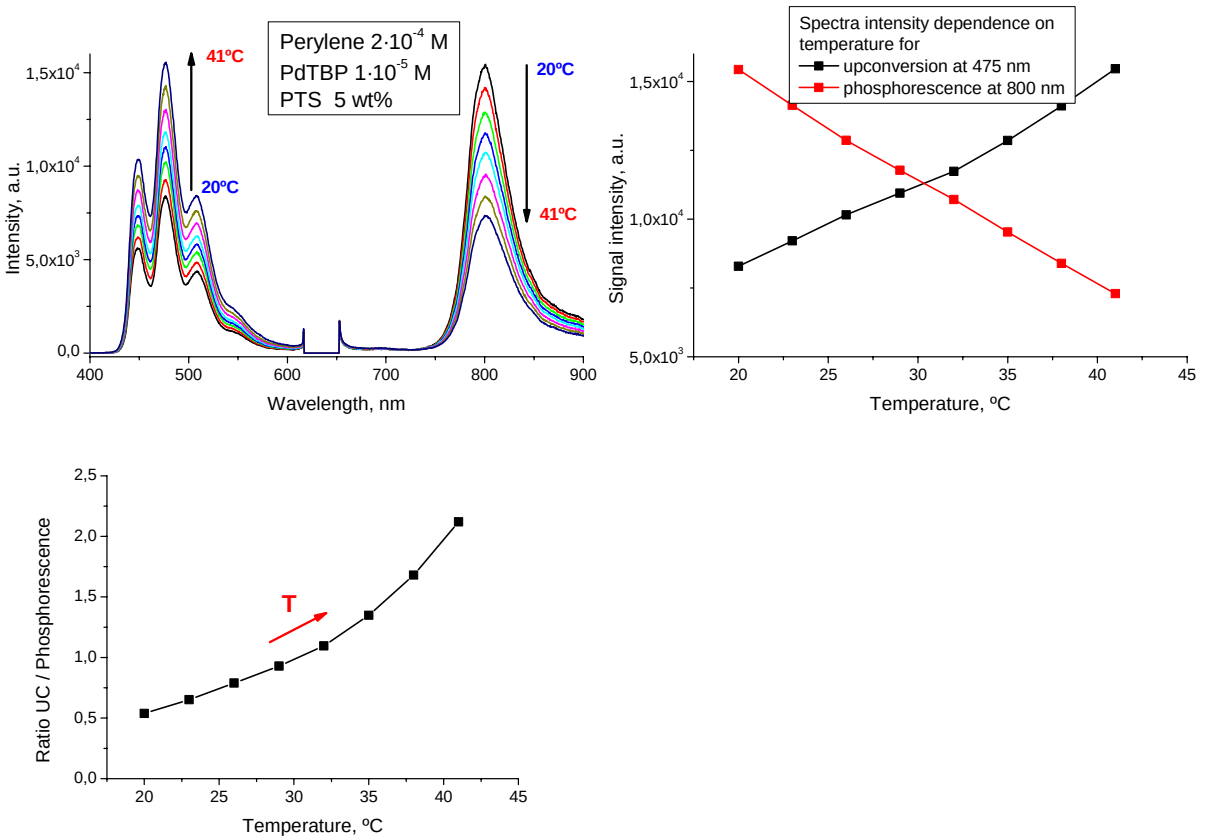

Figure 9.14 Emission spectra (top left), UC and phosphorescence signals intensity (top right) and ratio between them (bottom) in dependence on temperature for the sample containing PdTBP 1·10^{-5} M, perylene 2·10^{-4} M and PTS 5 wt%.

Each pulse duration was equal to 10 ms, pulse to pulse period was chosen to be 50 ms. Peak excitation intensity of the pulses was at the level of 1 W·cm^{-2} (a corresponding average excitation intensity for the modulated radiation is 5 times less).

The obtained oscillograms both for the phosphorescence and the UC signals are shown in Figure 9.15. It is seen, that the increase of the temperature of the system leads to a strong decrease of the decay time of triplet state of sensitizer. The decay time of the phosphorescence signal (taken at the level of 1/e) drops almost linearly from 155 μs down to 48 μs with the temperature grow (the dependencies are shown in Figure 9.16) that indicate the increased efficiency of the TTT. The decay time of the generated delayed fluorescence also decreases from 290 μs down to 115 μs that is a result of the changed mobility of the molecules at the temperature increase and the corresponding improvement of the efficiency of the triplet states annihilation.

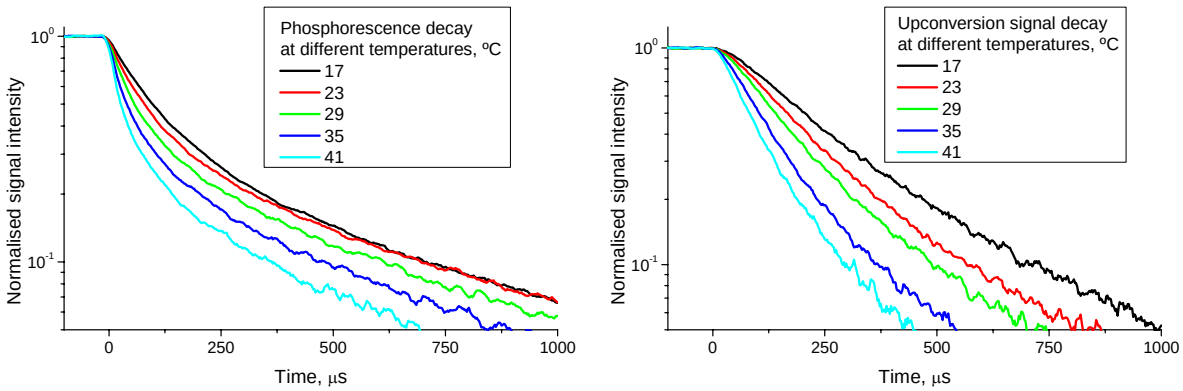

Figure 9.15 Normalized phosphorescence (left) and UC (right) signal intensities (logarithmic scale) in dependence on time for different temperature of the sample (PdTBP $1 \cdot 10^{-5}$ M, perylene $2 \cdot 10^{-4}$ M and PTS 5 wt%).

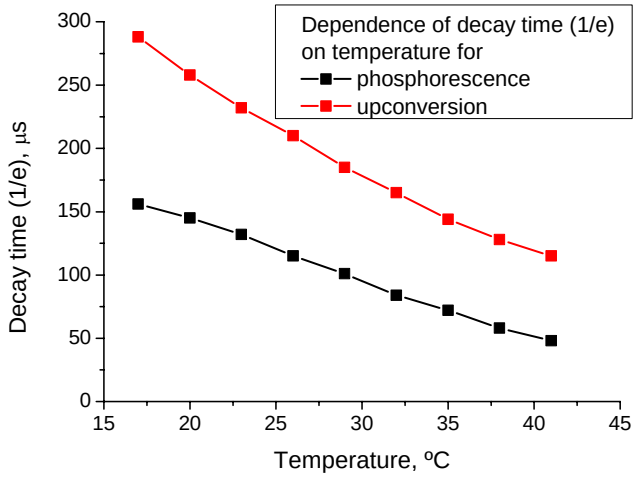

Figure 9.16 The dependence of the decay time (taken at 1/e level) of phosphorescence (black) and UC (red) signals on the temperature of the sample (PdTBP $1 \cdot 10^{-5}$ M, perylene $2 \cdot 10^{-4}$ M and PTS 5 wt%).

The emitter dye was proposed to be changed by the Y-635 emitter, which has the higher efficiency in a combination with PdTBP sensitizer, as the perylene (see part 8.1). The sample containing the same molar concentrations of dyes and surfactant, as for previous sample, was created. Surprisingly, at the temperature of 17 ºC the obtained UC efficiency was much lower in compare to the perylene – PdTBP pair and the phosphorescence signal was 24 times higher than the UC one (the generated emission spectra are shown in Figure 9.17). On the other hand, the sensitivity of the system on the temperature alteration improved significantly. Thus, the change of the temperature from 17 ºC up to 41 ºC was accompanied by 6 times increase of the UC signal (and corresponding Q.Y.) and more than twice decreased phosphorescence signal from the sensitizer. The ratiometric parameter (shown in the bottom right graph in Figure 9.17) changed in 13 times, that gives round $0.5 \cdot K^{-1}$ (50%·of ratio increase at increase of temperature on 1 K) of the temperature sensitivity.

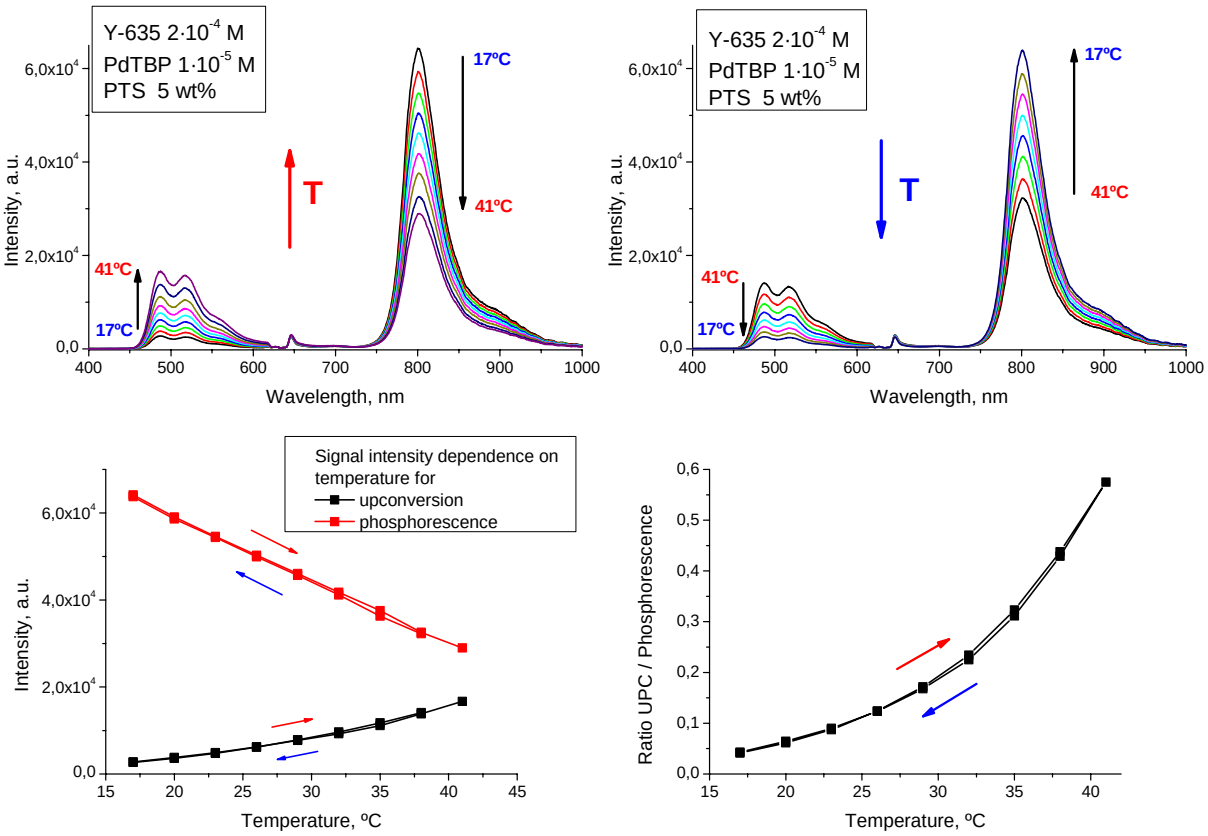

Figure 9.17 Emission spectra at heating (top left) and cooling (top right), UC and phosphorescence signals intensity (bottom left) and ratio between them (bottom right) in dependence on temperature for the sample containing PdTBP 1·10^{-5} M, Y-635 2·10^{-4} M and PTS 5 wt%.

Taking the error of the measurement of spectrum intensity at the level of 5%, the corresponding achievable temperature sensitivity can be estimated as round 0.1 K.

No significant hysteresis of the signal during heating and cooling of the sample (corresponding spectra are shown in Figure 9.17) was observed. The decrease of the temperature results in the reversed behavior of the dependencies – the UC efficiency drops down with the simultaneous growing of the phosphorescence.

It should be noted that the upper limit of the temperature for all the samples with PTS surfactant was limited by 41°C. At the samples heating up to 42-43°C the investigated micelle solution started to become turbid with a changing of the initial properties of the solution. Nevertheless, the UC process remained efficient. The optical transparency of the solution returned at the cooling of the sample under 41°C.

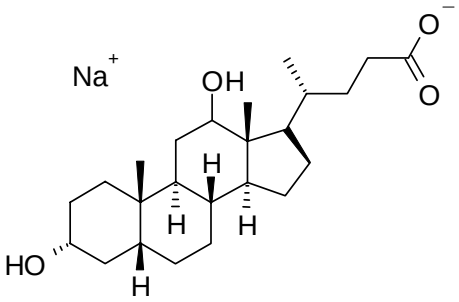

Figure 9.18 Chemical structure of sodium deoxycholate.

Other surfactants were suggested to be used in order to overcome this temperature limit. The samples with the UC system (PdTBP ($1 \cdot 10^{-5}$ M) and perylene ($2 \cdot 10^{-4}$ M)) were solubilized in the water by two surfactants from polyoxyethyleneether family, namely Triton X-100 (previously shown in Figure 9.4) and IGEPAL CA-630 (chemical structure is similar to Triton X-100), and sodium deoxycholate (the structure is shown in Figure 9.18).

The results of the UC generation in dependence on temperature in micelles solutions for Triton X-100 and IGEPAL CA-630 are shown in Figure 9.19 and Figure 9.20. It should be noted that because of almost the same chemical structure the obtained results were quite similar. The efficiency of the UC generation was extremely low at room temperature (21 ºC) but grew significantly with the temperature increase. The ratiometric parameter changed in around 600 times for Triton X-100 and 300 times for IGEPAL CA-630 at the temperature increase on 45 ºC. Both investigated solutions became turbid at around 70 ºC that is on 30 ºC higher than for PTS surfactant.

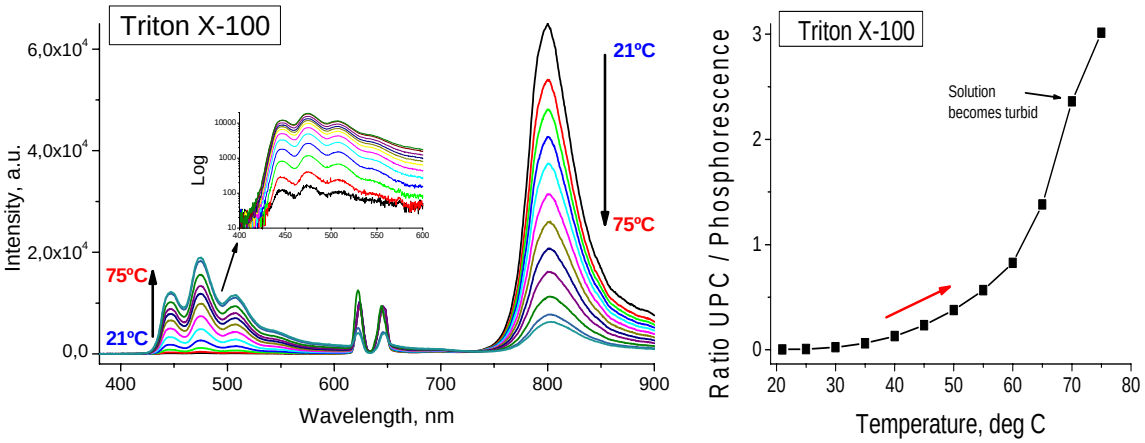

Figure 9.19 Emission spectra (left) with logarithmic scaled inset for UC signal and ratio between UC and phosphorescence signals (right) In dependence on the temperature for the samples containing PdTBP $1 \cdot 10^{-5}$ M and perylene $2 \cdot 10^{-4}$ M solubilized by Triton X-100 5 wt%.

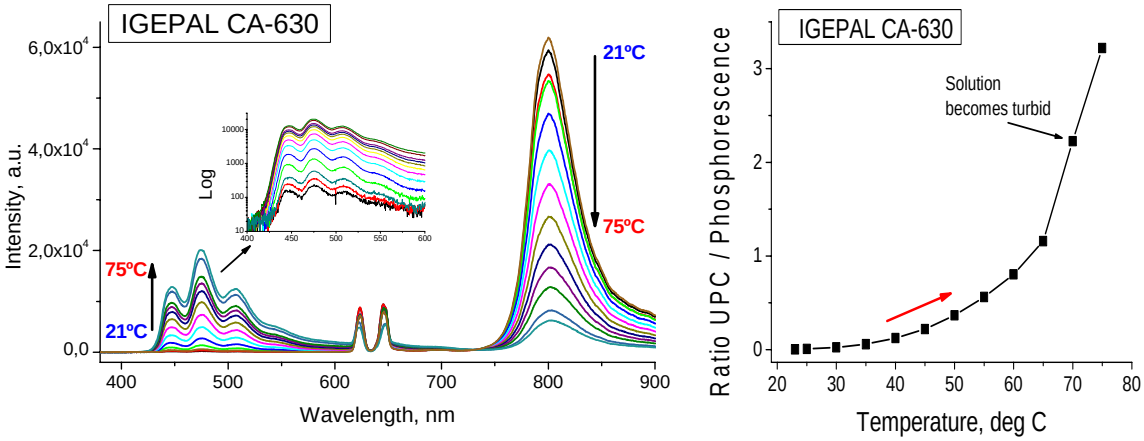

Figure 9.20 Emission spectra (left) with logarithmic scaled inset for UC signal and ratio between UC and phosphorescence signals (right) In dependence on the temperature for the samples containing PdTBP $1 \cdot 10^{-5}$ M and perylene $2 \cdot 10^{-4}$ M solubilized by IGEPAL CA-630 5 wt%.

The sample with the third proposed surfactant (sodium deoxycholate) remained transparent even at the temperatures higher than 75 ºC. Unfortunately, up to 60 ºC only the phosphorescence signal was clearly detectable. It decreased almost linearly with the temperature increase that is characteristic for metallated porphyrins [122]. The UC signal started to be distinguished from a noise only at 65 ºC and grew at the further temperature increase. Anyway, the increase of the temperature above 75 ºC was avoided from the security reasons. The pressure of the water vapor inside the glassy vitrotubes is growing significantly with a temperature increase and could result in an explosion of the sample.

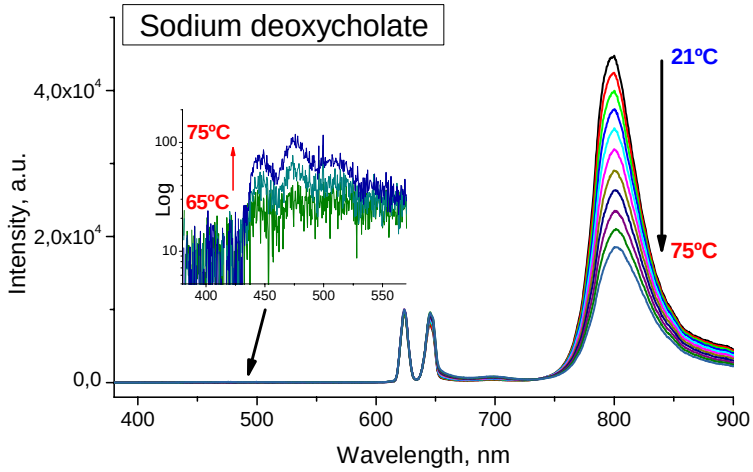

Figure 9.21 Emission spectra with logarithmic scaled inset for UC signal in dependence on the temperature for the sample PdTBP $1 \cdot 10^{-5}$ M, perylene $2 \cdot 10^{-4}$ M, solubilized by Sodium deoxycholate 5 wt%.

In conclusion, the embedding the hydrophobic dyes in the micellar structures results in a highly temperature sensitive system, that can be used for temperature sensing purposes. Small size of the micelles can be potentially used for the imaging of the local temperature distribution with a high resolution instead of the fluorescence lifetime imaging techniques [130] and with the sensitivity, improved in compare to other temperature-sensitive systems [131]. Because of the high bio-compatibility PTS micelles with encapsulated TTA – UC system can be directly used in biologically-oriented investigations for temperature sensing in the temperature range up to 41 ºC. As it was previously noted, there is no obvious restriction on the encapsulated UC system. Thus, TNP sensitizers with appropriate emitters can be used to transfer the UC system in the optical tissue transparency window with corresponding advantages.

In comparison to the PTS system, micelles created with Triton X-100 and IGEPAL CA-630 surfactants have restricted applicability in biological science because of surfactant's toxicity [132], but have extended temperature range (up to 70 ºC) and possess much higher sensitivity and, therefore, can be used in other fields of science for the temperature sensing.

Conclusions and outlook

There are three main directions in the research of the process of triplet-triplet annihilation assisted upconversion (TTA – UC):

- the increase of the overall efficiency of upconversion (UC) by the search of new sensitizer-emitter pairs,
- the fundamental investigation of the processes involved in the TTA – UC and a theoretical treatment of the limit of upconversion efficiency,
- an exploration of new application areas.

Due to the cooperation with the colleagues from our group, taking over the chemical part of the investigations, my physical background and continuous modification of the experimental setup, the aspects from all three categories are represented in the actual work.

As the overview of the publications show, on the way to the UC efficiency increase the main attention of other research groups is focused on the creation of new sensitizer molecules, whereas the standard commercially available dyes like 9,10-diphenylanthracene (DPA), perylene and rubrene are used as emitters. In contrast, the main idea of our group is the variation of the properties of emitters, synthesized mainly on the base of perylene, while only several dyes from families of octa-, benzo-, naphto and anthroporphyrins are used as sensitizers. Thus, the substitution of the perylene core with one or two phenyl, ethynyl or phenylethynyl group(s), decorated with alkyl chains, allows one to vary the spectral region of the dye emission from blue up to yellow and simultaneously to increase the quantum efficiency of the TTA – UC. As a result, the maximal quantum efficiency in a case of use of the TBP sensitizers reached 13.4%. Similarly, the sensitizers from the TNP family were combined with the emitters based on perylene-monoimide and Bodipy dyes. The maximal obtained quantum efficiency was as high as 3.6%.

During the optimization of conditions for the efficient TTA – UC observation, a strong influence of the excitation beam parameters on the resulting UC efficiency was found. Specifically, at the beam spot sizes on the sample lower than 200 μm a drastic reduction of quantum efficiency of UC was observed. The severity of this effect is dependent on the viscosity of the matrix, used for the UC solution, and increases with lowering the solvent's viscosity. The intensity of the excitation radiation also plays a critical role in the TTA – UC process. Despite the fact that upconverted emission can be detected at the extremely low

levels of irradiation (order of 1 $mW \cdot cm^{-2}$), the efficiency of TTA – UC increases with the raise of the excitation radiation intensity and tends to be maximal at the irradiation levels of unities of $W \cdot cm^{-2}$. Besides the excitation parameters, it was shown, that not so much the absolute values, but a relative ratio between the sensitizer and emitter concentrations influences the resulting quantum efficiency of the TTA – UC process in the UC medium.

The significant fundamental result is the demonstration of a new strategy of an effective UC emitter's creation by comprising the functions of two chromophors in a dyad. In such a molecule the function of the triplet-triplet transfer (TTT) and the triplet-triplet annihilation (TTA) are attributed to different parts of the molecule. As a result, the quantum efficiency of the TTA – UC with the synthesized bichromophore emitter can be significantly higher than for each dye separately or being mixed.

An important step for a practical application of the TTA – UC effect is the transfer of an UC medium into the water environment. This was achieved by the encapsulation of hydrophobic UC dyes into the micelles, formed by the PTS surfactant. The resulting efficiency of the TTA – UC is comparable with that in volatile organic media. It is significant that due to the high bio-compatibility of the obtained micellar system a further application in biology and other environmental science is possible. Additionally, an extremely strong dependence of the efficiency of the TTA – UC process on temperature in such micellar structures was observed. As a consequence, the use of PTS micelles for the local temperature sensing in biological objects is theoretically possible. It was also shown that by the variation of a surfactant the range of temperature sensitivity can be extended up to 70 ºC that can probably find the application even in technological systems.

For the past decade the investigation of process of TTA – UC has been moved far forward. The number of publications, patents and new research groups, working in this research area, is growing from year to year. Nevertheless, there are still many open questions like a strong influence of the UC efficiency from molecular oxygen, shift of the possible excitation range further into the infra-red spectrum, search for the suitable technological matrices for the UC medium and others. In the presented work the answers for at least some of these quastions are hopefully given.

Bibliography

1. Shen, Y., *Principles of nonlinear optics.* 2008.
2. Rumi, M. and J.W. Perry, *Two-photon absorption: an overview of measurements and principles.* Advances in Optics and Photonics, 2010. **2**(4): p. 451-518.
3. Boyd, G., et al., *Second-harmonic generation of light with double refraction.* Physical Review, 1965. **137**(4A): p. A1305.
4. Lewenstein, M., et al., *Theory of high-harmonic generation by low-frequency laser fields.* Physical Review A, 1994. **49**(3): p. 2117.
5. Boyd, R.W., *Nonlinear optics* 2002: Academic press.
6. Scheps, R., *Upconversion laser processes.* Progress in Quantum Electronics, 1996. **20**(4): p. 271-358.
7. Baluschev, S., et al., *Upconversion photoluminescence in poly(ladder-type-pentaphenylene) doped with metal (II)-octaethyl porphyrins.* Applied Physics Letters, 2005. **86**(6).
8. Parker, C. and C. Hatchard. *Sensitised Anti-Stokes Delayed Fluorescence*. in *Proc. Chem. Soc., London*. 1962.
9. Sternlicht, H., G. Nieman, and G. Robinson, *Triplet—Triplet Annihilation and Delayed Fluorescence in Molecular Aggregates.* The Journal of Chemical Physics, 1963. **38**(6): p. 1326-1335.
10. Parker, C., *Phosphorescence and delayed fluorescence from solutions.* Advances in Photochemistry, 1964. **2**: p. 305-383.
11. Parker, C., C. Hatchard, and T.A. Joyce, *Selective and mutual sensitization of delayed fluorescence.* Nature, 1965. **205**: p. 1282 - 1284.
12. Parker, C. and T.A. Joyce, *Determination of triplet formation efficiencies by the measurement of sensitized delayed fluorescence.* Trans. Faraday Soc., 1966. **62**: p. 2785-2792.
13. Baluschev, S., et al., *Up-conversion fluorescence: Noncoherent excitation by sunlight.* Physical Review Letters, 2006. **97**(14).
14. Baluschev, S., et al., *A general approach for non-coherently excited annihilation up-conversion: transforming the solar-spectrum.* New Journal of Physics, 2008. **10**.
15. Cheng, Y.Y., et al., *Improving the light-harvesting of amorphous silicon solar cells with photochemical upconversion.* Energy & Environmental Science, 2012. **5**(5): p. 6953-6959.
16. Huang, X., et al., *Enhancing solar cell efficiency: the search for luminescent materials as spectral converters.* Chemical Society Reviews, 2013.
17. Khnayzer, R.S., et al., *Upconversion-powered photoelectrochemistry.* Chemical Communications, 2012. **48**(2): p. 209-211.
18. Miteva, T., et al., *Annihilation assisted upconversion: all-organic, flexible and transparent multicolour display.* New Journal of Physics, 2008. **10**.
19. Miteva, T., et al., *Late-news paper: All-organic, transparent up-conversion displays with tailored excitation and emission wavelengths.* 2008 Sid International Symposium, Digest of Technical Papers, Vol Xxxix, Books I-Iii, 2008. **39**: p. 665-668.
20. Borisov, S.M., C. Larndorfer, and I. Klimant, *Triplet–Triplet Annihilation-Based Anti-Stokes Oxygen Sensing Materials with a Very Broad Dynamic Range.* Advanced Functional Materials, 2012: p. n/a-n/a.
21. Baluschev, S. and T. Miteva, *Non-Coherent Up-Conversion in Multi-Component Organic Systems.* Next Generation of Photovoltaics, 2012: p. 157-190.

22. Solovyov, K.N. and E.A. Borisevich, *Intramolecular heavy-atom effect in the photophysics of organic molecules.* Physics-Uspekhi, 2005. **48**(3): p. 231-253.
23. Scholes, G.D., *Long-range resonance energy transfer in molecular systems.* Annual review of physical chemistry, 2003. **54**(1): p. 57-87.
24. Hsu, C.-P., *The electronic couplings in electron transfer and excitation energy transfer.* Accounts of Chemical Research, 2009. **42**(4): p. 509-518.
25. Zhao, W. and F.N. Castellano, *Upconverted emission from pyrene and di-tert-butylpyrene using Ir(ppy)(3) as triplet sensitizer.* Journal of Physical Chemistry A, 2006. **110**(40): p. 11440-11445.
26. Monguzzi, A., et al., *Low power, non-coherent sensitized photon up-conversion: modelling and perspectives.* Physical Chemistry Chemical Physics, 2012. **14**(13): p. 4322-4332.
27. Rurack, K., *Fluorescence quantum yields: methods of determination and standards.* Standardization and Quality Assurance in Fluorescence Measurements I, 2008: p. 101-145.
28. Fischer, M. and J. Georges, *Fluorescence quantum yield of rhodamine 6G in ethanol as a function of concentration using thermal lens spectrometry.* Chemical Physics Letters, 1996. **260**(1-2): p. 115-118.
29. Kubin, R. and A. Fletcher, *Fluorescence quantum yields of some rhodamine dyes.* Journal of Luminescence, 1983. **27**(4): p. 455-462.
30. Bachilo, S.M. and R.B. Weisman, *Determination of triplet quantum yields from triplet-triplet annihilation fluorescence.* The Journal of Physical Chemistry A, 2000. **104**(33): p. 7711-7714.
31. Cheng, Y.Y., et al., *On the efficiency limit of triplet-triplet annihilation for photochemical upconversion.* Physical Chemistry Chemical Physics, 2010. **12**(1): p. 66-71.
32. Froese, R.D.J. and K. Morokuma, *Accurate calculations of bond-breaking energies in C< sub> 60</sub> using the three-layered ONIOM method.* Chemical Physics Letters, 1999. **305**(5): p. 419-424.
33. Cheng, Y.Y., et al., *Kinetic Analysis of Photochemical Upconversion by Triplet-Triplet Annihilation: Beyond Any Spin Statistical Limit.* Journal of Physical Chemistry Letters, 2010. **1**(12): p. 1795-1799.
34. Singh-Rachford, T.N. and F.N. Castellano, *Triplet Sensitized Red-to-Blue Photon Upconversion.* Journal of Physical Chemistry Letters, 2010. **1**(1): p. 195-200.
35. Baluschev, S., et al., *Blue-green up-conversion: Noncoherent excitation by NIR light.* Angewandte Chemie-International Edition, 2007. **46**(40): p. 7693-7696.
36. Foote, C.S., *Active oxygen in chemistry*1995: Chapman & Hall.
37. Vinogradov, S.A. and D.F. Wilson, *Metallotetrabenzoporphyrins. New phosphorescent probes for oxygen measurements.* Journal of the Chemical Society, Perkin Transactions 2, 1995. **0**(1): p. 103-111.
38. Niedermair, F., et al., *Tunable Phosphorescent NIR Oxygen Indicators Based on Mixed Benzo-and Naphthoporphyrin Complexes.* Inorganic chemistry, 2010. **49**(20): p. 9333.
39. Wu, W., et al., *Tuning the emissive triplet excited states of platinum (II) Schiff base complexes with pyrene, and application for luminescent oxygen sensing and triplet–triplet-annihilation based upconversions.* Dalton Transactions, 2011. **40**(43): p. 11550-11561.
40. Kochevar, I.E. and R.W. Redmond, *[2] Photosensitized production of singlet oxygen.* Methods in enzymology, 2000. **319**: p. 20-28.
41. DeRosa, M.C. and R.J. Crutchley, *Photosensitized singlet oxygen and its applications.* Coordination Chemistry Reviews, 2002. **233**: p. 351-371.

42. Demas, J.N. and G.A. Crosby, *Measurement of Photoluminescence Quantum Yields - Review.* Journal of Physical Chemistry, 1971. **75**(8): p. 991-&.
43. Olmsted, J., *Calorimetric determinations of absolute fluorescence quantum yields.* Journal of Physical Chemistry, 1979. **83**(20): p. 2581-2584.
44. Lakowicz, J.R., *Principles of fluorescence spectroscopy*. Vol. 1. 2006: Springer.
45. Brouwer, A.M., *Standards for photoluminescence quantum yield measurements in solution (IUPAC Technical Report).* Pure and Applied Chemistry, 2011. **83**(12): p. 2213-2228.
46. Montalti, M., et al., *Handbook of photochemistry*2006: CRC.
47. Karstens, T. and K. Kobs, *Rhodamine B and rhodamine 101 as reference substances for fluorescence quantum yield measurements.* The Journal of Physical Chemistry, 1980. **84**(14): p. 1871-1872.
48. Penzkofer, A. and W. Leupacher, *Fluorescence Behavior of Highly Concentrated Rhodamine 6g Solutions.* Journal of Luminescence, 1987. **37**(2): p. 61-72.
49. Magde, D., R. Wong, and P.G. Seybold, *Fluorescence Quantum Yields and Their Relation to Lifetimes of Rhodamine 6G and Fluorescein in Nine Solvents: Improved Absolute Standards for Quantum Yields*¶. Photochemistry and photobiology, 2002. **75**(4): p. 327-334.
50. Ferguson, M.W., et al., *Excited state and free radical properties of Rhodamine 123: a laser flash photolysis and radiolysis study.* Phys. Chem. Chem. Phys., 1999. **1**(2): p. 261-268.
51. Pal, P., et al., *Spectroscopic and photophysical properties of some new rhodamine derivatives in cationic, anionic and neutral micelles.* Journal of Photochemistry and Photobiology A: Chemistry, 1996. **98**(1): p. 65-72.
52. Braslavsky, S., *GLOSSARY OF TERMS USED IN PHOTOCHEMISTRY 3 rd EDITION.* Pure Appl. Chem, 2007. **79**(3): p. 293-465.
53. Singh-Rachford, T.N. and F.N. Castellano, *Photon upconversion based on sensitized triplet-triplet annihilation.* Coordination Chemistry Reviews, 2010. **254**(21-22): p. 2560-2573.
54. Singh-Rachford, T.N. and F.N. Castellano, *Low Power Visible-to-UV Upconversion.* Journal of Physical Chemistry A, 2009. **113**(20): p. 5912-5917.
55. Rachford, A.A., et al., *Boron Dipyrromethene (Bodipy) Phosphorescence Revealed in [Ir (ppy) 2 (bpy-C□ C-Bodipy)]+.* Inorganic chemistry, 2010. **49**(8): p. 3730-3736.
56. Islangulov, R.R., D.V. Kozlov, and F.N. Castellano, *Low power upconversion using MLCT sensitizers.* Chemical Communications, 2005(30): p. 3776-3778.
57. Zhao, J., S. Ji, and H. Guo, *Triplet–triplet annihilation based upconversion: from triplet sensitizers and triplet acceptors to upconversion quantum yields.* RSC Advances, 2011. **1**(6): p. 937-950.
58. Ji, S., et al., *Tuning the luminescence lifetimes of ruthenium (II) polypyridine complexes and its application in luminescent oxygen sensing.* J. Mater. Chem., 2010. **20**(10): p. 1953-1963.
59. Medlycott, E.A. and G.S. Hanan, *Designing tridentate ligands for ruthenium (II) complexes with prolonged room temperature luminescence lifetimes.* Chem. Soc. Rev., 2005. **34**(2): p. 133-142.
60. Abrahamsson, M., et al., *Bistridentate Ruthenium (II) polypyridyl-Type Complexes with Microsecond 3MLCT State Lifetimes: Sensitizers for Rod-Like Molecular Arrays.* Journal of the American Chemical Society, 2008. **130**(46): p. 15533-15542.
61. Ji, S., et al., *Ruthenium (II) Polyimine Complexes with a Long-Lived 3IL Excited State or a 3MLCT/3IL Equilibrium: Efficient Triplet Sensitizers for Low-Power Upconversion.* Angewandte Chemie International Edition, 2011. **50**(7): p. 1626-1629.

62. Du, P. and R. Eisenberg, *Energy upconversion sensitized by a platinum (II) terpyridyl acetylide complex.* Chemical Science, 2010. **1**(4): p. 502-506.
63. Damrauer, N.H., et al., *Effects of intraligand electron delocalization, steric tuning, and excited-state vibronic coupling on the photophysics of aryl-substituted bipyridyl complexes of Ru (II).* Journal of the American Chemical Society, 1997. **119**(35): p. 8253-8268.
64. Zhao, J., et al., *Transition metal complexes with strong absorption of visible light and long-lived triplet excited states: from molecular design to applications.* RSC Advances, 2012. **2**(5): p. 1712-1728.
65. Wu, W.H., et al., *Organic Triplet Sensitizer Library Derived from a Single Chromophore (BODIPY) with Long-Lived Triplet Excited State for Triplet-Triplet Annihilation Based Upconversion.* Journal of Organic Chemistry, 2011. **76**(17): p. 7056-7064.
66. Singh-Rachford, T.N., et al., *Boron dipyrromethene chromophores: Next generation triplet acceptors/annihilators for low power upconversion schemes.* Journal of the American Chemical Society, 2008. **130**(48): p. 16164-16165.
67. Turshatov, A., et al., *Synergetic Effect in Triplet–Triplet Annihilation Upconversion: Highly Efficient Multi-Chromophore Emitter.* Chemphyschem, 2012. **13**(13): p. 3112-3115.
68. Gouterman, M., *The Porphyrins*1978, New York: Academic Press.
69. Papkovsky, D.B. and T.C. O'Riordan, *Emerging applications of phosphorescent metalloporphyrins.* Journal of fluorescence, 2005. **15**(4): p. 569-584.
70. Baluschev, S., et al., *Metal-enhanced up-conversion fluorescence: Effective triplet-triplet annihilation near silver surface.* Nano letters, 2005. **5**(12): p. 2482-2484.
71. Baluschev, S., et al., *Two pathways for photon upconversion in model organic compound systems.* Journal of Applied Physics, 2007. **101**(2).
72. Islangulov, R.R., et al., *Noncoherent low-power upconversion in solid polymer films.* Journal of the American Chemical Society, 2007. **129**(42): p. 12652-+.
73. Keivanidis, P.E., et al., *Inherent Photon Energy Recycling Effects in the Up-Converted Delayed Luminescence Dynamics of Poly(fluorene)-Pt(II)octaethyl Porphyrin Blends.* Chemphyschem, 2009. **10**(13): p. 2316-2326.
74. Mezyk, J., et al., *Effect of an External Magnetic Field on the Up-Conversion Photoluminescence of Organic Films: The Role of Disorder in Triplet-Triplet Annihilation.* Physical Review Letters, 2009. **102**(8).
75. Singh-Rachford, T.N., et al., *Influence of temperature on low-power upconversion in rubbery polymer blends.* J. Am. Chem. Soc, 2009. **131**(33): p. 12007-12014.
76. Keivanidis, P.E., et al., *Electron-Exchange-Assisted Photon Energy Up-Conversion in Thin Films of pi-Conjugated Polymeric Composites.* Journal of Physical Chemistry Letters, 2011. **2**(15): p. 1893-1899.
77. Wohnhaas, C., et al., *Annihilation Upconversion in Cells by Embedding the Dye System in Polymeric Nanocapsules.* Macromolecular Bioscience, 2011. **11**(6): p. 772-778.
78. Haefele, A., et al., *Getting to the (Square) Root of the Problem: How to Make Noncoherent Pumped Upconversion Linear.* The Journal of Physical Chemistry Letters, 2012. **3**(3): p. 299-303.
79. Kim, J.H., F. Deng, and F.N. Castellano, *High Efficiency Low-Power Upconverting Soft Materials.* Chemistry of Materials, 2012. **24**(12): p. 2250-2252.
80. Baluschev, S., et al., *Upconversion with ultrabroad excitation band: Simultaneous use of two sensitizers.* Applied Physics Letters, 2007. **90**(18).
81. Singh-Rachford, T.N. and F.N. Castellano, *Supra-Nanosecond Dynamics of a Red-to-Blue Photon Upconversion System.* Inorganic chemistry, 2009. **48**(6): p. 2541-2548.

82. Monguzzi, A., R. Tubino, and F. Meinardi, *Multicomponent Polymeric Film for Red to Green Low Power Sensitized Up-Conversion.* Journal of Physical Chemistry A, 2009. **113**(7): p. 1171-1174.
83. Turshatov, A., et al., *Micellar carrier for triplet-triplet annihilation-assisted photon energy upconversion in a water environment.* New Journal of Physics, 2011. **13**.
84. Jankus, V., et al., *Energy Upconversion via Triplet Fusion in Super Yellow PPV Films Doped with Palladium Tetraphenyltetrabenzoporphyrin: a Comprehensive Investigation of Exciton Dynamics.* Advanced Functional Materials, 2012.
85. Monguzzi, A., et al., *White light generation by sensitized photon up-conversion.* Chemical Physics Letters, 2012. **521**: p. 17-19.
86. Yakutkin, V., et al., *Towards the IR Limit of the Triplet-Triplet Annihilation-Supported Up-Conversion: Tetraanthraporphyrin.* Chemistry-a European Journal, 2008. **14**(32): p. 9846-9850.
87. Schulze, T.F., et al., *Efficiency Enhancement of Organic and Thin-Film Silicon Solar Cells with Photochemical Upconversion.* The Journal of Physical Chemistry C, 2012.
88. Schulze, T.F., et al., *Photochemical Upconversion Enhanced Solar Cells: Effect of a Back Reflector.* Australian Journal of Chemistry, 2012. **65**(5): p. 480-485.
89. Singh-Rachford, T.N. and F.N. Castellano, *Pd(II) phthalocyanine-sensitized triplet-triplet annihilation from rubrene.* Journal of Physical Chemistry A, 2008. **112**(16): p. 3550-3556.
90. Clarke, R.H. and R.M. Hochstrasser, *Location and assignment of the lowest triplet state of perylene.* Journal of Molecular Spectroscopy, 1969. **32**(2): p. 309-319.
91. Lewitzka, F. and H.G. Löhmannsröben, *Investigation of Triplet Tetracene and Triplet Rubrene in Solution.* Zeitschrift für Physikalische Chemie, 1986. **150**(1): p. 69-86.
92. Wu, K. and A. Trozzolo, *Production of singlet molecular oxygen from the oxygen quenching of the lowest excited singlet state of rubrene.* Journal of Physical Chemistry, 1979. **83**(22): p. 2823-2826.
93. Wilson, T., *Excited singlet molecular oxygen in photooxidation.* Journal of the American Chemical Society, 1966. **88**(13): p. 2898-2902.
94. Herkstroeter, W. and P. Merkel, *The triplet state energies of rubrene and diphenylisobenzofuran.* Journal of Photochemistry, 1981. **16**(4): p. 331-341.
95. Loudet, A. and K. Burgess, *BODIPY dyes and their derivatives: Syntheses and spectroscopic properties.* Chemical Reviews, 2007. **107**(11): p. 4891-4932.
96. Ulrich, G., R. Ziessel, and A. Harriman, *The chemistry of fluorescent bodipy dyes: versatility unsurpassed.* Angewandte Chemie International Edition, 2007. **47**(7): p. 1184-1201.
97. Friedemann, K., et al., *Characterization via Two-Color STED Microscopy of Nanostructured Materials Synthesized by Colloid Electrospinning.* Langmuir, 2011. **27**(11): p. 7132-7139.
98. Wilke, C. and P. Chang, *Correlation of diffusion coefficients in dilute solutions.* AIChE Journal, 1955. **1**(2): p. 264-270.
99. Birks, J.B., *Photophysics of aromatic molecules*. Vol. 71. 1970: Wiley, New York.
100. Auckett, J.E., et al. *Efficient up-conversion by triplet-triplet annihilation*. in *Journal of Physics: Conference Series*. 2009. IOP Publishing.
101. Andrews, D.L., C. Curutchet, and G.D. Scholes, *Resonance energy transfer: beyond the limits.* Laser & Photonics Reviews, 2010. **5**(1): p. 114-123.
102. Benstead, M., G.H. Mehl, and R.W. Boyle, *4, 4'-Difluoro-4-bora-3a, 4a-diaza-< i> s</i>-indacenes (BODIPYs) as components of novel light active materials.* Tetrahedron, 2011. **67**(20): p. 3573-3601.

103. Whited, M.T., et al., *Singlet and Triplet Excitation Management in a Bichromophoric Near-Infrared-Phosphorescent BODIPY-Benzoporphyrin Platinum Complex.* Journal of the American Chemical Society, 2010. **133**(1): p. 88-96.
104. Cheng, Y.Y., et al., *Entropically Driven Photochemical Upconversion.* The Journal of Physical Chemistry A, 2011. **115**(6): p. 1047-1053.
105. Borisov, S., et al., *New NIR-emitting complexes of platinum (II) and palladium (II) with fluorinated benzoporphyrins.* Journal of Photochemistry and Photobiology A: Chemistry, 2009. **201**(2): p. 128-135.
106. Anderson, R.R. and J.A. Parrish, *The optics of human skin.* Journal of Investigative Dermatology, 1981. **77**(1): p. 13-19.
107. Tromberg, B.J., et al., *Non-invasive in vivo characterization of breast tumors using photon migration spectroscopy.* Neoplasia (New York, NY), 2000. **2**(1-2): p. 26.
108. Li, C., et al., *Rainbow perylene monoimides: easy control of optical properties.* Chemistry-a European Journal, 2008. **15**(4): p. 878-884.
109. Avlasevich, Y., C. Li, and K. Müllen, *Synthesis and applications of core-enlarged perylene dyes.* J. Mater. Chem., 2010. **20**(19): p. 3814-3826.
110. Sommer, J.R., et al., *Photophysical Properties of Near-Infrared Phosphorescent pi-Extended Platinum Porphyrins.* Chemistry of Materials, 2011. **23**(24): p. 5296-5304.
111. Rozhkov, V.V., M. Khajehpour, and S.A. Vinogradov, *Luminescent Zn and Pd tetranaphthaloporphyrins.* Inorganic chemistry, 2003. **42**(14): p. 4253-4255.
112. Tanaka, K., K. Inafuku, and Y. Chujo, *Environment-responsive upconversion based on dendrimer-supported efficient triplet–triplet annihilation in aqueous media.* Chemical Communications, 2010. **46**(24): p. 4378-4380.
113. Branco, M.C. and J.P. Schneider, *Self-assembling materials for therapeutic delivery.* Acta biomaterialia, 2009. **5**(3): p. 817-831.
114. Batrakova, E.V. and A.V. Kabanov, *Pluronic block copolymers: evolution of drug delivery concept from inert nanocarriers to biological response modifiers.* Journal of Controlled Release, 2008. **130**(2): p. 98-106.
115. Borowy-Borowski, H., et al., *Unique technology for solubilization and delivery of highly lipophilic bioactive molecules.* Journal of drug targeting, 2004. **12**(7): p. 415-424.
116. Naderi, J., et al., *Water-soluble formulation of Coenzyme Q 10 inhibits Bax-induced destabilization of mitochondria in mammalian cells.* Apoptosis, 2006. **11**(8): p. 1359-1369.
117. Lipshutz, B.H. and B.R. Taft, *Heck Couplings at Room Temperature in Nanometer Aqueous Micelles.* Organic Letters, 2008. **10**(7): p. 1329-1332.
118. Lipshutz, B.H., S. Ghorai, and G.T. Aguinaldo, *Ring-Closing Metathesis at Room Temperature within Nanometer Micelles using Water as the Only Solvent.* Advanced Synthesis & Catalysis, 2008. **350**(7-8): p. 953-956.
119. Lipshutz, B.H., et al., *Olefin Cross-Metathesis Reactions at Room Temperature Using the Nonionic Amphiphile "PTS": Just Add Water.* Organic Letters, 2008. **10**(7): p. 1325-1328.
120. Lipshutz, B.H. and A.R. Abela, *Micellar Catalysis of Suzuki− Miyaura Cross-Couplings with Heteroaromatics in Water.* Organic Letters, 2008. **10**(23): p. 5329-5332.
121. Stich, M.I., L.H. Fischer, and O.S. Wolfbeis, *Multiple fluorescent chemical sensing and imaging.* Chemical Society Reviews, 2010. **39**(8): p. 3102-3114.
122. Pope, M. and C.E. Swenberg, *Electronic processes in organic crystals*. Vol. 383. 1982: Clarendon Press Oxford.

123. Miteva, T., G. Nelles, and A. Yasuda, *Temperature and temperature distribution sensing with high resolution in microscopic electronic devices and biological objects*, 2007, Google Patents.
124. Turshatov, A.A. and S.B. Baluschev, *Triplet-Triplet Annihilation Assisted Upconversion: All-Optical Tools for Probing Physical Parameter of Soft Matter.* Handbook of Coherent-Domain Optical Methods, ISBN 978-1-4614-5175-4. Springer Science+ Business Media New York, 2013, p. 1289, 2013. **1**: p. 1289.
125. Mitchell, D.J., et al., *Phase behaviour of polyoxyethylene surfactants with water. Mesophase structures and partial miscibility (cloud points).* J. Chem. Soc., Faraday Trans. 1, 1983. **79**(4): p. 975-1000.
126. Mehta, S., et al., *Effect of temperature on critical micelle concentration and thermodynamic behavior of dodecyldimethylethylammonium bromide and dodecyltrimethylammonium chloride in aqueous media.* Colloids and Surfaces A: Physicochemical and Engineering Aspects, 2005. **255**(1): p. 153-157.
127. Chen, L.J., et al., *Temperature dependence of critical micelle concentration of polyoxyethylenated non-ionic surfactants.* Colloids and Surfaces A: Physicochemical and Engineering Aspects, 1998. **135**(1): p. 175-181.
128. Streletzky, K. and G.D.J. Phillies, *Temperature dependence of Triton X-100 micelle size and hydration.* Langmuir, 1995. **11**(1): p. 42-47.
129. Balmbra, R., et al., *Effect of temperature on the micelle size of a homogeneous non-ionic detergent.* Transactions of the Faraday Society, 1962. **58**: p. 1661-1667.
130. Okabe, K., et al., *Intracellular temperature mapping with a fluorescent polymeric thermometer and fluorescence lifetime imaging microscopy.* Nature communications, 2012. **3**: p. 705.
131. Donner, J.S., et al., *Mapping Intracellular Temperature Using Green Fluorescent Protein.* Nano letters, 2012. **12**(4): p. 2107-2111.
132. Dayeh, V.R., et al., *Evaluating the toxicity of Triton X-100 to protozoan, fish, and mammalian cells using fluorescent dyes as indicators of cell viability.* Ecotoxicology and Environmental Safety, 2004. **57**(3): p. 375-382.

List of the principal abbreviations

Bodipy (class of dyes)	Boron Dipyrromethene
Bodipy (dye)	1,3,5,7-tetramethyl-8-phenyl-2,6-diethyl dipyrromethane•BF_2)
Bodipy-A	Dyad 4-(perylene-3'-yl)-8-phenyl-1,3,5,7-tetramethyl -2,6-diethyl dipyrromethane•BF_2
Bodipy-A2	Dyad 4-(perylene-3'-yl)ethynyl-8-phenyl-1,3,5,7-tetramethyl- -2,6-dipyrromethane•BF2
CW	Continuous wave
DPA	9,10-diphenylanthracene
DMF	Dimethylformamide
FWHM	Full width at half maximum
ISC	Intersystem crossing
IR	Infra-red
milli-Q	"Ultrapure" water
NA	Numerical aperture
NIR	Near infra-red
OEP	Octaethylporphyrin
OD	Optical density
PdTBP, PdTPTBP	Pd (II) tetraphenyltetrabenzoporphyrin
PdTBP-W	Pd (II) tetra(4-carboxyphenyl)tetrabenzoporphyrin potassium salt
PdTNP	Pd (II) tetrakis-*meso*-(3,5-dimethoxyphenyl) tetranaphthaloporphyrin
PdOEP	Pd (II) 2,7,8,12,13,17,18-octaethyl-porphyrinato
PMI (class of dyes)	Perylene-monoimide
PMI (dye)	N-(2,6-diisopropylphenyl)perylene-3,4:9,10-perylenedicarboximide
PMI-Bodipy	Dyad (N-(2,6-diisopropylphenyl)perylene-3,4:9,10-perylenedicarboximide-yl)-8-phenyl-1,3,5,7-tetramethyl-2,6-diethyl dipyrromethane•BF_2
PS400	Oligo-styrene
PtTBP, PtTPTBP	Pt (II) tetraphenyltetrabenzoporphyrin
PtTNP	Pt (II) tetraphenyltetranaphtoporphyrin
PTS	Polyoxyethanyl-tocopheryl sebacate

List of the principal abbreviations

PtOEP	Pt (II) 2,7,8,12,13,17,18-octaethyl-porphyrinato
Q.Y.	Quantum yield
SC	Supercontinuum
TBP	Tetrabenzoporphyrin
THF	Tetrahydrofuran
Triton X-100	Polyoxyethylene octyl phenyl ether
TTA	Triplet-triplet annihilation
TTA – UC	Triplet-triplet annihilation photon upconversion
TNP	Tetranaphtoporphyrin
TTT	Triplet-triplet transfer
UC	Upconversion
UV	Ultra-violet
Y-635	3,10-bis(4-tert-butylphenyl)perylene
Y-789-W	1,1'-(4,4'-(perylene-3,10-diyl)bis(4,1-phenylene))bis(N,N',-trimethylmethanaminium) iodide
Y-792	3-(Hex-1-ynyl)perylene
Y-793	3,10-Di(hex-1-ynyl)perylene
Y-794	3-(4-*tert*-butylphenyl)perylene
Y-795	3,10-bis((4-tert-butylphenyl)ethynyl)perylene
Y-796	3-((4-*tert*-butylphenyl)ethynyl)perylene
Y-824	3-(3,3-Dimethylbutyn-1-yl)perylene
Y-805	3,10-bis(3,3-Dimethylbutyn-1-yl)perylene
Y-895	9-(4-*tert*-butylphenyl)-N-(2,6-diisopropylphenyl)perylene-3,4-perylenedicarboximide
Y-896	9-(3,3'-Dimethylbutynyl)-N-(2,6-diisopropylphenyl)perylene-3,4-perylenedicarboximide

Acknowledgments

This work was performed in the department of at the Max Planck Institute for Polymer Research in Mainz. I thank everyone who directly or indirectly influenced on this work and contributed its successful accomplishment.

First of all, I would like to thank xxxxxxxxxxx, Head of the Department of Physical Chemistry of Polymers, for the possibility to do this interesting and challenging work.

I would like also to thank xxxxxxxxxxx from the Johannes Gutenberg-University in Mainz, for his interest in this work and for being a second referee of my thesis.

Also I want to thank xxxxxxxxxxx from Johannes Gutenberg-University for his interest to the work and readiness to be a chairman during the thesis defense.

A special gratitude I would like to give to my supervisor xxxxxxxxxxx for his support and continuous guidance throughout this project. In addition, I would like to thank him for his enthusiasm, humor sense, life philosophy and stories, which all together create the main atmosphere in the Photophysical Chemistry group.

I want to thank for the cooperation and financial support our project partners in Sony Technology Center in Stuttgart, and especially xxxxxxxxxxx for the shared practical experience in upconversion and quantum yield measurements.

Also I thank the IMPRS-PRS for the financial assistance of the first year of my dissertation work.

I would like to thank xxxxxxxxxxx, who, being not involved in the upconversion research, was the supervisor of the project devoted to the home-build STED-microscope, for the creation and improvement of which I spent a lot of time.

I would like to show my appreciation to the personal department of MPIP, who cared about me to have the contract in time, xxxxxxxxxxx and xxxxxxxxxxx, who received probably a ton of different equipment, ordered by me, technical staff, keeping the functionality of the labor and helping to make it more comfortable, and mechanic workshop, which always cause my admiration on a reached precision.

My huge appreciation goes to my friends and colleagues, xxxxxxxxxxx and xxxxxxxxxxx, without whose help this work would not have been possible. Only because of their knowledge, ideas and activity we could go so far in this research. Also I would like to thank xxxxxxxxxxx, cooperation with which though is not represented in this thesis, but nevertheless takes a significant part in our investigations. The patience of all of them in the repeating of probably obvious things strongly enhances my understanding of chemistry.

Acknowledgments

I am grateful to xxxxxxxxxxx for the translation of the abstract on the German language and for the helpful and pleasant conversations during all years of our team-work.

I would like to appreciate the patience of xxxxxxxxxxx in reading round 120 pages of this thesis and correction of my perfect English language.

I would like to express my gratitude to xxxxxxxxxxx for the very helpful discussions about oxygen scavengers and friendly communication.

I am deeply grateful to xxxxxxxxxxx, who has been successfully enriching our men's team and keeping our good mood in the coffee corner all these years.

Also I would like to thank all colleagues for the nice atmosphere in the group during both working hours and grill-parties.

Especially I would like to thank my wife, whose support and encouragement was especially needed in the last year, and my son, playing with whom gave the needed rest to my mind during the thesis writing.

The largest thank I want to say to my parents and sister, supporting me all the time and which will finally see the end of this livelong journey to the Doctor title. I love all of you so much, that sometimes I cannot understand how you could let me go so far away.

List of publications

1. C. Wohnhaas, V. Mailänder, M. Dröge, M. Filatov, **D. Busko**, Y. Avlasevich, S. Baluschev, T. Miteva, K. Landfester, A. Turshatov, Triplet–Triplet Annihilation Upconversion Based Nanocapsules for Bioimaging Under Excitation by Red and Deep-Red Light // Macromolecular Bioscience, 2013
2. C. Wohnhaas, K. Friedemann, **D. Busko**, K. Landfester, S. Baluschev, D. Crespy, and A. Turshatov, All Organic Nanofibers As Ultralight Versatile Support for Triplet–Triplet Annihilation Upconversion // ACS Macro Letters, 2013, Vol. 2, pp. 446-450
3. A. Turshatov, **D. Busko**, Y. Avlasevich, T. Miteva, K. Landfester, S. Baluschev, Synergetic Effect in Triplet–Triplet Annihilation Upconversion: Highly Efficient Multi-Chromophore Emitter // ChemPhysChem, 2012, Vol. 13, Iss. 13, pp. 3112–3115
4. **D. Busko**, S. Baluschev, D. Crespy, A. Turshatov, K. Landfester, New possibilities for materials science with STED microscopy (review) // Micron, 2012, Vol. 43, pp. 583–588
5. A. Turshatov; **D. Busko**; St. Baluschev, T. Miteva, K. Landfester, Micellar carrier for triplet-triplet annihilation-assisted photon energy upconversion in a water environment // New Journal of Physics, 2011, Vol. 13

Erklärung

Diese Dissertation wurde in der Zeit von Mai 2009 bis Juli 2013 im Arbeitskreis Physikalische Chemie der Polymere von xxxxxxxxxx am Max-Planck-Institut für Polymerforschung in Mainz erstellt.

Ich versichere hiermit, dass ich diese Arbeit selbstständig angefertigt habe und keine anderen als die angegebenen Quellen und Hilfsmittel benutzt, sowie die wörtlich oder inhaltlich übernommenen Stellen als solche kenntlich gemacht habe.

Mainz, den

Dzmitry Busko